17515

NATIONAL LIBRARY
OTTAWA

CANADA

BIBLIOTHÈQUE NATIONALE
OTTAWA

NAME OF AUTHOR..FRED..Y..FUJIWARA.....

TITLE OF THESIS..NUCLEAR..MAGNETIC..RESONANCE.....
..STUDY..OF...HYDROGEN..BINARIES...
...IN...SOLUTION.....

UNIVERSITY.....Alberta.....

DEGREE FOR WHICH THESIS WAS PRESENTED.....Ph.D.....

YEAR THIS DEGREE GRANTED.....1973.....

Permission is hereby granted to THE NATIONAL LIBRARY OF CANADA to microfilm this thesis and to lend or sell copies of the film.

The author reserves other publication rights, and neither the thesis nor extensive extracts from it may be printed or otherwise reproduced without the author's written permission.

(Signed) F. Fujiwara....

PERMANENT ADDRESS:

....8228 - 116 ST.....

....EDMONTON, ALBERTA

.....

DATED....July 24.....1973

NL-91 (10-68)

THE UNIVERSITY OF ALBERTA

NUCLEAR MAGNETIC RESONANCE STUDY OF HYDROGEN BIHALIDE IONS IN SOLUTION

by

© FRED YUKIO FUJIWARA

A THESIS

SUBMITTED TO THE FACULTY OF GRADUATE STUDIES AND RESEARCH

IN PARTIAL FULFILMENT OF THE REQUIREMENTS FOR THE DEGREE

OF DOCTOR OF PHILOSOPHY

DEPARTMENT OF CHEMISTRY

EDMONTON, ALBERTA

FALL, 1973

THE UNIVERSITY OF ALBERTA

FACULTY OF GRADUATE STUDIES AND RESEARCH

The undersigned certify that they have read, and recommend to the Faculty of Graduate Studies and Research, for acceptance, a thesis entitled "Nuclear Magnetic Resonance Study of Hydrogen Bihalide Ions in Solution", submitted by Fred Yukio Fujiwara in partial fulfilment of the requirements for the degree of Doctor of Philosophy.

J.S. Martin

Supervisor

External Examiner

Date July 19, 1973

ABSTRACT

The hydrogen bihalide ions XHY^-, where X, Y = F, Cl, Br or I were studied in aprotic solvents by nmr spectroscopy. The ^1H nuclear shieldings in all ten bihalide ions, and the ^{19}F shieldings and H-F coupling constants in the four fluorine-containing bihalide ions were determined. The H-F coupling was also observed for hydrogen fluoride dissolved in a few aprotic solvents.

Solutions containing FHF^- were prepared from tetraethylammonium or tetrabutylammonium bifluoride salts. The solutions containing the other bihalide ions were prepared by adding a tetrabutylammonium halide to a dilute solution of a hydrogen halide. A quantitative proton transfer reaction occurs if the halide ion is a stronger base than the conjugate base of the hydrogen halide.

The shieldings of the bihalide ions were obtained by analysis of the halide ion concentration dependence of the observed shieldings, which are averaged by rapid exchange. However, in most cases the H-F coupling was not averaged by rapid proton exchange. The association constants for the formation of most bihalide ions were large and the shieldings and coupling constants of these complexes could be directly observed.

The ^1H shieldings of a hydrogen halide decreases

on the formation of bihalide ions and the largest change occurs on the formation of the homobihalide ion, XHX^-. In all four homobihalide ions, the shieldings are about 14 ppm less than that of the corresponding hydrogen halide in the gas phase. A description of the shielding in terms of atomic contributions indicates that the hydrogen charge density in the homobihalide ion is less than that in the corresponding molecule.

The formation of a hydrogen bond to the electrophilic hydrogen of hydrogen fluoride is shown to result in a decrease in the ^{19}F shielding. This decrease is consistent with that observed in ^{13}C, ^{14}N and ^{17}O proton donors involved in hydrogen bonds, but it cannot be explained in terms of a simple model involving the change in the paramagnetic shielding of fluorine as the polarity of the H-F bond changes.

The first examples of the effect of hydrogen bonding on the H-F coupling constant of hydrogen fluoride are reported. A large decrease in J(HF) occurs on the formation of a bihalide ion. These coupling constants are: FHF^-, 120.5 ± 0.1 Hz; $FHCl^-$, 403.4 ± 0.2 Hz; $FHBr^-$, 427.1 ± 0.2 Hz; and FHI^-, 437 ± 5 Hz. The coupling constant of hydrogen fluoride dissolved in a few basic solvents was observed to decrease as the base strength of the solvent increases. The increase in the ionic character of the H-F bond is suggested as a possible explanation for the trend in J(HF).

ACKNOWLEDGEMENTS

The author wishes to express his appreciation and gratitude to:

Dr. J. S. Martin for guidance and encouragement throughout this research,

Dr. R. D. Green who did the preliminary study of this project,

Dr. J. E. Bertie and Dr. A. J. Jones for many helpful suggestions in the preparation of this thesis,

Mr. G. W. Stockton and Dr. A Quirt for many interesting and useful discussions,

Mr. G. Bigam for his efforts in keeping the spectrometers operating,

The National Research Council of Canada for financial support.

TABLE OF CONTENTS

	Page
ABSTRACT	iv
ACKNOWLEDGEMENT	vi
LIST OF TABLES	xi
LIST OF FIGURES	xiv
1. INTRODUCTION	1
1.1 Properties of the Hydrogen Bihalide Ions	2
1.1.1 Structure	3
1.1.2 Hydrogen Bond Strengths	7
1.2 Nmr Studies of Hydrogen Bonding	10
1.2.1 ^{1}H Nmr Studies	11
1.2.2 Nmr Studies of other Nuclei	14
1.2.3 Coupling Constants	18
1.3 Scope of the Thesis	21
2. EXPERIMENTAL	24
2.1 Materials	24
2.1.1 Hydrogen Halides	24
2.1.2 Halide Salts	25
2.1.3 Solvents	28
2.2 Procedures	30
2.3 Chemical Shift Scale	33
2.4 Analysis of 1:1 Complexes	37

Table of Contents cont'd.

		Page
3.	RESULTS OF A PROTON NMR STUDY OF BIHALIDE ION EQUILIBRIA IN SOLUTION	40
	3.1 Solvents Used	40
	3.2 Homobihalide Ions	41
	3.2.1 Proton Shielding	41
	3.2.2 Association Constants	47
	3.2.3 Solvent Dependence	49
	3.2.4 Cation Dependence	51
	3.2.5 Temperature Dependence	52
	3.3 Heterobihalide Ions	54
	3.3.1 Identification of the Species in Solution	54
	3.3.2 Analysis of 1:1 Complexes	63
	3.3.3 Solutions Involving Proton Transfer Reaction	65
	3.4 Summary	71
4.	RESULTS OF THE NMR STUDY OF HYDROGEN FLUORIDE COMPLEXES	74
	4.1 Bifluoride Ion	74
	4.1.1 Nuclear Shieldings and Coupling Constant	78
	4.1.2 Temperature Dependence	81

Table of Contents cont'd

Page

4.1.3 Deuterium Bifluoride Ion 82

4.2 Heterobihalide Ions 84

4.3 Hydrogen Fluoride in Solution 90

4.3.1 Non-Basic Solvents 92

4.3.2 Basic Solvents 94

4.4 Summary 96

5. DISCUSSION OF THE PROTON SHIELDING 100

5.1 Absolute Shieldings of the Hydrogen Bihalides 100

5.2 Proton Shielding in the Homobihalide Ions . 104

5.2.1 Theory of Proton Shielding 107

5.2.2 Dependence of the Shielding on the Charge Distribution 113

5.2.3 Evaluation of the Charge Densities . . 116

5.3 Proton Shielding in the Heterobihalide Ions 120

5.4 Electrostatic Model 121

5.5 Dependence of Proton Shielding on Hydrogen Bond Strength 125

6. DISCUSSION OF THE FLUORINE SHIELDINGS 134

6.1 Effect of Hydrogen Bonding 134

6.2 Theory of Fluorine Shielding 137

6.3 Application to Hydrogen Bonding of HF . . . 140

Table of Contents cont'd.

		Page
7.	DISCUSSION OF THE COUPLING CONSTANTS	146
	7.1 Effect of Hydrogen Bonding	146
	7.2 Theory of Nuclear Spin-Spin Coupling . . .	148
	7.3 Interpretation of Hydrogen Bonding Effects on the Coupling Constant	152
	7.4 Variation of J(HF) with Base Strength . . .	161
8.	CONCLUSION	165
	REFERENCES	170
	APPENDIX	184

LIST OF TABLES

Table		Page
I	Changes in enthalpy for the formation of the hydrogen bihalide ions	8
II	Absolute fluorine shieldings of the references at 34°C	36
III	Complex shifts of the tetra-n-butylammonium homobihalide ions in sym-tetrachloroethane at 34°C	44
IV	Association constants for the formation of the tetra-n-butylammonium homobihalide ions in sym-tetrachloroethane at 34°	48
V	Solvent dependence of the proton shieldings of tetrabutylammonium bihalides at 34°	50
VI	Temperature dependence of shieldings of tetrabutylammonium bihalide ions	53
VII	Complex shift and association constants for the heterobihalide ions assuming 1:1 complex	

List of Tables cont'd.

Table		Page
	formation in sym-tetrachloroethane	64
VIII	Nuclear shieldings and coupling constant in tetraethylammonium bifluoride at infinite dilution	80
IX	Temperature dependence of the shieldings in the bifluoride ion	83
X	Nuclear shieldings and coupling constants in the tetrabutylammonium heterobihalides in acetonitrile	87
XI	Nuclear shieldings and coupling constants in 0.22M hydrogen fluoride solutions	91
XII	Proton shieldings in parts per million of the hydrogen halides in the gas phase	101
XIII	Proton shielding of the bihalide ions	103

List of Tables cont'd.

Table		Page
XIV	Calculated absolute hydrogen shieldings in the hydrogen halides	114
XV	Calculation of bihalide hydrogen charge densities	118
XVI	Computed ion-molecule electrostatic potential energies	124
XVII	Proton shieldings in solutions containing 0.1M HBr and Bu_4NCl in sym-tetrachloroethane	187
XVIII	Proton shieldings in solutions containing 0.2M HI and Bu_4NCl in sym-tetrachloroethane	188
XIX	Proton shieldings in solutions containing 0.2M HI and Bu_4NBr in sym-tetrachloroethane	189

LIST OF FIGURES

Figure		Page
1	Dependence of the proton shielding of the hydrogen halides on the halide ion concentration: homobihalide systems	42
2	Proton shieldings at low salt concentrations	45
3	Proton shieldings in solutions containing HCl and Br^-, and HBr and Cl^-	55
4	Proton shieldings in solutions containing HCl and I^-, and HI and Cl^-	56
5	Proton shieldings in solutions containing HBr and I^-, and HI and Br^-	57
6	Infrared spectrum of a solution containing HBr and an excess of Cl^-	58
7	Infrared spectra of solutions containing HCl or HBr, and Br^-	62

List of Figures cont'd.

Figure		Page
8	Comparison of the observed and calculated shieldings in solutions containing HBr and Cl^-	69
9	Comparison of the observed and calculated shieldings in solutions containing HI and Cl^- or Br^-	70
10	The ^1H spectrum of FHF^-	75
11	The ^{19}F spectrum of FHF^- and FDF^-	76
12	The ^1H spectrum of $FHCl^-$	86
13	Correlation between the proton shielding and coupling constant in hydrogen-bonded complexes of hydrogen fluoride	97
14	Correlation between the ^1H and ^{19}F shieldings of the hydrogen-bonded complexes of hydrogen fluoride	99

List of Figures cont'd.

Figure		Page
15	Dependence of the complex shift on the proton affinities of the halide ions	127
16	Correlation between the changes in the ^{1}H shielding and in the ir stretch frequency of hydrogen fluoride	130
17	Variation of π_{AB} with a_1	159
18	Correlation between the changes in the coupling constant and the ir stretch frequency of hydrogen fluoride	163

CHAPTER 1

INTRODUCTION

The hydrogen bihalide ions are a class of hydrogen-bonded anion-molecule complexes of the form XHY^-, where X and Y are halogens. The best known of these complexes is the hydrogen bifluoride ion, FHF^-, which contains the strongest hydrogen bond known (1). This anion is stable in a variety of ionic crystals and has been extensively studied by a variety of techniques (2-4).

In 1909, Kaufler and Kunz (5) reported the synthesis and analysis of a large number of hydrogen bihalides and correctly deduced both the ionic nature and the order of the atoms in the XHX^- moiety. This paper appears to have been overlooked and it was not until 1954, when the isolation of tetraethylammonium hydrogen bichloride was reported (6), that an active interest in these compounds developed.

The impetus for the interest in the hydrogen bihalide ions can be attributed to their relevance in two major areas. Firstly, the triatomic XHY^- anion represents the simplest framework within which hydrogen bonding can be studied. These anions can be readily studied in solid compounds or in solution and they provide excellent examples of strong hydrogen bonding. Secondly, the formation of ion-molecule hydrogen-bonded complexes has been

found to play an important role in the solution chemistry of aprotic solvents. Recently a comprehensive review of acid-base behavior in aprotic solvents has been published (7). The behavior of acids in aprotic solvents very often involves a proton transfer to a base followed by the formation of a hydrogen-bonded complex between the conjugate base formed and the acid. Kolthoff (8) has coined the phrases, homoconjugation and heteroconjugation, to distinguish reactions involving an acid and its conjugate base from reactions involving an acid and the conjugate base of a different acid. A similar procedure will be used here to distinguish the hydrogen bihalide ions of the form XHX^- from those containing two different halogens. The terms homobihalide and heterobihalide will be used to designate these two classes of hydrogen bihalides.

1.1 Properties of the Hydrogen Bihalide Ions

An extensive survey of the literature on the hydrogen bihalide ions will not be presented here since there are recent reviews available (3,4,9). However, since the interpretation of the nmr results depend on the structure of these ions and the hydrogen bond strengths, these aspects will be reviewed.

1.1.1 Structure

The halogen-halogen distances have been determined only for the four homobihalide ions (10-12). In each case the distance is about 0.5 Å shorter than twice the van der Waals radius of the corresponding halide ion.

The position of the hydrogeh atom has been firmly established only for the hydrogen bifluoride ion. Hamilton and Ibers (2) have presented the evidence supporting the centrosymmetric structure of FHF^- and have discussed the difficulties involved in the structural determination of potentially symmetric hydrogen bonds.

Evans and Lo (13) have obtained infrared spectra of a large number of crystals containing the $ClHCl^-$ or $ClDCl^-$ ions. They found that the very broad absorption bands attributed to the $ClHCl^-$ ion were considerably perturbed by its environment in the crystals. There appeared to be two kinds of bichloride ions in crystals. Type I consisted of the cesium, tetramethylammonium, and hexadecyltrimethylammonium salts, and Type II consisted of the tetraethylammonium, tetrapropylammonium, and tetrapentylammonium salts. The unusual crystal $CsCl\ 1/3(H_3O \cdot HCl_2)$ has also been found to be of Type II (14). The tetrabutylammonium bichloride was classed as intermediate between these two types. In solution, the bichloride spectra were essentially independent of the cation and closely resembled

the solid-phase spectra of the Type II salts.

Evans and Lo tentatively concluded that the bichloride ions in the Type I salts have a linear asymmetric structure ($C_{\infty v}$ symmetry), and those in Type II salts have a centrosymmetric structure ($D_{\infty h}$ symmetry).

Subsequent studies on $CsHCl_2$ have shown that the bichloride ion in this salt cannot be centrosymmetric. Nibler and Pimentel (15) observed a weak peak in the $CsHCl_2$ spectrum at about 600 cm^{-1} which sharpened and increased in intensity when cooled to 20°K. They assigned this feature to the fundamental bending frequency, ν_2, and reassigned the much more intense feature at 1200 cm^{-1} to the overtone, $2\nu_2$, rather than to the fundamental as previously proposed (13). The enhancement of the overtone was explained in terms of the abnormally large dipole second derivative which occurs in the hydrogen bonds because of the large charge mobility along the bond (15). Nibler and Pimentel proposed, on the basis of the symmetry requirements for the enhancement of the overtone, that Type I ions have either $C_{\infty v}$ or lower symmetry. Inelastic neutron scattering studies (16) have confirmed this reassignment of ν_2 in $CsHCl_2$. In addition, these studies found that the symmetric stretching mode involved the motion of the hydrogen atom, which cannot occur in a centrosymmetric bichloride ion (17,18).

The evidence relating to the structure of the bichloride ion in Type II salt is less conclusive. An X-ray study (10) found that the bichloride ion in $CsCl \cdot 1/3(H_3O \cdot HCl_2)$ is in a symmetric environment, and the interpretation of the infrared and Raman spectra indicated that the bichloride ion has a centrosymmetric structure in the crystal (14). The only other crystallographic study (12) of a crystal containing the bichloride ion found that the bichloride ion in the Type I tetramethylammonium salt is not in a symmetric environment.

Evans and Lo's (13) classification has been supported by the nuclear quadrupole resonance studies of these bichloride salts. In the Type I salts, tetramethylammonium (19,20) and caesium (20) bichlorides a single signal was observed at approximately 20 MHz for the ^{35}Cl resonance. In the Type II salts, tetraethylammonium bichloride (19,21) and $CsCl \cdot 1/3(H_3O \cdot HCl_2)$ (20), a single resonance was observed at approximately 12 MHz. A semi-empirical calculation (19), based on a linear asymmetric structure for Type I bichloride ions, predicted a second resonance below 10 MHz. This prediction could not be verified because the frequencies below 10 MHz were inaccessible to the spectrometer. Using the same empirical parameters, the resonance frequency for the centrosymmetric case was predicted to be 12.8 MHz. The self-

consistency of these calculations lends further support to the postulate that the chlorines in Type I bichloride ions are not equivalent and that they may be equivalent in the Type II ions.

The hydrogen bibromide ions have been less extensively studied. Evans and Lo (22) observed the same Type I-Type II classification for the tetraalkylammonium bibromides and the compound $CsBr \cdot 1/3(H_3O \cdot HBr_2)$ has been classed as Type II (13). It is not known whether the biiodide salts also exhibit this behavior.

Milligan and Jacox (23,24) have contended that the spectra assigned by Pimentel and coworkers (25,26) to the hydrogen bihalide radicals isolated in argon matrices should be assigned to the anion XHX^-. Both groups agree with the interpretation of the spectra in terms of a centrosymmetric structure for the triatomic species. The fundamental frequencies assigned to ν_1 and ν_3 for ClHCl and BrHBr, or for the corresponding anions, are almost identical to those for the Type II bihalide ions. Whatever the outcome of this controversy, these studies do indicate that the unperturbed configuration of these species is of $D_{\infty h}$ symmetry.

1.1.2 Hydrogen Bond Strengths

The change in enthalpy, ΔH, for the reaction,

[1.1] $$HX_{(g)} + R_4NY_{(crystal)} \longrightarrow R_4NXHY_{(crystal)}$$

where R is an alkyl group has been measured for several hydrogen bihalide ions. An enthalpy change of -37 kcal $mole^{-1}$ was measured for the formation of tetramethylammonium bifluorides (1). The magnitude of ΔH for the formation of the other homobihalides was found to increase as the size of the tetraalkylammonium cation was increased and ΔH appeared to approach a limiting value for the tetra-n-butylammonium cation (27). These limiting values of ΔH are tabulated in Table I.

Calorimetric measurements have been recently carried out for the formation of the bihalide ions derived from HCl in sulfolane (28). The observed enthalpy changes were combined with the solvation energy of HCl to obtain the ΔH for the reaction,

[1.2] $$HCl_{(g)} + Bu_4NX_{(solution)} \longrightarrow Bu_4NClHX_{(solution)}$$

where Bu_4N^+ is the tetra-n-butylammonium cation. The values of ΔH obtained are tabulated in Table I.

The strength of a hydrogen bond is best defined as the ΔH for the formation of the hydrogen-bonded complex in the gas phase. The enthalpy changes observed in

Table I. Changes in enthalpy for the formation of the hydrogen bihalide ions.

Ion	ΔH, kcal.mole^{-1}		
	Equation [1.1][a]	Equation [1.2][b]	gas[c]
$ClHCl^-$	-14.2	-13.9	-24
$ClHBr^-$		-10.7	-16
$ClHI^-$		-8	
$BrHBr^-$	-12.8		-18
IHI^-	-12.4		

a. Reference 27.

b. Reference 28.

c. Reference 32.

reactions shown in Equations [1.1] and [1.2] differ from those for a totally gas-phase reaction by the differences between the crystal or solvation energies of the bihalide salt and the halide salt. There is evidence that these energy differences are appreciable. Waddington (29) has corrected the observed enthalpy changes for the formation of the alkali metal bifluorides in the crystal by calculating the changes in the crystal lattice energies and obtained a value of -58 ± 5 kcal $mole^{-1}$. These calculations have been recently refined (30,31) by considering the charge distribution in FHF^- rather than treating FHF^- as a single ion. An expression for the gas phase ΔH was derived for the formation of each alkali metal bifluoride as a function of the charge separation in FHF^-. The best solution to these equations gave a ΔH of -60 kcal $mole^{-1}$ and a charge of -0.73 esu on the fluorine.

Kebarle (32) has measured the equilibrium constant for the reactions of the form,

[1.3] $$X^-(HX)_{n-1} + HX \rightleftharpoons X^-(HX)_n$$

in the gas phase as a function of temperature using a mass spectrometer. Unfortunately, at the temperatures required to observe the case where n=1, ΔH could not be

measured. However the ΔH's given in Table I were estimated by extrapolating from the results for higher complexes. These results are significantly larger than those observed for the formation of the bihalide ions by Equation [1.1] or [1.2].

1.2 Nmr Studies of Hydrogen Bonding

The parameters which can be most conveniently obtained from high resolution nuclear magnetic resonance (nmr) spectroscopy are the chemical shifts and the nuclear spin - spin coupling constants. The interaction between the applied field and the electrons surrounding the nucleus produces a small magnetic field at the nucleus which is usually opposed to the applied field. This "shielding" of a nucleus is defined by the relationship,

$$\nu_i = \frac{\gamma}{2\pi}(1 - \sigma_i)H_o, \qquad [1.4]$$

where ν_i is the resonance frequency, H_o is the applied magnetic field, and γ is the magnetogyric ratio of the nucleus. σ_i is the shielding constant and the chemical shift is defined as $(\sigma_i - \sigma_r)$ where σ_r is the shielding of the reference. The coupling constant J(AB) (in units of Hz) arises from the magnetic interaction between two nuclear spins which are coupled indirectly by the elec-

tronic environment, and is defined by the expression,

[1.5] $$E_{AB} = h\, J(AB)\, I_A \cdot I_B,$$

where E_{AB} is the energy of interaction between the two nuclei with spins I_A and I_B (in dimensionless units). The changes in the nuclear shieldings and coupling constants which occur on the formation of hydrogen bonds provide a convenient and a sensitive method for investigating hydrogen bonding.

1.2.1 ^{1}H Nmr Studies

Most nmr studies of hydrogen bonding in solution have involved the measurement of the changes in the shielding of the electrophilic hydrogen in the proton donor molecule (33). The shielding of this proton is very sensitive to the formation of a hydrogen bond and in virtually every case, the proton resonance is shifted to lower field. The only exceptions to this behavior are connected with the association to aromatic solvents which induce changes in the shielding as a result of magnetic anisotropy effects (34).

The magnitude of the downfield shift has been found to be a useful qualitative measure of the relative strengths of the interactions between a proton donor and various proton acceptors. Several linear correlations

between these proton shifts and enthalpy changes have been established but the quantitative applications of these correlations are rather limited (35). These correlations require a correction of the proton shifts for any neighbour anisotropy effects (34) arising from the proton acceptor molecule, because these effects are usually not related to the changes in enthalpy (35).

The chemical shift of the hydrogen bonded complex usually cannot be directly observed because the lifetime of the complex is too short on the nmr time scale. To observe both the associated and unassociated states in an equilibrium of the form,

[1.6] $$XH + B \rightleftharpoons XHB$$

the lifetime of each state must be longer than the reciprocal of the difference in the chemical shift (expressed in frequency units) between XH and XHB (36). For a typical difference of 500 Hz, lifetimes of greater than 10^{-3} sec would be required to observe separate signals for HX and XHB. As the lifetimes become shorter, the increased exchange rate results in a broadening of the separate signals which coalesce into a single peak when the lifetime reaches the value (36)

$$\frac{\sqrt{2}}{2\pi\ \Delta\nu}$$

where $\Delta\nu$ (in units of Hz) is the separation of the two signals in the absence of exchange. This formula assumes equal population of the two sites. A further decrease in the lifetimes results in a narrowing of the single peak whose position corresponds to an apparent shielding given by

$$[1.7] \qquad \sigma = \sum_i p_i \sigma_i$$

where p_i is the fractional population of species i with shielding σ_i participating in the exchange.

In addition to the "whole molecule" exchange process of the proton donor molecule between the free and complexed forms, intermolecular proton exchange can also occur. This is usually the case since the electrophilic protons of most proton donors can readily undergo intermolecular exchange. This proton exchange process will have no effect on the average shielding of HX and XHB in Equation [1.7], if the solution contains no other exchangeable protons. This exchange process can be detected in the nmr spectra in cases where the electrophilic proton is coupled to another nucleus in the molecule. Rapid proton exchange will cause a collapse of the multiplets arising from this spin-spin coupling into a single signal (36).

1.2.2 Nmr Studies of Other Nuclei

Large changes in the shielding of the heavy atom nucleus at the hydrogen bonding site have been observed in the limited number of cases which have been studied. The ^{13}C shieldings of chloroform (38) dissolved in a variety of solvents were measured relative to that of a dilute solution of chloroform in cyclohexane. In basic solvents, the ^{13}C shieldings were observed to decrease over a range of 4 ppm. A similar study of the ^{14}N shieldings in pyrroles, amides, and indole found a decrease of 1 to 15 ppm when the N-H bonds act as the proton donors (39,40). The decrease in the heavy atom shieldings were found to be linearly correlated with the corresponding decrease in the ^{1}H shieldings, which strongly suggests that the changes in the heavy atom shieldings are dominated by hydrogen bonding effects (38,39).

The effects of hydrogen bonding on the ^{15}N shieldings in ammonia and amines, the ^{17}O shieldings in water and methanol, and the ^{19}F shielding in hydrogen fluoride have been studied. Downfield shifts were observed on going from the gas phase to the condensed phase for water (41), ammonia (42), methylamine (43), and hydrogen fluoride (44,45). The contributions of hydrogen bonding to these shifts are difficult to deduce since these molecules can act as proton donors or acceptors, and in these

highly associated liquids a molecule can be involved in both roles.

The ^{15}N shielding of ammonia, extrapolated to infinite dilution, has been measured in several solvents, mainly amines, alcohols, and ethers (46). In all cases, the ^{15}N shielding of ammonia in these solutions was less than the shielding in the gas phase. A simple empirical model was used to separate the solvent dependence of the ^{15}N shielding into several components. Large downfield shifts (from 11 to 23 ppm) were attributed to various interactions between the solvent and the nitrogen lone pair, and small high field shifts (from 2 to 3 ppm) were attributed to the effects of hydrogen bonding between the ammonia protons and the solvent. The interactions between the ammonia lone pair and the $-CH_3$, $-C_2H_5$, -OH and -NH functional groups of the solvent, and hydrogen bonding between the ammonia protons and the solvent oxygen and nitrogen basic sites, were considered.

Studies of the solvent dependence of the ^{15}N shieldings in aniline, methylamine, and N-methylacetamide found that while hydrogen bonding, via the N-H bond, seems to contribute to the observed downfield shifts, other, less well defined solvent interactions were also important (43).

Reüben (47) divided the 36 ppm (41) gas-to-liquid downfield shift for the ^{17}O shielding of water into two contributions by the following reasoning. The ^{17}O shielding of water in a dilute solution in dioxane was found to be 18 ppm downfield from its value in the vapour; this shift was attributed to the hydrogen bond formed between water and dioxane, where water only acts as the proton donor. The average number of these hydrogen bonds formed was calculated from the data of a ^{1}H nmr study of this system. With the further assumption, that in liquid water each water molecule is involved in four hydrogen bonds (two via the hydrogen atoms and two by donation of the oxygen lone pairs), Reuben separated the effect of forming an $HO-H\cdots OH_2$ hydrogen bond into the following contributions: a -12 ppm shift for the proton donor and a -6 ppm shift for the proton acceptor. In other systems (page 15), large downfield shifts were observed for non-hydrogen bonding interactions with the lone pair. Therefore, the difference in the ^{17}O shieldings of water in the gas phase and in dioxane solution cannot be completely attributed to the formation of hydrogen bonds by the O-H protons, and the -12 ppm shift for the proton donor is probably overestimated.

The ^{17}O resonance of a series of solutions containing 0.2 M methanol and 0.6 M tetrabutylammonium halide in dichloromethane has been measured (48). The shifts in the ^{17}O shieldings in these solutions, measured relative to methanol at the same concentration, were: for F^-, -0.9 ppm; for Cl^-, -7.9 ppm; for Br^-, -5.7 ppm; for I^-, -8.0 ppm. These downfield shifts can be attributed to the effects of hydrogen bonding since most of the methanol is complexed to the anion at these concentrations (49).

There have been very few studies of the effects of hydrogen bonding on the ^{19}F shielding of hydrogen fluoride. The ^{19}F shielding was found to decrease on the formation of hydrogen-bonded polymers in the gas (44,45). In aqueous solutions, the ^{19}F shieldings of the following species increased in the order (50),

$$F^- < FHF^- < HF.$$

These shieldings were deduced from the concentration dependence of the observed exchange-averaged chemical shifts and the known equilibrium constants for the equilibria involved. The ^{19}F spectra of the bifluoride salt of primary, secondary, tertiary, and quaternary butyl ammonium, as molten salts have also been reported (51). ^{19}F nmr studies of hydrogen fluoride dissolved in carbon tetrachloride, benzene, and dioxane have been previously reported (52).

The effect of hydrogen bonding on the atom at the basic site of the proton acceptor molecule is rather interesting. The shielding change of the proton acceptor atom appears to depend on its bonding to the rest of the molecule. The shielding of atoms which are π bonded have been observed to increase on forming a hydrogen bond. This behavior has been observed for the ^{13}C shielding in methylisocyanide (53), the ^{14}N shieldings in acetonitrile (53) and pyridine (54), the ^{15}N shielding in quinoline (43), and for the ^{17}O shielding in acetone (55). In contrast, a decrease in the shielding of the atom at the proton acceptor site in water (47), methanol (47), ammonia (46) and trimethylamine (43) have been observed on hydrogen bonding.

1.2.3 Coupling Constants

The solvent dependence of the spin-spin coupling constant has been well established (56-58). There is a number of cases in which the coupling constant between the electrophilic hydrogen in a proton donor molecule and the atom to which it is bonded has been found to be solvent dependent. The effect of hydrogen bonding on the couplings is generally quite small. Consequently the separation of the effect of hydrogen bonding from other effects

is often difficult (56-58).

There are very few examples in which the changes in the coupling constant of proton donors have been attributed to the effect of hydrogen bonding. The variation of the ^{13}C-H coupling constant observed in chloroform dissolved in a number of aprotic solvents has been interpreted in terms of hydrogen bonding (56, 59). The coupling constant was found to range from 208.1 Hz in cyclohexane solutions to 217.7 Hz in dimethylsulfoxide solution. Linear correlations were observed between the increase in the coupling constant and the decrease in the ^{1}H and ^{13}C shieldings (38). An increase in the magnitude of J (^{13}CH) in a number of different halomethanes has also been attributed to the effects of hydrogen bonding (60).
The one-bond ^{15}N-H coupling constant in aniline, acting as a proton donor towards a number of acceptors, has been observed to increase in magnitude by 5% (48). A recent review (57) has presented several other examples of solvent dependent coupling constants in which hydrogen bonding effects may also be important.

The coupling constant in hydrogen fluoride has been observed by nmr only in liquid hydrogen fluoride at very low temperature. A value of 521 Hz was found for this coupling constant (61). The H-F coupling constant has also been deduced for hydrogen fluoride in the gas

phase from the molecular beam electric resonance spectrum and was found to be +530 ± 23 Hz (62). This determination is too imprecise to allow a comparison of the coupling constant between the gas and the liquid state. However, this study did establish the sign of the coupling constant.

Exchange processes will also affect the observed coupling constant. Rapid whole molecule exchange processes such as in Equation [1.6], will result in an observed coupling constant which is a population-weighted average of the coupling constants in the free and associated forms. Rapid proton exchange will cause a collapse of the multiplet arising from a coupling to the exchanging proton into a single peak. This effect arises from the averaging of the relative orientations of the coupled nuclear spins. Slow exchange results in a broadening of the individual peaks in the multiplet and a decrease in the separation of the peak maxima. The multiplet will coalesce into a single broad peak when the lifetime τ equals $\sqrt{2}/(2\pi\Delta\nu)$, where $\Delta\nu$ is the separation in the multiplet (in Hz) in the absence of exchange (36). The separation of the peaks in the slow exchange region is given by the expression (assuming equal populations) (36)

$$[1.8] \quad \frac{\text{separation of peaks}}{\text{separation of peaks for large } \tau} = \left[1 - \frac{1}{2\pi^2\tau^2\Delta\nu^2}\right]^{1/2}$$

Lifetimes in the region of slow exchange can be estimated by (36)

[1.9] $$\tau = \frac{1}{\pi \Delta \nu_{1/2}} ,$$

where $\Delta \nu_{1/2}$ is the width at half-height due to the exchange broadening.

1.3 Scope of the Thesis

This thesis presents a study of the hydrogen bihalide ions in solution. ^{1}H and ^{19}F nmr spectroscopy was used to study solutions prepared by dissolving a hydrogen halide and a halide salt in an aprotic solvent.

The results of the study of solutions containing a hydrogen halide (except HF) and a tetraalkylammonium halide are presented in Chapter 3. Ideally, the formation of the hydrogen bihalide in solution can be described by the following equilibrium

$$HX + Y^- \rightleftharpoons XHY^-$$

However, in some of the mixed systems, where X and Y are not the same halogen, other equilibria were found to be present. One aspect of this study was to identify the species present in solutions containing a hydrogen halide and a halide ion. An attempt was made to identify the

equilibria involved and to measure the association constants. The ^{1}H nuclear shieldings in the hydrogen bihalide ions (except those containing fluorine) are presented in Chapter 3. The dependence of these shieldings on the solvent, temperature, and the cation were investigated.

Chapter 4 presents the results of the study of solutions containing the hydrogen bihalide ion of the form FHX^{-}, where X = F, Cl, Br, and I. The ^{1}H and ^{19}F shieldings, and the ^{19}F-H coupling constants in these four bihalide ions were measured. Dilute solutions of hydrogen fluoride in aprotic solvents were also studied to extend the rather limited data presently available regarding the effects of hydrogen bonding on heavy atom shieldings and coupling constants in proton donor molecules.

A discussion of the ^{1}H shieldings is presented in Chapter 5. An attempt is made to relate the observed decrease in the ^{1}H shielding on hydrogen bonding to the changes in the electronic structure between the hydrogen halide and the corresponding bihalide ion. The dependence of the proton shielding on the strength of the hydrogen bond, the base strength of the proton acceptor, and on the acid strength of the proton donor is discussed.

Chapter 6 contains a qualitative discussion of

the changes in the ^{19}F shieldings. At present, the changes in the heavy atom shieldings in the proton donor molecules on hydrogen bonding are not very well understood. The simple structure of hydrogen fluoride eliminates some of the complexities associated with other proton donor molecules. The changes in the ^{19}F shieldings are discussed in terms of a model which has been found to be useful in the understanding of fluorine shieldings in small molecules.

The variation of the F-H coupling constant in hydrogen fluoride on hydrogen bonding is discussed in Chapter 7. The change in the F-H coupling constant was found to be in an opposite direction to the changes previously found for proton donor molecules. A possible explanation for this behavior is presented. The correlation between the variation in the coupling constant and the strength of the hydrogen bond is investigated.

CHAPTER 2

EXPERIMENTAL

2.1 Materials

2.1.1 Hydrogen Halides

Matheson reagent gases, HCl, HBr, HI, were introduced into a vacuum system through anhydrous $CaSO_4$, frozen with liquid nitrogen, and the noncondensible gases pumped off until the pressure was less than 5 microns. The solid hydrogen halides were sublimed three times through a series of U-tubes at a temperature at least 10° below their melting points (HCl from a methylcyclohexane slush bath at -126°, HBr from a methanol slush bath at -98°, and HI from an acetone/CO_2 mixture at -78°). No peaks attributed to water vapour were observed in the infrared spectra of the purified gases (10 cm path length, 300 torr pressure) in the region 4000-500 cm^{-1} and also in the region 300-100 cm^{-1} in the case of HCl and HBr. The HI was used within one day after purification. After longer periods, the proton resonance of a freshly prepared solution of HI was found to be shifted downfield and gave a nonlinear temperature dependence. This behavior could be the result of the presence of iodine produced by the decomposition of HI in the gas (63).

Matheson HF (99.9%) was stored in a polytrifluorochlorethylene tube attached to a monel and copper vacuum system, and was purified by three trap to trap distillations.

2.1.2 Halide Salts

Eastman reagent grade tetraalkylammonium halide salts were predried in a vacuum desicator over P_2O_5. The tetra-n-butylammonium chloride (Bu_4NCl) and iodide salts were recrystallized 2 or 3 times from acetone/diethylether (3:1 V/V). Final drying of all salts was performed by heating the salt (below its melting point) while pumping until the pressure was less than 10^{-3} torr.

The tetrabutylammonium salts were analyzed for halide ion by titration with $AgNO_3$, using a potentiometric method to determine the endpoint. Analysis: Bu_4NCl, found 12.77%, calculated 12.76%; Bu_4NBr, found 24.76%, calculated 24.79%; Bu_4NI, found 34.42%, calculated 34.36%. Melting points were measured in sealed capillary tubes with a calibrated thermometer and were found to be: Bu_4NCl, 75.0-75.8; Bu_4NBr, 117.8-118.0; Bu_4NI, 144.0-145.0 °C.

Tetraethylammonium fluoride (Et_4NF), obtained from Eastman Kodak, contained water which could not be completely removed by drying under vacuum at room temperature. After drying for one week, the salt was analyzed

for fluoride ion by a gravimetric method as triphenyltin fluoride (64), and for water by the Karl Fischer titration (65). The analysis was consistent with a hydrate $Et_4NF(H_2O)_{1.5}$. An aqueous solution of this salt had a pH of about 8 which indicates that there was no acid present.

The Et_4NF hydrate decomposed to produce the bifluoride salt when slowly heated to 100° under vacuum. The volatile components were collected in a liquid nitrogen cold trap and were identified by nmr as triethylamine, ethylene, and water. The presence of ethylene was confirmed by its reaction with bromine in carbon tetrachloride to produce 1,2-dibromoethane. The thermal decomposition of the hydrated tetraethylammonium fluoride, as a solid or in solution, has been previously reported and the following two step process was postulated (66):

[2.1] $$Et_4NF \xrightarrow{100°} Et_3N\cdot HF + C_2H_4$$

[2.2] $$Et_4NF + Et_3N\cdot HF \longrightarrow Et_4NHF_2 + Et_3N.$$

Reaction [2.1] is analogous to the Hoffmann elimination reaction of quaternary ammonium hydroxides (67). The F^- ion could take the same role as the OH^- ion in this elimination reaction. A possible alternative mechanism could involve a proton transfer from H_2O to F^-, resulting in the formation of FHF^- and Et_4NOH which would decompose by

the Hoffmann reaction.

The Et_4NHF_2 was precipitated twice from acetonitrile by adding diethylether and then dried for several days at 100° under vacuum. The melting point of the salt, determined in a sealed capillary, was 158.5-160.0°, with evolution of a gas. Analysis for F^-, as triphenyltin fluoride, and for titratable acid in aqueous solution gave the following results: F^-, found 22.31%, calculated 22.45%; H^+, found 0.5895%, calculated 0.5955%. Water content by Karl Fischer method was less than 0.2% by weight.

A mixture of Et_4NHF_2 and Et_4NDF_2 was prepared by dissolving Et_4NHF_2 in D_2O and then evaporating the water. The partially deuterated salt was purified as described above.

An aqueous solution of Bu_4NF was prepared from the bromide salt by exchange on a Dowex 21K anion exchange column in the fluoride form. This solution had a pH of 8 which is consistent with a simple fluoride salt. After concentrating the solution by removing most of the water by vacuum distillation at 40°, the remaining liquid water was removed by freeze drying. The resulting off-white colored crystals initially melted into a clear liquid when heated to 50° under vacuum and then solidified after several hours. On further heating under vacuum, the solid was slowly converted into a transparent, light brown

liquid with evolution of gases. After two weeks the solid had completely disappeared and the liquid produced waxy crystals with a melting point of 30 ± 2°C. The ^{1}H and ^{19}F nmr spectra of the final product in acetonitrile solution showed the presence of only Bu_4N^+ and FHF^-. This behavior is consistent with the formation of the hydrated Bu_4NF salt which decomposes on heating to form Bu_4NHF_2. During the course of this reaction an additional peak was observed at 5 ppm below TMS in the ^{1}H nmr spectrum. This peak completely disappeared on further heating. This peak is probably due to $F^-(H_2O)_x$ where x is about 1 or 2 since a peak was observed in the same position in the spectrum of $Et_4NF(H_2O)_{1.5}$.

The tetraalkylammonium bifluorides were handled as solids or as solutions in aprotic solvents in glass apparatus. No etching of the glass was visible after several weeks.

2.1.3 Solvents

Most solvents were treated with a drying agent and then fractionally distilled. The middle 50-75% fractions were collected and stored over 4A molecular sieves in a nitrogen atmosphere glove box. Drying tubes containing anhydrous $CaSO_4$ were used to protect the solvent from

atmospheric water during distillation at atmospheric pressure. Fischer reagent grade sym-tetrachloroethane and dichloromethane were refluxed overnight through a Soxhlet apparatus containing 4A molecular sieves. Both solvents were fractionated and the middle fractions, which had boiling ranges of less than one degree, were collected. Approximately 4% pentachloroethane, which should not significantly alter the solvent properties, was detected in the nmr spectrum of the purified tetrachloroethane.

Fischer reagent grade acetonitrile was stirred with CaH_2 for two days, then decanted and fractionally distilled from P_2O_5. This distillate was then refluxed over CaH_2 for two hours and fractionally distilled.

Dimethylsulfoxide and propylene carbonate were stirred with CaH_2 and then fractionally distilled under reduced pressure at temperatures below 70°. N,N-dimethylformamide was stirred with P_2O_5 for three days, with KOH for one hour, and then fractionally distilled under reduced pressure at temperatures below 70°. Diethylether and cyclohexane-d_{12} were fractionated from $LiAlH_4$. Eastman spectrograde nitromethane was fractionated under reduced pressure from $CaSO_4$. Trichlorofluoromethane was fractionated. Tetramethylsilane was stored over 4A molecular sieves; no water was detected in the nmr spectrum of this material.

2.2 Procedures

Solutions containing hydrogen bihalide ions were prepared by condensing the hydrogen halide into a solution containing the tetraalkylammonium halide. The tetraalkylammonium halide solutions were prepared in a glove box under a nitrogen atmosphere. A large open dish of P_2O_5 was used to remove water vapour from the glove box. The halide solutions were made up in two milliliter volumetric tubes. Using a calibrated 1 ml syringe, 0.500 ml (±0.003 ml) of the solution was transferred to a 5 mm o.d. nmr sample tube. The sample tube was fitted with a ground glass joint which could be connected to an auxiliary stopcock to exclude air. During the course of this work, this stopcock assembly was replaced by a less bulky metal valve with O-ring compression fittings. The tube was connected to a vacuum rack, frozen with liquid nitrogen, and pumped to less than 10^{-2} torr. Hydrogen halide gas, measured by a mercury manometer in a calibrated volume (typically 35 torr in 25 ml) was condensed onto the frozen solution, and the sample tube was sealed. More dilute samples in 12 mm tubes were prepared in a similar manner.

Hydrogen bifluoride solutions were prepared directly from the tetraalkylammonium salt. These solutions were found to be stable in glass sample tubes.

Hydrogen fluoride was handled in a vacuum system constructed from copper tubing, monel valves, and monel fittings. The cold trap and storage containers were fabricated from 3/4 inch polytrifluorochloroethylene rod and attached to the vacuum system by compression fittings. Pressure measurements were made with a Helicoid bourdon gauge (Type 460-K monel) which had a pressure range of 0 to 1 atmosphere.

The nmr sample tubes for hydrogen fluoride solutions were fabricated from polypropylene tubing (0.125 in o.d. with 0.016 in wall). The sample tube was attached to the vacuum line by an O-ring compression fitting (Cajon Ultra-Torr) and sealed by heating a thin glass sleeve, fitted snugly around the tube, with a hot air gun. These tubes will fit inside medium wall glass nmr tubes, which allows the sample to be spun in the spectrometer.

The hydrogen fluoride gas was measured by pressure in a known volume at a constant temperature (26 ± 1°), and then condensed into the sample tube cooled with liquid nitrogen. The actual amount of hydrogen fluoride used at a given pressure was calibrated to take into account polymer formation in the gas. Aqueous solutions, containing the same amounts of hydrogen fluoride as were used in the

nmr samples, were prepared by the same procedure and then titrated with NaOH using phenolphthalein as an indicator. The quantity of HF condensed into the sample tube was found to be reproducible to within 1%.

The nmr spectra were obtained on a Varian HA-60 or HA-100 spectrometer. For the ^{1}H spectra, the internal reference, tetramethylsilane, was used for the lock signal. The peak positions were measured by setting the sweep oscillator at resonance and measuring the difference between its frequency and that of the lock oscillator. The ^{19}F spectra were obtained at 56.445 and 96.4 MHz. A solution of trifluoroacetic acid in acetonitrile (50% by volume) was used as an external reference to provide a lock signal. For samples in polypropylene tubes, the external reference was placed in the space between the inner polypropylene tube and the outer supporting glass tube. The external references were placed in capillary tubes for solutions in glass nmr tubes. Unless otherwise stated, spectra were obtained at ambient probe temperature, 34 ± 1°, in both spectrometers.

The infrared spectra in the region 4000-500 cm^{-1} were obtained on a Perkin-Elmer Model 337 spectrometer, and on a Beckman IR-11 spectrometer for the region 300-100 cm^{-1}. Solution spectra were obtained using sample cells with 0.1 or 0.5 mm path lengths. Solutions of

hydrogen bihalides (except those containing fluorine) gave identical spectra in cells with NaCl or KBr windows in all cases.

2.3 Chemical Shift Scale

The chemical shift of a nucleus can be defined as the difference between its absolute shielding and the absolute shielding of a reference nucleus (34). The absolute shielding, σ, referenced to the bare nucleus, is defined by the condition required for resonance given in Equation [1.4].

Throughout this work, all chemical shifts will be reported in parts per million (ppm) relative to a reference. The symbol σ will be used for both the absolute shieldings, and the chemical shifts or "relative shieldings". σ will always be accompanied by the reference when it is used to represent a relative shielding. The sign convention used throughout this thesis for the relative shielding scales is defined by

$$\sigma_i \text{ vs. } R = \sigma_i - \sigma_R$$

where R is the reference. Consequently a positive value means that the nucleus is more shielded than the reference.

DOCUTAIR
BELL & FAST BIND

The difference between the shieldings of a hydrogen halide, HX, and the hydrogen bihalide ion XHY^-, will be called the complex shift, Δ_c, and is defined as

[2.3] $$\Delta_c = \sigma_{XHY^-} - \sigma_{HX}$$

The hydrogen-bond shift, Δ, is defined as

[2.4] $$\Delta = \sigma_{obs} - \sigma_{HX}$$

where σ_{obs} is the observed average shielding of a solution containing HX and XHY^-. Therefore negative values of Δ or Δ_c indicate that the shielding has decreased or, in terms of the nmr spectra, that the resonance has shifted downfield.

An absolute shielding scale referenced to the bare nucleus has been established for ^1H and ^{19}F shieldings. The ^1H shielding scale was established (68) by combining a measurement of the ratio of the electron and proton g factors for atomic hydrogen, with a measurement by Lambe (69) of the ratio of the g factor for the electron in a hydrogen atom to that of a proton in liquid water. The value for the shielding of water reported in Reference (68) was recalculated, using a subsequent, more precisely determined value of the ratio of the electron and proton g factors for atomic hydrogen (70) and the

BELL-FAST-BOND
50% COTTON

result of a recent theoretical calculation of the proton shielding in atomic hydrogen (71), to give

$$\sigma\ (H_2O,\ \text{liquid, sphere}) = 25.60 \pm 0.17\ \text{ppm.}$$

The absolute shielding of methane gas at zero pressure, determined from the relative shieldings of H_2O, C_6H_6, and CH_4 (72), is

$$\sigma\ (CH_4) = 30.55 \pm 0.17\ \text{ppm.}$$

Hindermann and Cornwell (72) have established an absolute shielding scale for fluorine based on HF in the gas at zero pressure which has a value of

$$\sigma_F\ (HF) = 410.0 \pm 6\ \text{ppm.}$$

All fluorine shieldings were measured relative to the internal reference, CF_4, in order to compare shieldings in different solutions without the necessity of correcting for the differences in the diamagnetic susceptibilities (34). The absolute fluorine shieldings of 0.1 M CF_4 in solution are presented in Table II. The shieldings of CF_4 in solution were measured relative to an external reference and converted to the absolute scale using the absolute shielding of a cylindrical sample of liquid $CFCl_3$ (72). The shieldings of CF_4 in solution relative to that of the external reference were corrected (34)

Table II. Absolute fluorine shieldings of the references at 34°C.

Reference	Relative Shieldings, ppm	$-\chi_v \times 10^6$	Absolute Shielding, ppm
$CFCl_3$ (liq, cyl.)	0	-	188.7 ± 6[a]
CF_4 in diethylether	63.42	0.534[b]	252.2
nitromethane	63.23	0.391[b]	252.6
tetramethylsilane	63.02	0.533[c]	252.9
acetonitrile	62.43	0.534[b]	252.2
trichlorofloromethane	62.43	0.638[b]	252.4
N,N-dimethylformamide	62.04	0.503[c]	251.8
propylene carbonate	61.56	-	
CF_4 gas	-	-	259.0[a]
CF_3COOH in acetonitrile (liq. cyl.) (50% by volume)	77.72	-	266.4

a. Reference 72.

b. R.C. Weast, Ed., "Handbook of Chemistry and Physics", (The Chemical Rubber Co., Cleveland, Ohio, 1968).

c. Calculated from Pascal's constants (Reference 34).

for the volume diamagnetic susceptibility, χ_v, of the solvent by adding $-2\pi\chi_v/3$ before converting to the absolute scale. The relative values of the shieldings in Table II are accurate to within 0.1 ppm.

2.4 Analysis of 1:1 Complexes

In the simplest case, the association of a proton donor HX and a proton acceptor B can be described by the equation,

$$HX + B \rightleftharpoons XHB$$

Such a system is readily studied by nmr in two limiting cases. In the case of slow exchange, separate signals will be observed for HX and XHB, and their concentrations may be evaluated independently.

In the case of rapid exchange, only a single, population-weighted average shielding will be observed. The shielding of the complex and the association constant can be calculated using the Benesi-Hildebrand-Scott (BHS) equation (73,74)

[2.5] $$\frac{[B]}{\Delta} = \frac{[B]}{\Delta_c} + \frac{1}{K\Delta_c}$$

Where K is the association constant defined by,

$$K = \frac{[XHB]}{[HX][B]} ,$$

and Δ_c and Δ are defined in Equations [2.3] and [2.4]. An iterative procedure was used since the concentration of the uncomplexed base [B] is not known. Initially the total base concentration, C_B, was used to approximate [B], and the value of Δ_c, determined from a least squares fit to Equation [2.5] can be used to arrive at a better estimate of [B], since

$$[B] = C_B - \frac{\Delta}{\Delta_c} C_H \qquad [2.6]$$

where C_H is the initial concentration of HX. These values of [B] can be used for a second BHS analysis, yielding better values of Δ_c, and so on to self-consistency.

Error estimates of Δ_c and K were determined from the least squares analysis and include the uncertainty in $[B]/\Delta$ arising from experimental errors in measuring peak positions and concentrations.

The complex shift, Δ_c, can be accurately determined for an equilibrium with a large association constant since the limiting value corresponding to the shielding of the complex can be directly observed in the presence of large excess of the proton acceptor. On the other hand, the precise determination of the association constant by

DOMTAR
BELL-FAST BOND

the BHS equation becomes more difficult for larger association constants (75,76). The association constant can also be calculated from Δ_c and the observed shift Δ, of an individual sample. The fraction of the HX complexed will be equal to Δ/Δ_c and the association constant can be calculated from

[2.7] $$K = \frac{x}{(1 - x)(C_B - xC_H)}$$

where $x = \Delta/\Delta_c$. The precision of this method is also limited since the quantity $(1 - x)$ approaches zero for large association constants.

CHAPTER 3

RESULTS OF A PROTON NMR STUDY OF BIHALIDE ION EQUILIBRIA IN SOLUTION

The results of the nmr study of the hydrogen bihalide ions XHY^-, where X, Y = Cl, Br, and I, are presented in this chapter. The object of the study was to obtain the nuclear magnetic shielding of the hydrogen bonded complex, XHY^-, and to measure the association constant in solution.

3.1 Solvents Used

The choice of solvents is governed by somewhat contradictory requirements. The solvent must dissolve adequate amounts of salt (to ca. 0.5M) but must not contain labile or strongly electrophilic hydrogens. Basic aprotic solvents are unsuitable, since they are readily protonated by strong acids such as the hydrogen halides (77). Dichloromethane, sym -tetrachloroethane, and acetonitrile were used although even these were not entirely satisfactory. Acetonitrile reacts with the hydrogen halides (77), but it was found that the reversible nature of this reaction allows the formation of most hydrogen bihalides. The halogenated solvents undergo slow halide ex-

change with the dissolved salts making it necessary to obtain the nmr spectra soon after preparation of the solutions. Where exchange was perceptible, it was possible to extrapolate back to the time of preparation of the sample and obtain reproducible results.

3.2 Homobihalide Ions

The homobihalide ions $ClHCl^-$, $BrHBr^-$, and IHI^- were studied by adding a small amount of hydrogen halide to solutions containing various amounts of the corresponding tetraalkylammonium halide salt. In all cases, only a single proton signal was observed, whose linewidth was determined by the magnetic field inhomogeneity (0.2 Hz), in all but a few concentrated viscous solutions. The occurrence of a single concentration-dependent signal indicates that a rapid exchange process is occurring and the observed shielding is a population-weighted average over all species to which the proton has access.

3.2.1 Proton Shielding

Figure 1 shows the effect on the proton shielding of 0.1M hydrogen halide, caused by the addition of tetrabutylammonium halide in sym -tetrachloroethane at ambient probe temperature (34°). The shieldings of HCl, HBr, and HI, referenced to TMS, are -0.9, 2.73, and 11.21

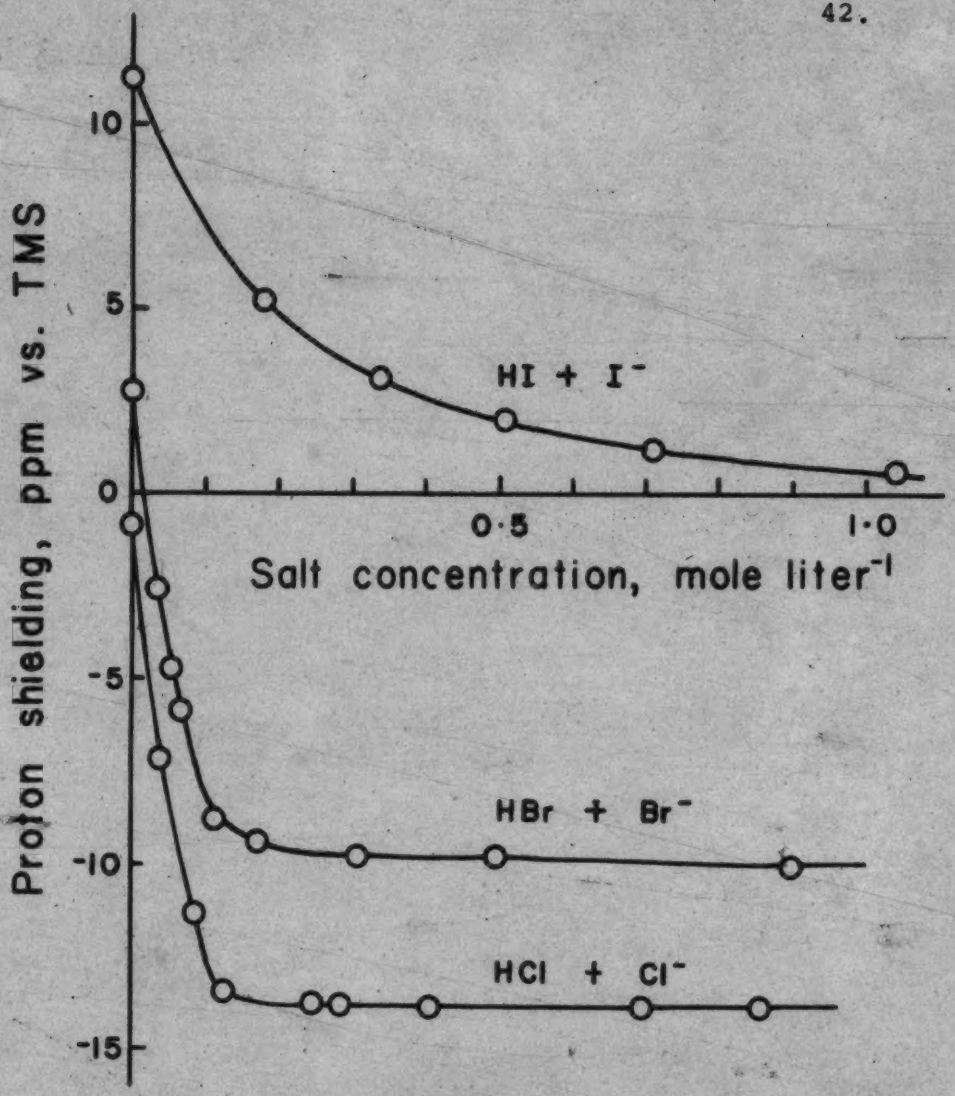

Figure 1. Dependence of the proton shielding on the tetrabutylammonium halide concentration: homobihalide systems. Hydrogen halide at 0.1M in sym-tetrachloroethane at 34°.

ppm, respectively. These observed hydrogen halide shieldings in solution are 1 to 2 ppm less than those in the gas phase (78-80). The concentration dependence of the shieldings of the hydrogen halides in solution in the range 0.05 to 0.2M was less than 0.02 ppm which indicates that there is no significant self-association.

The HCl and HBr shieldings decrease and approach limiting values near the equimolar points. Further change, in excess halide, is of the order of 0.1 ppm. This limiting value is taken to be the shielding of the 1:1 complex, XHX^-.

Table III presents the complex shifts Δ_c deduced for several concentrations C_H of the hydrogen halide. These values were determined by an iterative procedure using the BHS equation. The "mean" values were determined by fitting the combined data with different values of C_H to a single BHS plot. Points in the region where the hydrogen halide was in excess were omitted from the analysis presented in Table III, since evidence of the formation of higher complexes of the form, $X(HX)_n^-$ was observed in this region. Figure 2 shows the points at low salt concentration in the chloride and bromide systems. In each case, the observed downfield shifts exceeds that which would arise from quantitative formation of XHX^-

Table III. Complex shifts of the tetra-n-butylammonium homobihalide ions in sym-tetrachloroethane at 34°C.

Bihalide Ion	C_H moles ℓ^{-1}	Δ_c in ppm	σ (XHY^-) ppm vs. TMS
$ClHCl^-$	0.200	-13.14 ± 0.11	
	0.100	-13.01 ± 0.06	
	0.0508	-12.85 ± 0.09	
	mean	-13.01 ± 0.05	-13.91
$BrHBr^-$	0.200	-13.02 ± 0.18	
	0.100	-12.90 ± 0.08	
	0.0508	-12.83 ± 0.09	
	mean	-12.90 ± 0.05	-10.17
IHI^-	0.200	-12.16 ± 0.12	
	0.100	-12.10 ± 0.12	
	mean	-12.11 ± 0.07	-0.90

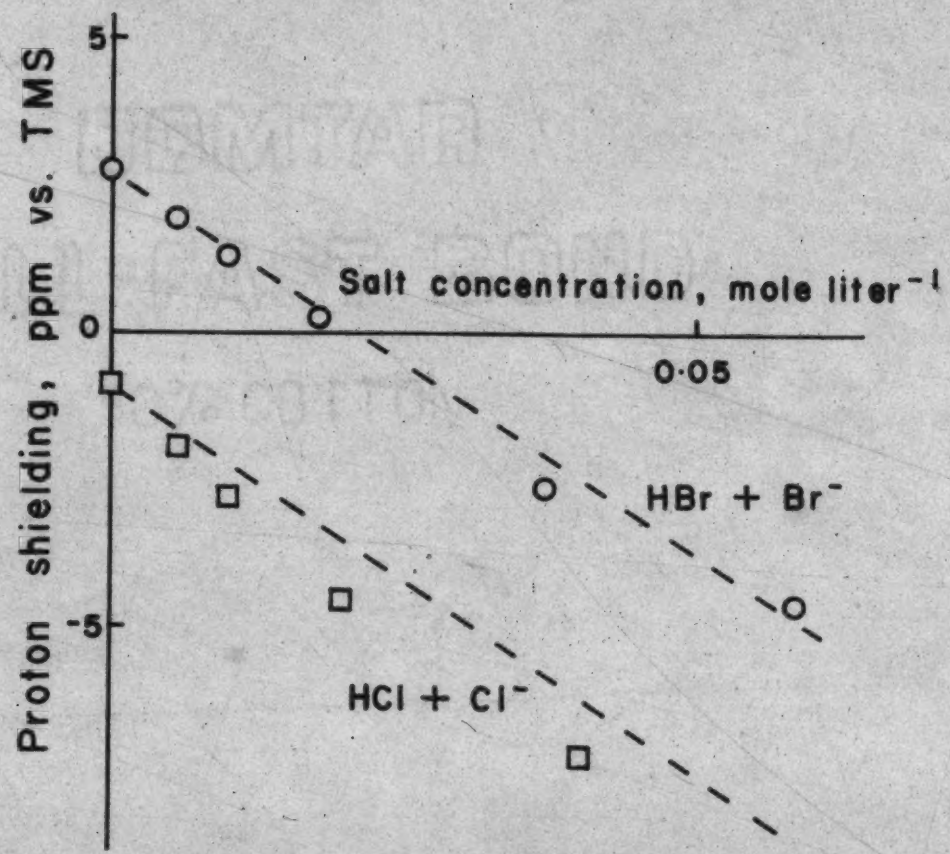

Figure 2. Proton shielding at low salt concentrations, showing shifts in excess of that computed for 1:1 ion-molecule association. Hydrogen halides at 0.1M.

(shown by the dashed line). Evidently, more than one molecule of XH is participating in complex formation per ion X^-. Multiple equilibria of this type have also been observed in the chloride (13,27) bromide (27) and iodide (27) systems, in the reaction between the solid halide salt and the hydrogen halide gas.

Samples containing 0.01M HCl and HBr were studied but the observed shieldings were not reproducible nor consistent with the other sets. In the region of excess halide, the observed downfield shifts were smaller than expected. This effect was most noticeable in the hydrogen bichloride system. The observed proton resonance tended to shift back upfield as the chloride concentration was increased, in the region of excess chloride. The observed discrepancies of 1 to 2 ppm to high field from the expected value could arise from trace amounts of water. The shielding of 0.1M H_2O was found to shift from -1.52 ppm to -2.85 ppm vs. TMS on the addition of 0.9M Bu_4NBr (81). On the basis of the trend in the proton shieldings of alcohol-halide ion complexes (49), the shielding of H_2O in the presence of Cl^- is expected to be less than -4 ppm. A water content of 0.01% in the chloride salt would be sufficient to account for the discrepancy in the 0.01M HCl solution, since the protons of

the water-halide complexes would be averaged into the observed shielding.

Solutions containing HI became discolored after an hour due to the formation of iodine. These samples were kept frozen in liquid nitrogen after preparation, until their spectra could be obtained. The spectra of these solutions were monitored over the interval from 5 to 30 minutes after the samples were removed from the liquid nitrogen. The observed change in this interval was less than 0.1 ppm to high field, and the shieldings used were obtained by graphically extrapolating back to zero time.

3.2.2 Association Constants

Table IV presents the association constants for the formation of the homobihalide ions in sym -tetrachloroethane at 34°. The values listed under Method 1 were determined from the BHS equation using the same data used to calculate the mean values of Δ_c in Table III. The values listed under Method 2 were calculated from Equation [2.7] using the observed shift Δ, of individual points near the equimolar point, and the complex shift Δ_c. The errors quoted for the values in Method 2 are standard deviations from 11 determinations in each case.

Table IV. Association constants for the formation of the tetra-n-butylammonium homobihalide ions in sym -tetrachloroethane at 34°

Bihalide	K, ℓ mole^{-1}	
	Method 1	Method 2
$ClHCl^-$	ca. 600	660 ± 105
$BrHBr^-$	220 ± 62	240 ± 44
IHI^-	7.41 ± 0.23	-

3.2.3 Solvent Dependence

Table V compares shieldings in acetonitrile and dichloromethane with those observed in tetrachloroethane.

Acetonitrile reacts with the hydrogen halides (with the exception of HF) to form compounds with the stoichiometry, $CH_3CN \cdot 2HX$, which can be isolated as solids (82). Infrared studies (82,83) and a neutron diffraction study of the HCl adduct (84), have shown that these compounds are acetohalogenimidium halides of the form,

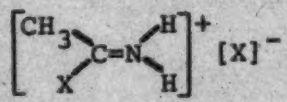

A white precipitate was observed in acetonitrile solutions of the hydrogen halides when the sample was thawed after preparation. This solid readily dissolved on warming. The nmr spectrum of the HCl solution showed a signal at -4.0 ppm, but in the HBr and HI solutions no proton signal attributable to the N-H proton could be observed. This presumably is a consequence of a slow proton exchange mechanism which broadens the signal. However, on the addition of Cl^- or Br^- to the HCl and HBr solutions, sharp peaks were observed at low field which became independent of the salt concentration at high salt concentrations. These limiting values are reported as

Table V. Solvent dependence of the proton shieldings of tetrabutylammonium bihalides in ppm at 34°C.

System	in $CHCl_2CHCl_2$	in CH_2Cl_2	in CH_3CN
Δ_c of $ClHCl^-$	-13.01 ± .05	-13.22 ± .13	-
σ of HCl, vs. TMS	-0.90	-1.03	-
σ of $ClHCl^-$, vs. TMS	-13.91	-14.25	-14.2
Δ_c of $BrHBr^-$	-12.90 ± .05	-13.25 ± .09	-
σ of HBr, vs. TMS	+2.73	+2.67	-
σ of $BrHBr^-$, vs. TMS	-10.17	-10.58	-10.9
Δ_c of IHI^-	-12.11 ± .07	-	-
σ of HI, vs. TMS	+11.21	-	-
σ of IHI^-, vs. TMS	-0.90	-	-

$ClHCl^-$ and $BrHBr^-$ shieldings in Table V.

No peak which could be assigned to IHI^- was observed when excess I^- was added to the HI solutions in acetonitrile. The HI-acetonitrile complex appears to be more stable than the biiodide ion.

The values in Table V indicate that the shieldings of the bihalide ions show a small solvent dependence. The observed variation between solvents is of the order of a few tenths of a part per million, which is comparable to the solvent dependence of nonlabile protons (85).

The association constants in dichloromethane for the bichloride and bibromide ions were similar to those in sym -tetrachloroethane. The association constants in acetonitrile could not be determined because of the reaction of the hydrogen halides with this solvent.

3.2.4 Cation Dependence

The tetraethylammonium bichloride, the tetra-n-pentylammonium bichloride, and the tetra-n-heptylammonium bibromide were studied to determine the effect of changing the counterion. In all cases, the complex shift and the association constant agreed, to within experimental error, with the values obtained for the corresponding tetrabutylammonium bihalides.

3.2.5 Temperature Dependence

The complex shifts of the homobihalide ions were measured at various temperatures using the same procedure employed to obtain the values reported at 34°C. These values are presented in Table VI. The complex shifts were found to be independent of temperature, to within ±0.1 ppm, and the shieldings of the homobihalide ions showed a very small temperature dependence which paralleled the changes in the shielding of the parent hydrogen halides.

The attempts to measure the changes in enthalpy for the formation of the bihalide ions in solution from a study of the temperature dependence of the association constants were not very successful. The association constant for the bichloride ion was too large to be measured accurately, and the biiodide solutions were not extensively studied because a new set of samples had to be prepared for each temperature. An enthalpy change of -3.3 ± 0.3 kcal $mole^{-1}$ was obtained for the formation of the bibromide ion in tetrachloroethane from measurements in the range -40 to 34°C. This value is much smaller in magnitude than those observed for the formation of the bibromide ion from isolated constituents (see 1.1.2). In solution, the observed enthalpy change contains an endothermic contribution due to the difference of solvation energies between the reactants and the product (28).

Table VI. Temperature dependence of shieldings (in ppm) of the tetrabutylammonium bihalide ions.

Bihalide	Temperature °C	σ_{HX}	Δ_c	σ_{XHX^-}
$ClHCl^-$ [a]	26	-1.06	-13.3 [b]	-14.4
	8	-1.12	-13.4	-14.5
	-10	-1.21	-13.4	-14.6
	-29	-1.29	-13.4	-14.7
	-47	-1.36	-13.4	-14.8
	-66	-1.45	-13.4	-14.8
	-80	-1.51	-13.4	-14.9
$BrHBr^-$ [a]	26	2.65	-13.1 [b]	-10.5
	8	2.58	-13.1	-10.5
	-10	2.50	-13.1	-10.6
	-29	2.43	-13.1	-10.7
	-47	2.34	-13.1	-10.8
	-66	2.25	-13.1	-10.8
	-80	2.19	-13.1	-10.9
IHI^- [c]	34	11.21	-12.1 [b]	-0.9
	0	11.06	-12.0	-1.0

a. in dichloromethane

b. ±0.1

c. in tetrachloroethane

3.3 Heterobihalide Ions

Figure 3 shows the dependence of the proton shielding of HCl on the addition of Br^-, and of HBr on the addition of Cl^- in sym -tetrachloroethane at 34°. The behavior of the corresponding chloride-iodide and bromide-iodide systems are shown in Figures 4 and 5. The same type of behavior was observed in dichloromethane and in acetonitrile solutions.

3.3.1 Identification of the Species in Solution

These six systems show two distinct types of behavior. The proton shieldings of the following solutions,

$$HBr + Cl^-$$

$$HI + Cl^-$$

$$HI + Br^-$$

exhibit exceptionally large downfield shifts and do not reach a limiting value until more than a two fold excess of halide ion has been added. The limiting values of the proton shieldings in these solutions clearly indicate that the bichloride ion is formed, when an excess of Cl^- is added to HBr or HI. Similarly, the bibromide ion is formed on the addition of excess Br^- to HI. The infrared spectra of these solutions unambiguously confirms the presence of the homobihalide ion in the region of excess halide. Figure 6 shows the ir spectrum of a solution

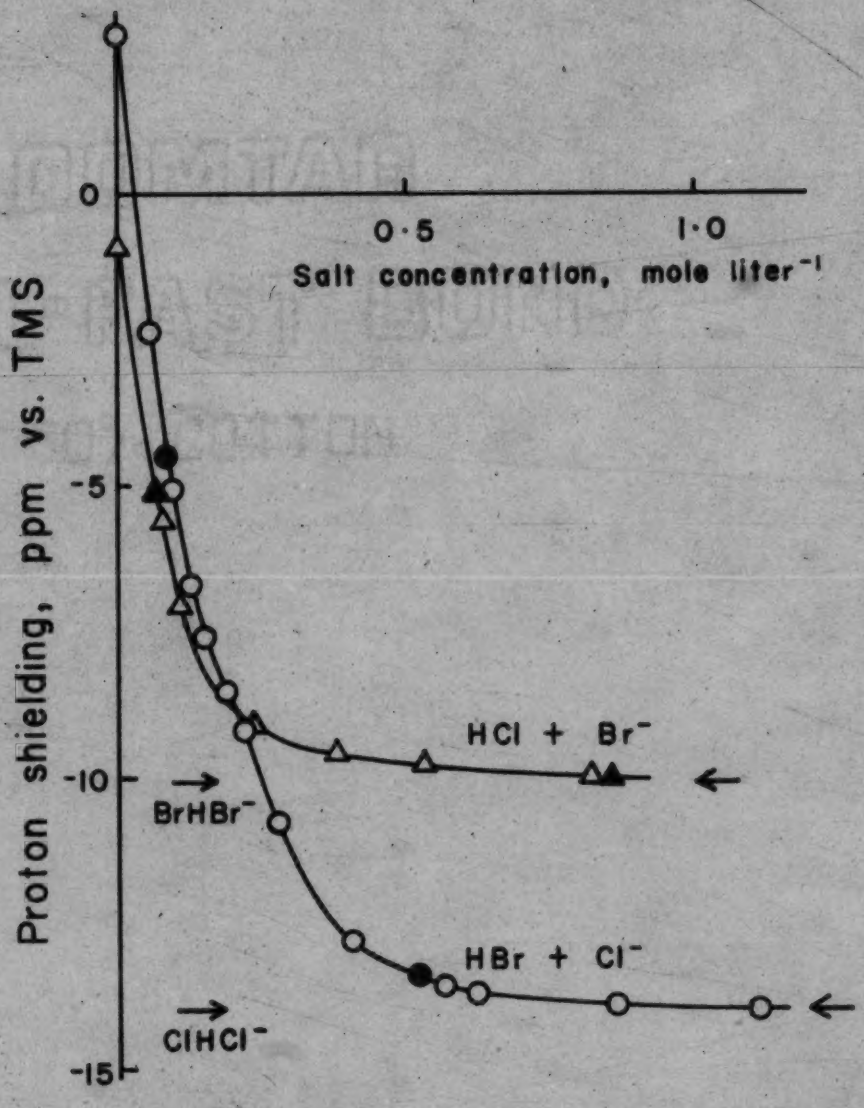

Figure 3. Proton shieldings in solutions containing 0.2M HCl and Bu_4NBr, and 0.2M HBr and Bu_4NCl in sym-tetrachloroethane at 34°.

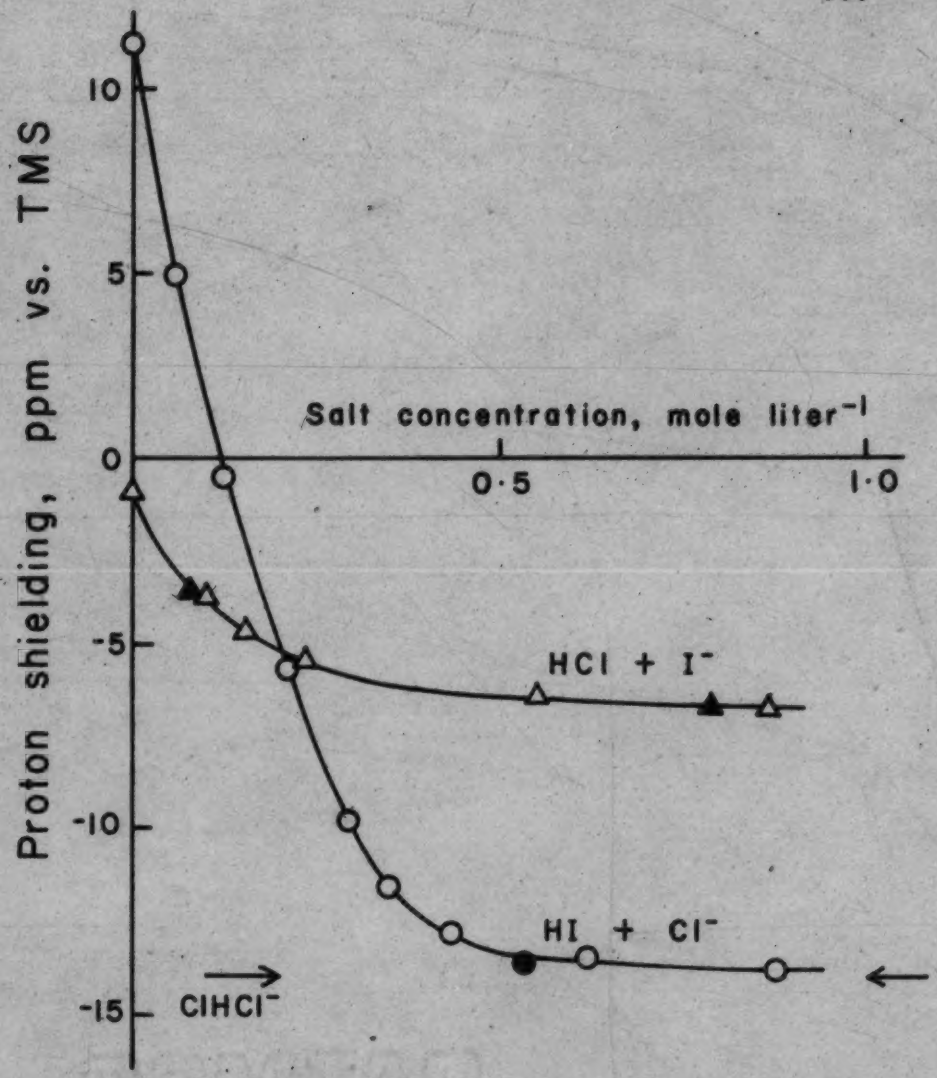

Figure 4. Proton shieldings in solutions containing 0.2M HCl and Bu_4NI, and 0.2M HI and Bu_4NCl in sym-tetrachloroethane at 34°.

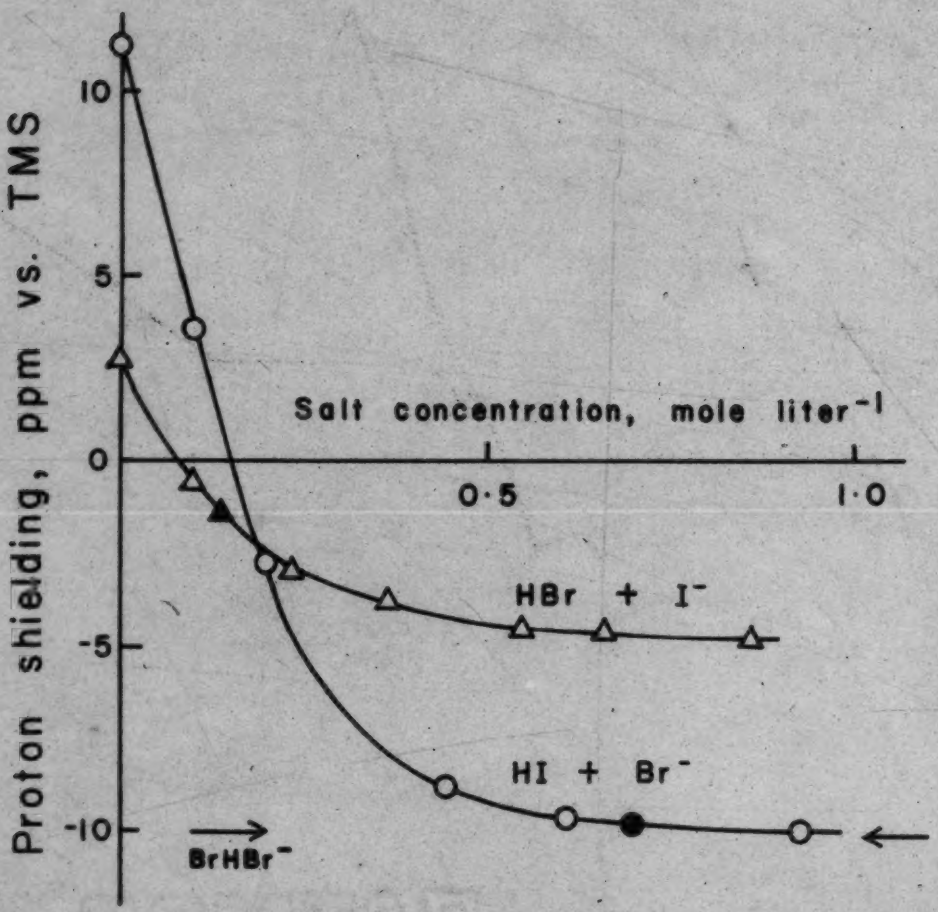

Figure 5. Proton shieldings in solutions containing 0.2M HBr and Bu_4NI, and 0.2M HI and Bu_4NBr in sym-tetrachloroethane at 34°.

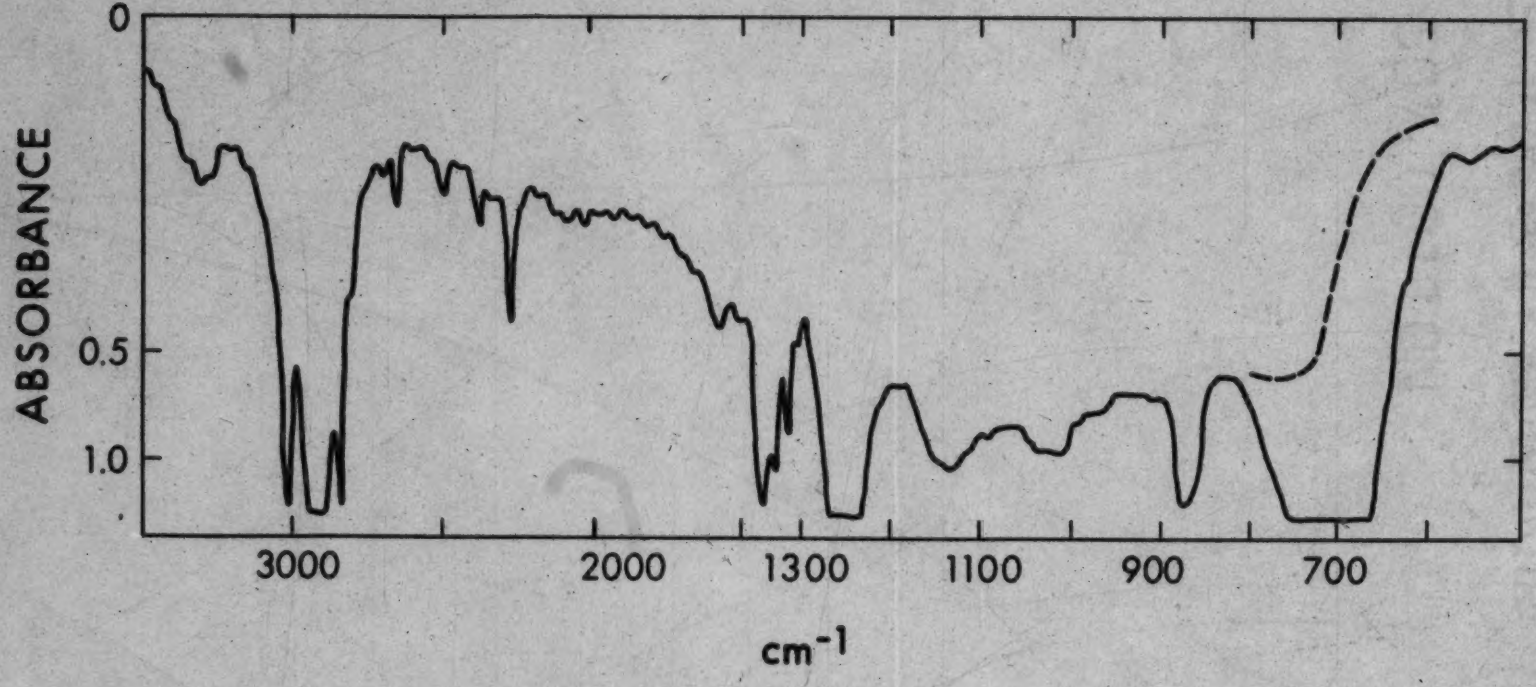

Figure 6. Infrared spectrum of a solution containing HBr and Bu_4NCl in dicholoromethane; $[HBr]:[Cl^-]=1:2.7$. The dashed line represents the absorbance observed for a corresponding acetonitrile solution.

containing HBr and an excess of Bu_4NCl. This spectrum was indistinguishable from the solution spectrum of $ClHCl^-$. The spectrum of $ClHCl^-$ was in good agreement with the spectrum previously published (13).

The halide ion added in these three solutions is a stronger base than the conjugate base of the acid. A proton transfer to the stronger base and the subsequent reaction of the hydrogen halide formed in this process would result in the formation of the homobihalide ion. The occurrence of the proton transfer step was confirmed by examining the gas phase over these solutions by infrared spectroscopy. Solutions containing 0.2M hydrogen halide, and halide ion concentrations ranging from 0.1 to 0.4M, gave the following results:

over $HBr + Cl^-$: HCl gas

over $HI + Cl^-$: HCl gas

over $HI + Br^-$: HBr gas

This proton exchange process has also been reported for the reaction between the hydrogen halide gas and the alkali metal halide crystal (86).

Solutions containing HX ($X \neq F$) and F^- were not studied because a dry soluble fluoride salt could not be prepared. These solutions are expected to result in the formation of the homobihalide ion FHF^- in every case,

when the F^- is in excess. The formation of FHF^- has been observed when any hydrogen halide was condensed onto an alkali metal fluoride surface (86,87).

The concentration dependence of the proton shieldings in the other three systems is consistent with the formation of the heterobihalide ions by the following equilibria:

[3.1] $$HCl + Br^- \rightleftharpoons ClHBr^-$$

[3.2] $$HCl + I^- \rightleftharpoons ClHI^-$$

[3.3] $$HBr + I^- \rightleftharpoons BrHI^-$$

The limiting shielding observed in solutions containing HCl and Br^- however, was identical to the shielding of $BrHBr^-$. Therefore, it may be possible that the following process may be occurring:

[3.4] $$HCl + Br^- \text{ (excess)} \longrightarrow BrHBr^- + Cl^-$$

In order to identify the species present, ir spectra of solutions prepared from HCl and Br^- were measured in the region 4000 to 500 cm^{-1}. Solutions in dichloromethane and in acetonitrile were studied since the absorption peaks of tetrachloroethane obscured the areas of interest. The spectra of solutions containing HCl and Br^-

or HBr and Br^- in dichloromethane are shown in Figure 7. These spectra were obtained using an empty reference cell; consequently the absorption peaks of the solvent are also present. The vertical arrows indicate the broad absorption peaks arising from the bihalide ions. The dashed line estimates the absorbance due to the bihalide ion in the region obscured by this solvent. The absorbances in the region below 900 cm^{-1} were estimated from the acetonitrile solutions which were not obscured by strong solvent absorption in this region. These spectra compare very well with the solution spectra of $ClHBr^-$ and $BrHBr^-$ previously reported (22, 89).

The absorption peaks of the bihalide ions are very broad, but the ir spectra of $ClHBr^-$ can be readily distinguished from that of $BrHBr^-$. The absence of the strong absorption of $BrHBr^-$ in the region from 700 to 1050 cm^{-1} in the spectra of the solutions containing HCl and Br^- is quite evident. However, small amounts of $BrHBr^-$ would be difficult to detect since its very broad absorption peaks could be masked by the cation and solvent absorptions. The lack of a change in the general features of the $ClHBr^-$ spectra in Figure 7 (a) and (b) as the ratio of the concentrations of $HCl:Br^-$ is changed from 1:1 to 1:3, also indicates that very little $BrHBr^-$ is being formed.

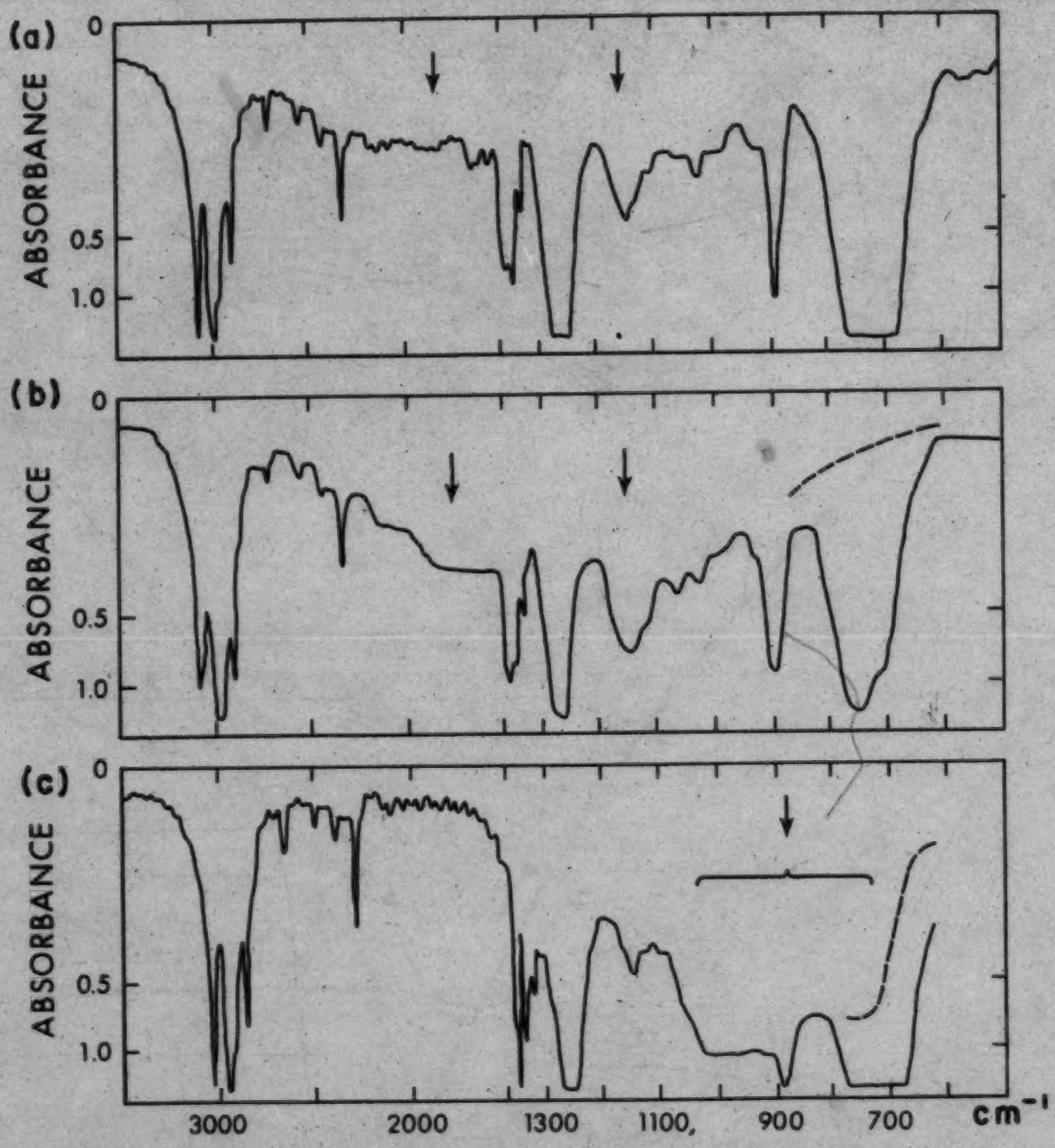

Figure 7. Infrared spectra of solutions containing HCl or HBr, and Bu_4NBr in dichloromethane.
(a) $[HCl]:[Br^-]=1:1$, (b) $[HCl]:[Br^-]=1:2.8$, (c) $[HBr]:[Br^-]=1:1$. The dashed lines represent the absorbances observed for corresponding acetonitrile solutions. Arrows indicate bihalide ion absorptions.

Furthermore, in the gas phase over solutions containing HCl and Br^-, no HBr, whose presence would support the postulate of Equation [3.4], was observed in the ir spectrum. Thus, the ir data show that large amounts of $BrHBr^-$ are not formed in solutions containing HCl and Br^-. The nmr data show that the observed shieldings in the region of excess Br^- becomes almost independent of the Br^- concentration. Although this evidence does not exclude the presence of significant amounts of $BrHBr^-$, it can be concluded that the proton shielding in $ClHBr^-$ must be very similar to the shielding in $BrHBr^-$.

The spectrum of a solution containing HCl and Bu_4NI contained a very broad, strong absorption band centered at 2100 cm^{-1} which agrees with the value of 2025 cm^{-1} reported for Bu_4NClHI in the crystal (89). A second weaker band reported at 990 cm^{-1} was not observed.

No peaks, which could be assigned with any confidence to $BrHI^-$, were observed in the ir spectrum of solutions containing HBr and Bu_4NI. The ir spectrum of $BrHI^-$ has not been reported.

3.3.2 Analysis of 1:1 Complexes

Table VII presents the complex shifts and association constants deduced from the BHS equation assuming

Table VII. Complex shift and association constants for the heterobihalide ions assuming 1:1 complex formation in sym -tetrachloroethane at 34°C.

Complex*	C_H moles ℓ^{-1}	K, ℓ mole^{-1}	$\Delta_{C'}$ ppm	σ, ppm vs TMS
$ClHBr^-$	0.200	97 ± 47	-9.26 ± .13	
	0.100	114 ± 49	-9.24 ± .08	
	mean	107 ± 28	-9.25 ± .06	-10.15
$ClHI^-$	0.200	24 ± 6	-6.28 ± .10	
	0.100	20 ± 4	-6.25 ± .09	
	0.0508	20 ± 4	-6.19 ± .09	
	mean	21 ± 3	-6.23 ± .06	-7.13
$BrHI^-$	0.200	27 ± 4	-7.99 ± .08	
	0.100	25 ± 3	-7.92 ± .05	
	0.0508	25 ± 2	-7.67 ± .04	
	mean	27 ± 4	-7.80 ± .06	-5.07

*tetra-n-butylammonium cation.

1:1 complex formation as described by Equations [3.1] to [3.3]. Data for solutions containing an excess of hydrogen halide were not used in the analysis since complexes of the form $Y^-(HX)_n$, where n is greater than one, may have been present.

The association constants and complex shifts in Table VII are reasonably independent of the hydrogen halide concentration which is consistent with the formation of 1:1 complexes.

3.3.3 Solutions Involving Proton Transfer Reactions

In Figures 3 to 4, solutions containing equimolar amounts of HX and Y^-, or HY and X^- have the same average shielding. The infrared spectra of these solutions were indistinguishable which indicates that the composition of these two solutions are identical. This indicates that these solutions are in thermodynamic equilibrium with respect to proton transfer. As a further check, several samples were made up which duplicated previous runs in over-all halide and proton concentrations. To duplicate a solution with C_H molar HX and C_S molar Y^-, a solution would be made up containing HX, HY, X^-, and Y^- such that

$$[HX] + [HY] = C_H$$
$$[HX] + [X^-] = C_H$$
$$[HY] + [Y^-] = C_S$$

These solutions gave the filled points in Figures 3 to 5. The excellent agreement between these solutions implies that complete and rapid equilibration of the proton transfer reactions takes place.

The equilibria involved in these solutions will be considered using the $HBr\text{-}Cl^-$ system as an example. The proton transfer process could be described as

[3.5] $$HBr + Cl^- \rightleftharpoons ClHBr^- \rightleftharpoons HCl + Br^-$$

or more simply as

[3.6] $$HBr + Cl^- \rightleftharpoons HCl + Br^-$$

Since the equilibrium constant for Equation [3.6] in solution is expected to be very large, the proton transfer can be considered to be quantitative. This has been found to be the case in the totally gas-phase reaction and in the reaction between the hydrogen halide in the gas and the solid halide salt. The forward reaction in Equation [3.6] was observed in the gas phase using ion cyclotron double resonance, while the reverse reaction could not be detected (90). The solid $Bu_4NClHBr$ salt was found to decompose

into HCl and Br^- on heating (89). Mass spectral studies of the vapour phase over solid NaCl at 190°K in contact with HBr showed that after the admission of HBr, gaseous HCl was present and only a trace of HBr remained after a 30 second exposure to the surface (86).

The composition of solutions which result from a quantitative proton transfer from HBr to Cl^- will depend on the relative amounts of these two components initially added to the solution.

When the number of moles of Cl^- added are less than the number of moles of HBr added, all the Cl^- will be converted to HCl and the following equilibria will be established:

$$HCl + Br^- \rightleftharpoons ClHBr^-$$

$$HBr + Br^- \rightleftharpoons BrHBr^-.$$

When equimolar amounts of HBr and Cl^- are added, all the HBr and Cl^- will be converted into HCl and Br^- and the solution can be described by the single equilibrium,

$$HCl + Br^- \rightleftharpoons ClHBr^-.$$

When an excess of Cl^- is added, the solution will contain no HBr and the solution can be described by the equilibria,

$$HCl + Cl^- \rightleftharpoons ClHCl^-$$
$$HCl + Br^- \rightleftharpoons ClHBr^-.$$

When a large excess of Cl^- is added, the predominant bihalide species will be $ClHCl^-$ since the association constant for its formation is larger than that for the formation of $ClHBr^-$. Also the Cl^- concentration will be larger than the Br^- concentration which is limited by the amount of HBr initially added.

If a quantitative proton transfer reaction is assumed, the equilibrium concentrations of all species can be calculated since the association constants for all the equilibria assumed to be present are known. Since the shieldings of all of these species are also known, the average shielding can be calculated. Figure 8 shows the concentrations of the proton containing species calculated for solutions containing Bu_4NCl and an initial concentration of 0.1M HBr in tetrachloroethane. A comparison between the observed shieldings and the calculated values (solid line) is also shown in Figure 8. The corresponding comparisons for solutions containing HI and Cl^- or Br^- are shown in Figure 9. The details of these calculations are presented in the Appendix.

The agreement between the calculated and observed

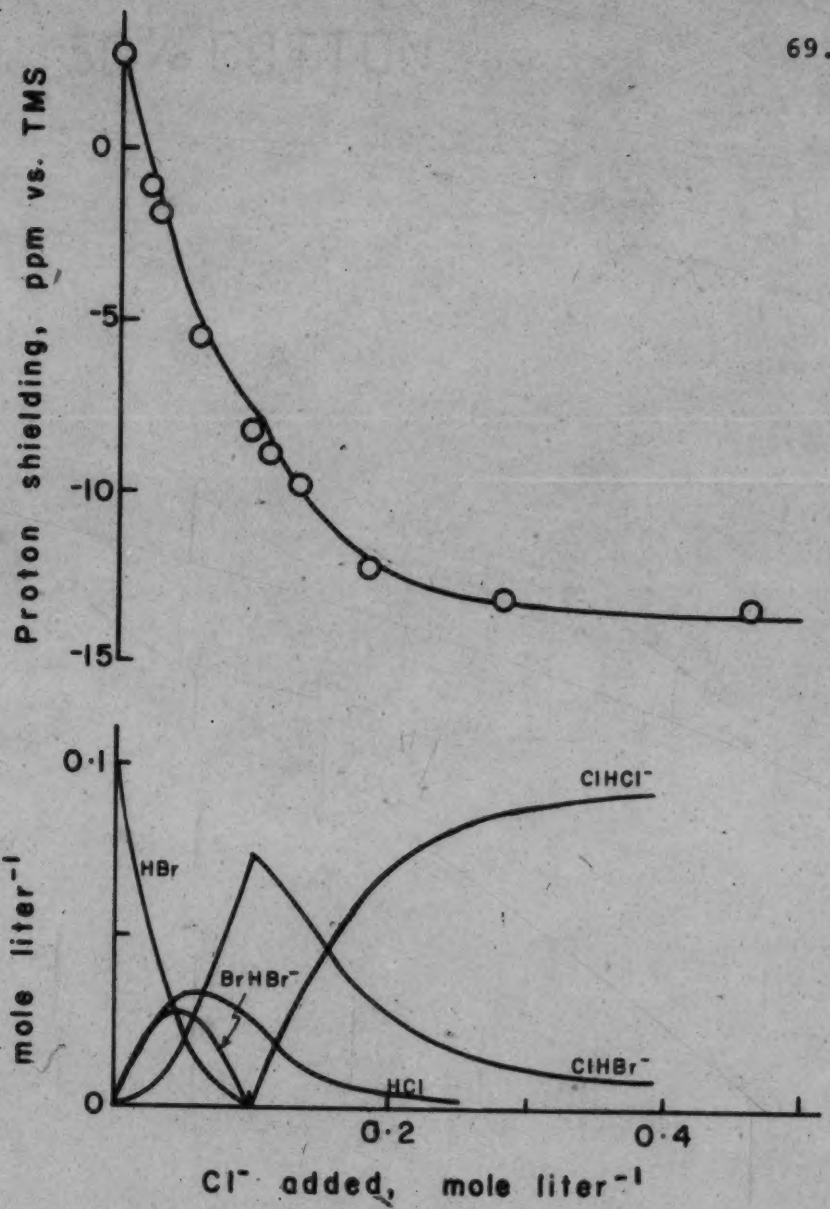

Figure 8. Comparison of the observed shieldings in solutions containing 0.1M HBr and Bu_4NCl with the calculated values (solid line). The bottom figure shows the calculated concentrations of the proton containing species.

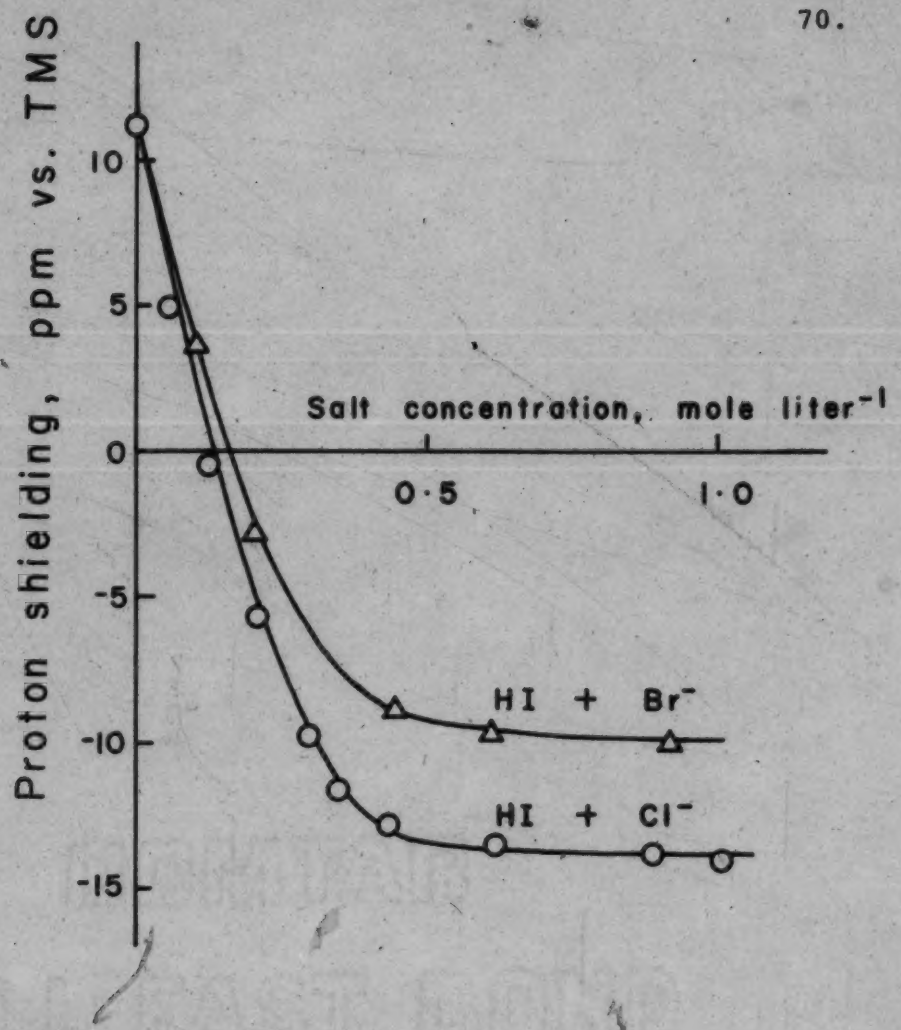

Figure 9. Comparison of the observed shieldings in solutions containing 0.2M HI, and Bu_4NCl or Bu_4NBr, with the calculated values (solid line).

shieldings is satisfactory. The largest discrepancies occur at low salt concentrations and are probably due to the neglect of complexes of the form $X^-(HY)_n$.

3.4 Summary

The postulated 1:1 association of HX and X^- appears to be adequate to describe the shielding in solution when the halide ion is in excess. The deduced bihalide ion shieldings are fairly insensitive to the temperature, the nature of the tetraalkylammonium cation, and the solvent.

The heterobihalide ion XHY^- appears to be formed when an excess of the halide ion Y^- is added to the hydrogen halide HX, where Y has a larger atomic number than X. The requirement that Y has a larger atomic number is consistent with a weaker base strength of Y^- compared to X^-. When the halide ion added to a solution is a stronger base than the conjugate base of the hydrogen halide present, the proton is transferred from the hydrogen halide to the halide ions. The nmr and ir spectra of these solutions could be adequately described by assuming that the species present in solution are formed from the products of a quantitative proton transfer reaction.

The shieldings in the homobihalide ions are

remarkable in two respects. The downfield shifts of 13 ppm are exceptionally large and are about the same in all three bihalide ions.

Some trends in the complex shifts and the association constants are evident. For a given hydrogen halide, the magnitudes of the complex shifts and the association constants increase as the halide ion becomes smaller. There is a good linear correlation between Δ_c and log K for the bihalide ions containing HCl.

The magnitudes of Δ_c for the hydrogen halides complexed to a given halide ion vary in the order HI > HBr > HCl. There is no consistent trend apparent in the association constants for the hydrogen halides complexed to a given halide ion.

There has been a nmr study of the hydrogen bihalide ions containing HCl recently reported (91). The shieldings reported for the bihalide ions $ClHCl^-$, $ClHBr^-$, and $ClHI^-$ in sulfolane were -15.9 ± 0.3, -11.7 ± 0.4, and -9.7 ± 0.5 ppm versus TMS, respectively. These shieldings are ca. 2 ppm further downfield than the corresponding values reported here. These discrepancies are probably too large to be the result of solvent effects. The procedure employed to study the bihalide ions in sulfolane was similar to the procedure used here, except that larger concentrations of HCl were used (0.2 to 0.46M) and

the shielding in the region of excess halide was not studied. The shieldings reported for the bihalide ions in sulfolane may not be as reliable since corrections had to be made for the presence of water which was found at concentrations from 0.02 to 0.025M. At these concentrations the exchangeable water protons amounted to 10 to 20% of the HCl concentration.

CHAPTER 4

RESULTS OF THE NMR STUDY OF HYDROGEN FLUORIDE COMPLEXES

This chapter presents the nmr study of the hydrogen-bonded complexes of hydrogen fluoride. The hydrogen bihalide ions of the form, FHX^-, where X=F, Cl, Br, and I were studied as well as solutions of HF in several aprotic solvents. In these complexes of HF, the effect of hydrogen bonding on the ^{19}F shielding and on the H-F nuclear spin-spin coupling constant can be observed in addition to the change in the ^{1}H shielding.

4.1 Bifluoride Ion

Solutions of the bifluoride ion were prepared directly from the tetraalkylammonium bifluoride salt. Figures 10 and 11 show the proton and fluorine spectra of the bifluoride ion of the tetraethylammonium salt dissolved in acetonitrile. The identical separation, in Hz, of the peaks in the triplet and doublet in the ^{1}H and ^{19}F spectra indicate that a H-F spin-spin coupling of a proton with two equivalent fluorines is being observed. This is consistent with the previously established centrosymmetric structure of this ion (2).

The H-F coupling was not observed in a previous nmr study of the bifluoride ion in an aprotic solvent (51),

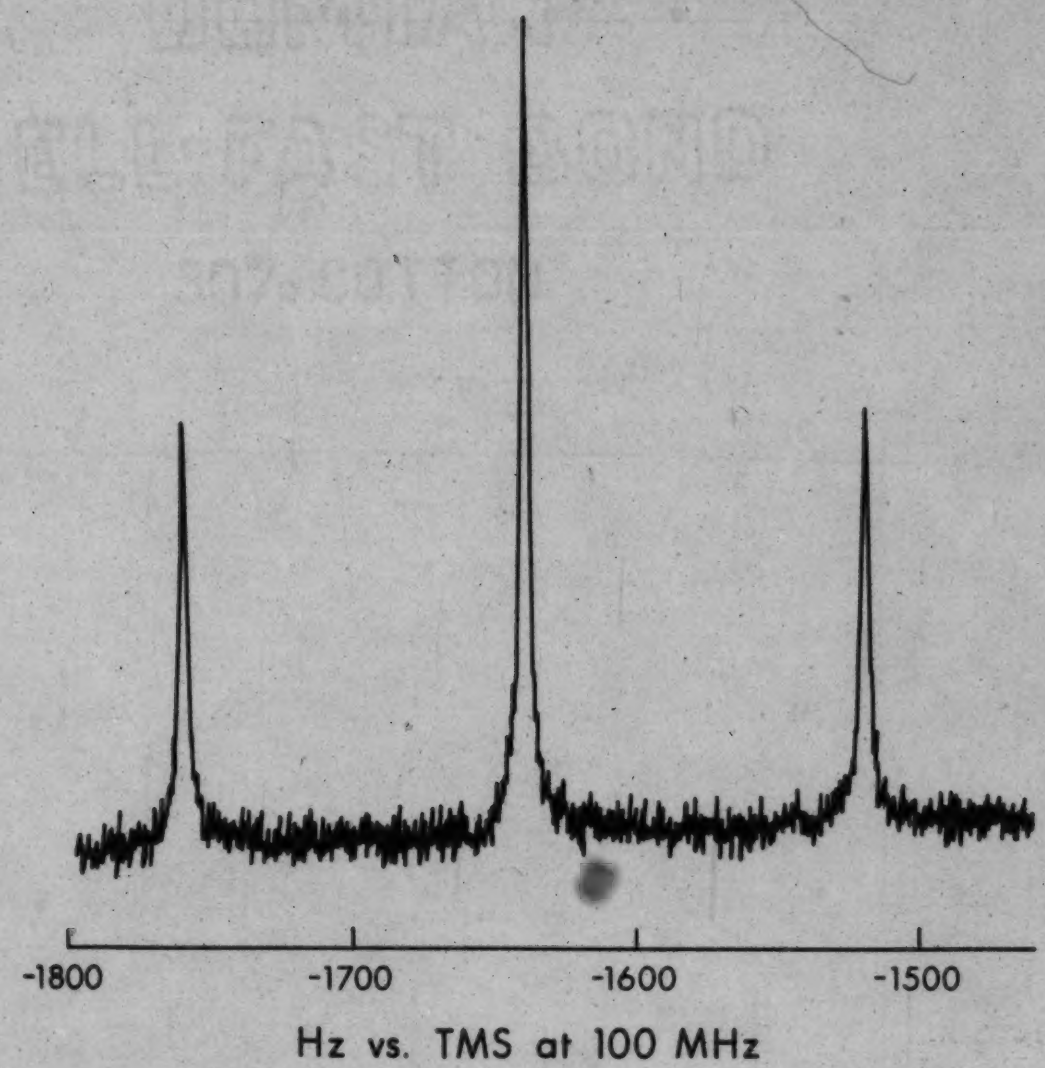

Figure 10. ^{1}H nmr spectrum of bifluoride ion of the tetraethylammonium salt in acetonitrile at -30°.

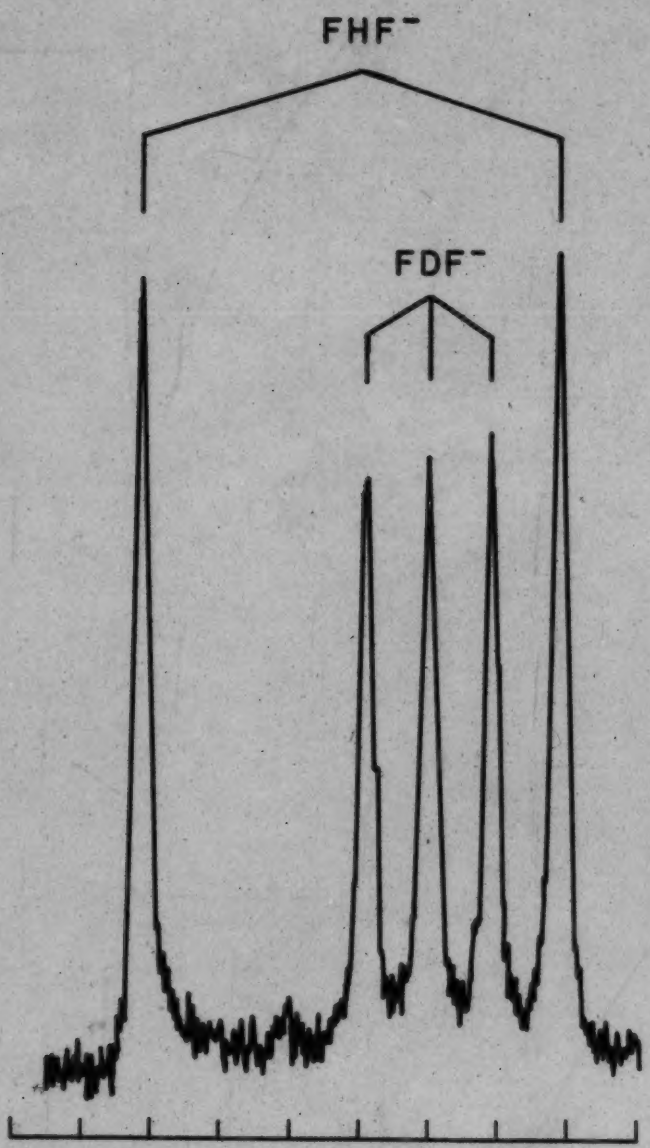

Figure 11. ^{19}F nmr spectrum of FHF^- and FDF^- ions of the tetraethylammonium salts in acetonitrile at -10°. The scale is marked in intervals of 20 Hz.

or in the study of HF dissolved in aprotic solvents (52). The only previous H-F coupling observed by nmr was in liquid HF at very low temperatures (61). The surprising lack of exchange averaging of the coupling constant observed in this study can be attributed to the lack of sufficient amounts of impurities which catalyze proton transfer reactions (36), and to the large association constant for the equilibrium,

[4.1] $$HF + F^- \rightleftharpoons FHF^-$$

A large association constant implies that the rate constant for the dissociation of FHF^- is relatively small compared to the rate constant for its formation. Consequently, the average lifetime of the FHF^- ion is long enough to allow observation of the H-F coupling in the nmr spectra. The lifetime of FHF^- can be estimated from the line broadening due to exchange. At 34°, the width at half-height of the absorption peaks of FHF^- in acetonitrile was about 5 Hz, which would correspond to a lifetime of $(5\pi)^{-1}$ sec. or 64 msec., if the contribution from the natural linewidth in the absence of exchange is neglected.

4.1.1 Nuclear Shieldings and Coupling Constant

The ^{1}H and ^{19}F nuclear shieldings and the coupling constant J(HF), for the bifluoride ion are given in Table VIII. The solvents used were acetonitrile (AN), N,N-dimethylformamide (DMF), and nitromethane (NM). The proton and fluorine shieldings are referenced to internal TMS and CF_4 respectively, and positive shieldings indicate that the nuclei are more shielded than the reference.

The H-F coupling was observed in the spectra of acetonitrile and DMF solutions at temperatures below 60°, but in nitromethane, the coupling was not observed until the sample was cooled down to 0°. In acetonitrile, the linewidths at half-height were about 5 Hz at 34° and sharpened to 1 Hz on cooling to -30°. The linewidths in DMF solutions were slightly larger than in acetonitrile, and in nitromethane, the sharpest lines observed were about 5 Hz at half-height. In the chlorinated solvents, carbon tetrachloride and sym -tetrachloroethane, only a single very broad peak was observed which could not be resolved on cooling.

In the concentration range studied (from 0.05 to 0.5M), only small changes in the shieldings were observed, about 0.02 ppm for the proton and 0.2 ppm for the fluorine shieldings. There was no concentration

dependence observed for the coupling constant. Corresponding solutions containing tetrabutylammonium bifluoride were also studied and there were no observable changes in the bifluoride spectra. Therefore the bifluoride spectra may be regarded as substantially invariant to the concentration and the cation.

There has been a nmr study of the bifluoride salts of primary, secondary, tertiary, and quaternary butylammonium salts previously reported (51). The spectra were obtained from the molten salts at 30° and the proton signal of FHF^- was a broad singlet appearing at -12.03 to -12.13 ppm vs. TMS. Only $Bu_2NH_2HF_2$ was studied in $CDCl_3$ solution and the proton signal of FHF^- was reported at -12.67 ppm vs. TMS. The ^{19}F shieldings reported ranged from 150.4 to 167.9 ppm vs. $CFCl_3$, for the series from the primary to the quaternary ammonium bifluoride salts. These fluorine shieldings converted to CF_4 (internal) as a reference range from 89 to 105 ppm. Since the results for Bu_4NFHF were only reported for the molten salt, a direct comparison with the results reported here is uncertain. However the ^1H shieldings appear to be insensitive to the cation for this series and the discrepancy between the proton shielding of FHF^- in chloroform and those reported here is too large to be attributed to solvent effects.

Table VIII. Nuclear shieldings and coupling constant in tetraethylammonium bifluoride at infinite dilution.

Solvent	T, °C	σ_H, ppm vs. TMS	σ_F, ppm vs. CF_4	J(HF), Hz
AN	34	-16.29 ± 0.01	86.09 ± 0.03	120.5 ± 1.0
	-30	-16.37 ± 0.01	83.35 ± 0.03	120.5 ± 0.1
DMF	34	-16.63 ± 0.01	86.30 ± 0.05	120 ± 2
	-40	-16.77 ± 0.01	82.70 ± 0.05	118.8 ± 0.1
NM	34	-15.87 ± 0.03	90.9 ± 0.1	-
	-30	-16.27 ± 0.03	87.4 ± 0.1	120.5 ± 0.2

AN, acetonitrile

DMF, N,N-dimethylformamide

NM, nitromethane

This discrepancy of 4 ppm could result from the presence of impurities with exchangeable protons which are more shielded than the proton in FHF^-. Rapid exchange processes among these protons would shift the observed ^1H resonance to high field.

The fluorine shielding of FHF^- in water has also been determined (50). The concentrations of F^-, HF, and FHF^- were calculated from the known equilibrium constants for the formation of FHF^- and for the acid dissociation of HF in water. From the observed fluorine shieldings of solutions containing various amounts of these species, the shielding of FHF^- relative to F^- was found to be 33 ± 1 ppm. This value is equivalent to 89 ppm vs. CF_4 (internal), which is in excellent agreement with the values reported here for the aprotic solutions.

4.1.2 Temperature Dependence

The multiplets arising from the H-F coupling in FHF^- were observed to broaden on heating and coalesced at 70°. However, on cooling, the linewidths were significantly broader. Presumably HF attacks the solvent at high temperatures and produces impurities which catalyze proton exchange reactions. A similar behavior was observed for FHF^- in DMF solutions. A more extensive investigation

of the exchange processes, which gives rise to the collapse of the coupling constant, could not be carried out since the line shapes were not reproducible.

The temperature dependences of the ^{1}H and ^{19}F shieldings with respect to TMS and CF_4, respectively, were linear in the temperature range -40 to 34°. These temperature dependences are given in Table IX. No temperature dependence of the H-F coupling constant was observed within the uncertainty in measuring the peak positions.

4.1.3 Deuterium Bifluoride Ion

The deuterium isotope effect on the fluorine shielding was determined from solutions containing a mixture of FHF^- and FDF^- in acetonitrile. The fluorine spectrum of the tetraethylammonium salts is shown in Figure 11. The deuterium isotope shift, defined as $\sigma_{FDF^-} - \sigma_{FHF^-}$ is +0.40 ± 0.02 ppm. This isotope effect was found to be independent of the concentration and temperature. The isotope effect in the bifluoride ion is much smaller than the corresponding deuterium isotope shift in hydrogen fluoride which is 1.64ppm in the liquid (45) and 2.5 ppm in the gas phase (44).

A D-F coupling constant of 18.1 ± 0.3 Hz was observed for FDF^- in acetonitrile at -30°. This value of

Table IX. Temperature dependence of the shieldings in the bifluoride ion in the range -40 to 34 °C.

Solvent	$d\sigma_H/dT$, x 10^3 ppm deg.$^{-1}$	$d\sigma_F/dT$, x 10^2 ppm deg.$^{-1}$
acetonitrile	1.2 ± 0.1	4.3 ± 0.1
N,N-dimethylformamide	2.0 ± 0.1	4.8 ± 0.2
nitromethane	6.0 ± 0.7	5.7 ± 0.3

J(DF) gives $(\gamma_H/\gamma_D)J(DF)=117.9 \pm 2.1$ Hz which should be equivalent to J(HF)=120.5 ±0.1 Hz in the absence of an isotope effect on the coupling constant. The difference of 2.6 ± 2.1 Hz is not significant since the separation of the peaks arising from the D-F coupling are smaller than the actual value of J(DF) because of exchange effects (see section 1.2.3). If the lifetime of FDF^- in solution is approximated by Equation [1.9], Equation [1.8] would predict that the observed J(DF) is about 0.1 Hz smaller than the actual value. A change of this magnitude is sufficient to account for the difference between $(\gamma_H/\gamma_D)J(DF)$ and J(HF).

4.2 Heterobihalide Ions

The heterobihalide ions were prepared by adding a small amount of HF to solutions containing tetrabutylammonium halide.

The nmr spectra of a dilute solution of HF in acetonitrile indicate that HF is present as HF molecules. A doublet with a separation of 476 Hz was observed in both the ^1H and ^{19}F spectra. This doublet arises from a coupling of one proton to one fluorine and the magnitude of the separation strongly suggests that these nuclei are directly bonded. This coupling constant is significantly smaller than the coupling constant of 521 Hz observed in liquid HF (61) which suggests that HF is complexed to the solvent. Infrared studies have also found that HF, in

dilute solutions in acetonitrile, exists as a molecular complex with the solvent (92,93).

On the addition of chloride or bromide to a 0.22M solution of HF, the proton and fluorine resonances shifted downfield and reached a limiting value in the region of excess halide. The doublet due to the H-F coupling constant collapsed when a small amount of halide was added and reappeared only in the region of excess halide. The H-F coupling constant in the presence of an excess of halide was also invariant to the halide concentration. These observations indicate that the heterobihalide ions are formed and that the association constant for the reaction,

[4.3] $$HF + X^- \rightleftharpoons FHX^-$$

where X is Cl or Br, is large. The linewidths of the doublets in the spectra of FHX^- were broad but well resolved at ambient temperature and sharpened, on cooling to -40°, to ca. 5 Hz at half-height. Figure 12 shows a proton spectrum of $FHCl^-$ at -40° in acetonitrile.

The ^1H and ^{19}F shieldings of $FHCl^-$ and $FHBr^-$ were determined by the BHS equation and are presented in Table X.. The coupling constants reported in Table X were those observed in the region of a large halide ion

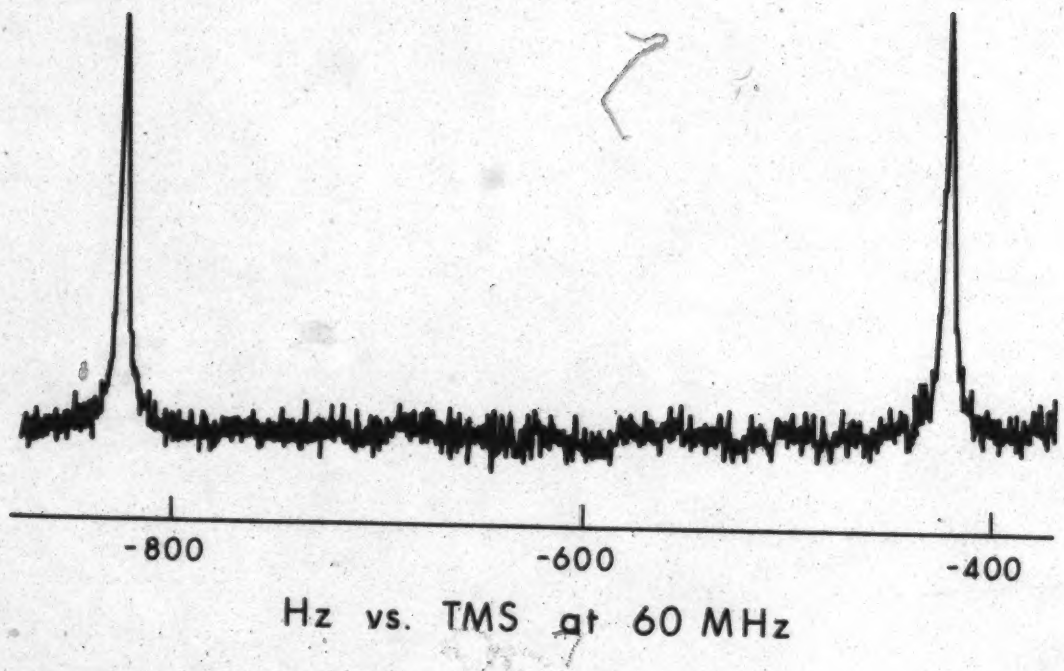

Figure 12. The ^{1}H nmr spectrum of $FHCl^{-}$ ion of the tetra-n-butylammonium salt in acetonitrile at -30°.

Table X. Nuclear shieldings and coupling constants in the tetrabutylammonium heterobihalides in acetonitrile.

Species	T °C	σ_H, ppm vs. TMS	σ_F, ppm vs. CF_4	J(HF), Hz
HF	34	-7.20 ± 0.05	121.4 ± 0.1	479 ± 4
	-40	-7.64 ± 0.02	118.7 ± 0.1	476 ± 1
$FHCl^-$	34	-10.34 ± 0.06	84.6 ± 0.4	404 ± 2
	-40	-10.43 ± 0.03	83.3 ± 0.3	403.4 ± 0.2
$FHBr^-$	34	-8.76 ± 0.05	84.4 ± 0.5	428 ± 2
	-40	-8.88 ± 0.03	83.2 ± 0.3	427.1 ± 0.2
FHI^-	-40	-7.4 ± 0.2	82 ± 4	437 ± 5

concentration where the coupling constants were independent of the halide ion concentration.

The dependence of the fluorine shielding and the H-F coupling constant on the concentration of FHX^-, where X = Cl or Br, was studied by using solutions containing a large constant amount of X^- (0.7M) and varying the HF added from 0.05 to 0.22M. The fraction of HF complexed to X^- in these solutions is expected to be almost constant.* The fluorine shielding at -40° was found to decrease by 0.5 ppm as the HF concentration was decreased from 0.22 to 0.05M. No change in the coupling constant was observed within the uncertainty (±1 Hz) in measuring the peak positions of the dilute samples. Therefore the values in Table X are representative of the infinite dilution values.

The association constant for the formation of FHI^- was much smaller. The fluorine shielding and the observed coupling constant continued to change as the iodide concentration was increased and did not reach a limiting value. This behavior is consistent with a rapid

---

*A calculation, assuming a reasonable value of 100 ℓ $mole^{-1}$ for the equilibrium constant, found that the fraction of HF complexed in these solutions varies by only 0.4%.

exchange process described by Equation [4.3], and the observed shieldings and coupling constants are population -weighted averages of the solvated hydrogen fluoride and bihalide values. The continuous resolution of the coupling constant indicates very little occurrence of reactions such as,

[4.4] $$FHI^- \rightleftharpoons F^- + HI,$$

or other processes which would average the relative orientations of the nuclear spins of a given H-F and result in a collapse of the spin-spin coupling. The linewidths at -40° were ca. 40 Hz at half-height which corresponds to an average lifetime of FHI^- of the order of $1/40\pi$ sec. or 8 msec. In the proton spectra, the same variation of J(HF) with iodide concentration was observed, but there was almost no change in the proton shielding. Apparently the proton shieldings of HF in acetonitrile and in FHI^- are about the same.

The fluorine shielding of FHI^- given in Table X was determined by a BHS analysis. At the highest concentration of I^- used (0.8M) approximately 85% of the HF was complexed to I^-. The coupling constant for FHI^- listed in Table X is an average of five values calculated from spectra which contained well resolved doublets. The

separation of the peaks in the doublet was assumed to be a population-weighted average of the coupling constants in HF (476 Hz) and FHI^-. The amounts of HF and FHI^- present in the solution were calculated from the observed fluorine shift Δ and the fluorine complex shift Δ_c calculated from the BHS equation.

The association constant in acetonitrile for the iodide complex derived from the BHS analysis was 2.8 ± 0.5 ℓ^{-1} mole at -40°. The association constant for the Cl^- and Br^- complexes could not be determined accurately since the BHS method does not yield good determinations of large association constants (75,76). The determinations were further complicated by the partial collapse of the doublets in the critical equimolar region. The very broad peaks observed in this region made it impossible to measure their positions accurately. The best estimate for the association constants for the formation of $FHCl^-$ and $FHBr^-$ at -40° were 250 ± 100 and 100 ± 50 ℓ $mole^{-1}$ respectively.

4.3 Hydrogen Fluoride in Solution

The observed properties of hydrogen fluoride dissolved in aprotic solvents are given in Table XI. Gutmann's donor numbers (94), which are a measure of the solvent base strength, have been included.

Table XI. Nuclear shieldings and coupling constants in 0.22M hydrogen fluoride solutions.

	Solvent	Donor No.[a]	T, °C	σ_H, ppm vs. TMS	σ_F, ppm vs. CF_4	J(HF), Hz
1.	gas	-	30	-2.2[b]	151[b,c]	+530 ± 23[d]
2.	tetramethylsilane[e]	-	34	-3.93	132.1	-
3.	cyclohexane-d_{12}[e]	-	34	-3.97	-	-
4.	trichlorofluoromethane[e]	-	34	-4.07	133.0	-
5.	acetonitrile	14.1	34	-7.20	121.4	479 ± 4
			-40	-7.64	118.7	476 ± 1
6.	diethylether	15.1	-40	-9.05	124.5	464 ± 5
7.	propylene carbonate	19.2	-40	-8.43	120.6	453 ± 5
8.	N,N-dimethylformamide	26.6	-40	-11.80	117.5	412 ± 1
9.	dimethylsulfoxide	29.8	34	-10.44	104.9	410 ± 10

a. Reference 94.
b. Reference 72.
c. Referenced to CF_4 (gas).
d. Reference 62.
e. Concentration of HF is less than 0.22M.

4.3.2 Non-Basic Solvents

Tetramethylsilane (TMS), cyclohexane-d_{12}, and trichlorofluormethane are solvents of very low basicity. In these solvents, HF gave sharp, single-line, exchange-averaged spectra. The signal intensities in the TMS and cyclohexane-d_{12} solutions indicated that only a small portion of the HF condensed into the sample tube was in solution. The rest was presumably in the gas phase. These concentrations could not be measured with any precision because of the low signal-to-noise ratio.

The H-F coupling was not observed in these solvents or for HF in the gas phase (44,45) because of rapid exchange processes. The exchange process in the gas phase has been attributed to proton transfer reactions involving cyclic polymers (45). This process could also account for the exchange-averaging of the H-F coupling observed in the non-basic solvents since HF is probably self-associated to some extent in these solvents.

A qualitative estimate of the degree of self-association of the HF in the non-basic solvents can be obtained from a comparision of the proton shielding in solution and in the gas phase. The gas-to-solution shifts

in the proton shieldings can be attributed mainly to the effects of hydrogen bonding since other solvent effects are generally quite small (56). The differences of about 1.8 ppm between the proton shieldings of HF in the gas and in the non-polar solvents are smaller than the difference of 5.7 ppm observed between gaseous and liquid HF (44), which is highly self-associated. This indicates that HF, dissolved in the non-polar solvents, is significantly less associated than in liquid HF. The same degree of self-association of the HF in these solvents cannot be assumed from the observation that the proton shieldings are almost identical, since solvent effects and HF concentrations are probably different.

The fluorine shieldings in HF in the non-basic solvents exhibit large gas-to-solution shifts (defined as $\sigma_{solution} - \sigma_{gas}$). The fluorine shieldings of HF in the gas, given in Table XI, cannot be directly compared to the other shieldings because the shielding in the reference, CF_4, also exhibits a gas-to-solution shift of about -6 ppm. However, all the fluorine shieldings can be converted to the absolute shielding scale using the values listed in Table II. The total gas-to-solvent shift for HF dissolved in $CFCl_3$ and TMS is -25 ppm. This shift is larger than the -20.5 ppm (44) observed for the gas-to-

liquid shift for pure HF. Since HF in the non-basic solvents is only partially self-associated, non-hydrogen bonding solvent effects strongly influence its fluorine shielding. The solvent effects observed here are comparable with those observed for other fluorine compounds. Large gas-to-solution shifts in the range -3 to -16 ppm have been observed for the fluorine shieldings of non-polar molecules, such as SF_6 and SiF_4, dissolved in non-polar solvents (95). These solvent effects have been attributed to van der Waals interaction between the solute and the solvent (95,96).

A previous study (52) reported fluorine shieldings of 130 and 131 ppm relative to CF_4 (internal) in dilute solutions of HF in carbon tetrachloride and benzene, respectively, which are in good agreement with those reported in Table XI for the non-basic solvents.

4.3.2 Basic Solvents

In the basic aprotic solvents in Table XI, spin-coupled spectra of dissolved molecular HF were observed. In most cases, the H-F coupling constant could be observed only at low temperatures.

Infrared studies of dilute solutions of HF in basic aprotic solvents have found that HF forms bimolecular complexes with the solvent (92). Polymers of the

form, ···F-H···F-H···B, where B is a Lewis base were only observed at HF concentrations much larger than those used here. There appears to be very little self-association of HF in the basic solvents studied here. The proton and fluorine shieldings of HF dissolved in acetonitrile were found to be independent of the concentration to within 0.05 ppm in the range 0.05 to 0.22M. The coupling constant of HF in acetonitrile was also found to be independent of the HF concentration and of the temperature (from -40 to 34°) to within 3 Hz.

The changes observed in the coupling constant when HF is dissolved in the basic solvents are exceptionally large. The fractional changes in J(HF) are about five times larger than those observed in $J(^{13}CH)$ of chloroform (59) or $^{1}J(^{15}NH)$ of aniline (43) in the same solvents. J(HF) in HF is also observed to decrease in magnitude which is in contrast to the increase in the magnitudes of the coupling constants observed for chloroform and aniline. The coupling constant in HF tends to decrease as the base strength of the solvent as measured by the donor numbers increases. This behavior strongly suggests that the decrease in the H-F coupling constant can be attributed to the effects of hydrogen bonding.

The fluorine shieldings of HF dissolved in the basic solvents are much smaller than that of HF in the

gas phase. These differences cannot be completely attributed to the effects of hydrogen bonding since non-hydrogen bonding solvent effects are also important. However, the shieldings in the basic solvents are 10 to 30 ppm smaller than the shielding observed in HF dissolved in the non-polar solvents. These results show that the formation of a hydrogen bond to the proton in HF results in a decrease in the fluorine shieldings. However, the poor correlation between the fluorine shieldings and the base strengths of the solvents indicates that other effects are also important.

4.4 Summary

Figure 13 shows the relationship between the proton shielding and the H-F coupling constant, for HF complexed to a halide ion or dissolved in a polar aprotic solvent. The proton shielding and the H-F coupling constant of HF complexed to a halide ion decrease as the base strength of the halide ion increases. The coupling constant of HF dissolved in the basic solvents was observed to consistently decrease as the base strength of the solvent increases. In Figure 13, there appears to be an approximate trend between the coupling constant and the proton shielding, of HF dissolved in the aprotic sol-

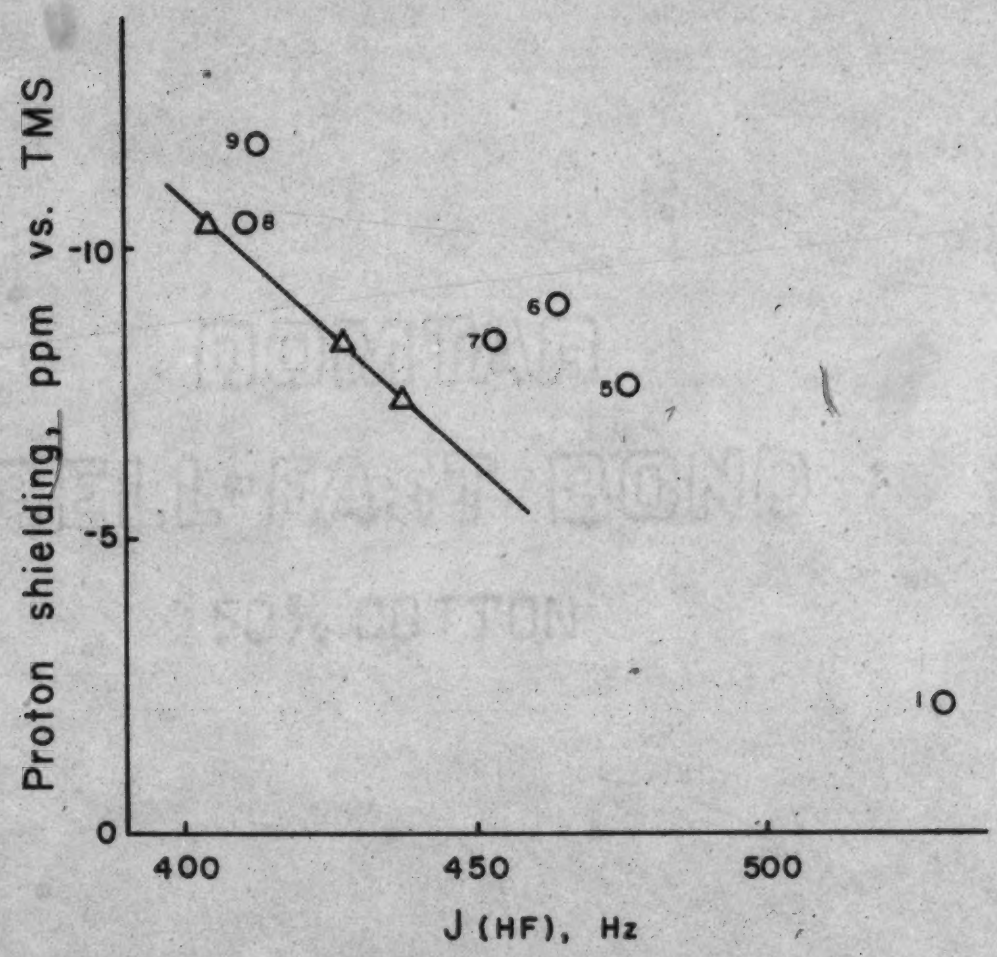

Figure 13. Correlation between the proton shielding and the coupling constant in hydrogen-bonded complexes of hydrogen fluoride: Δ, bihalide ions; o, HF in solution (numbers refer to Table XI).

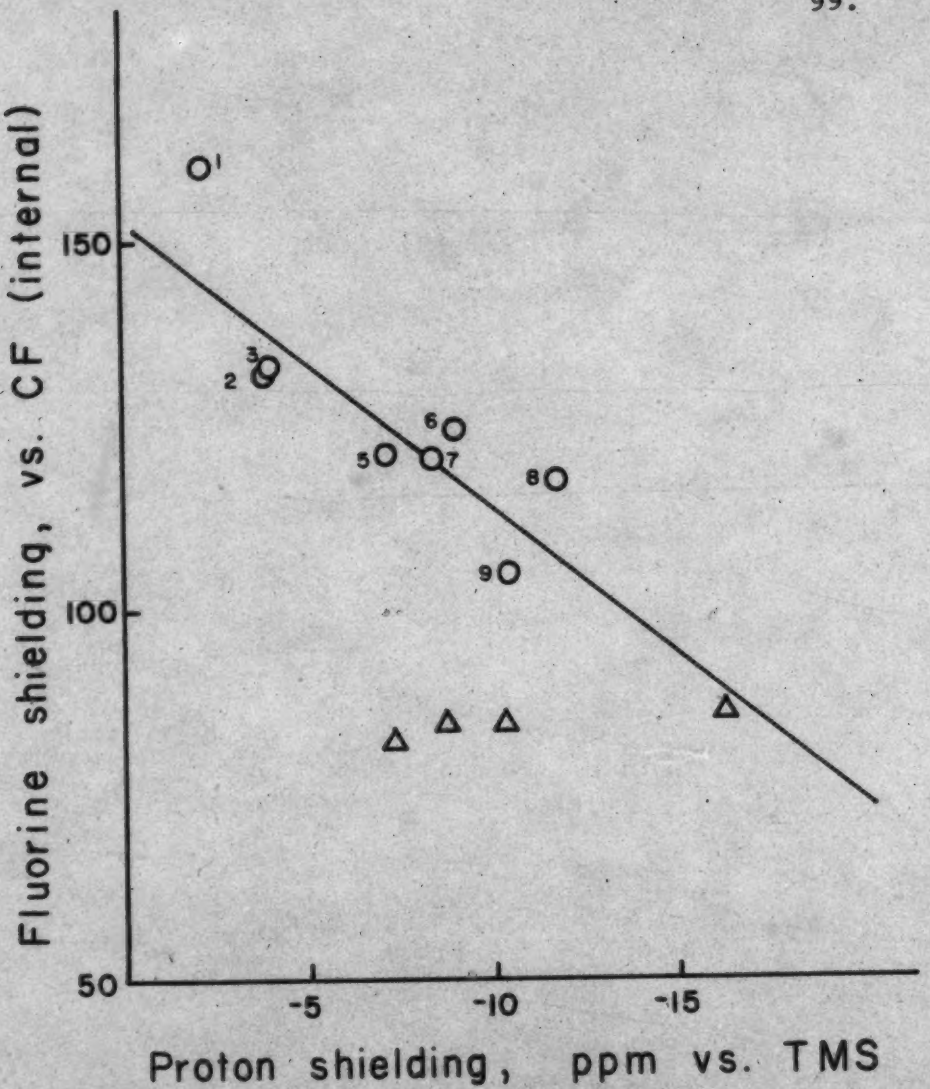

Figure 14. Correlation between the ^{1}H and ^{19}F shieldings of hydrogen fluoride: Δ, bihalide ions; o, HF in solution (numbers refer to Table XI).

vents. However, Figure 13 clearly shows that there is no common relationship between the coupling constant and the proton shielding for HF hydrogen bonded to a halide ion and HF hydrogen bonded to a molecular base.

The point for FHF^- was omitted from Figure 13 because it was far removed from the other points and fell well below the line drawn through the points for the heterobihalide ions.

Figure 14 shows the relationship between the proton and fluorine shieldings of HF. All the shieldings observed are smaller than their values for HF in the gas phase, and there is a rough trend between the proton and fluorine shieldings of HF dissolved in the aprotic solvents. The shieldings in the bifluoride ion are consistent with this trend but the fluorine shieldings in the heterobihalide ions are anomalous. In all four bihalide ions, the fluorine shieldings are almost identical.

CHAPTER 5

DISCUSSION OF THE PROTON SHIELDINGS

In this chapter, the decrease in the ^1H shielding of the hydrogen halides on the formation of a hydrogen bond is discussed. The close relationship between the charge density on the hydrogen and its shielding is used to show that the decrease in the shielding could be accounted for by a lower hydrogen charge density in the bihalide ions. The relationship between the change in the proton shielding and the change in enthalpy on the formation of a hydrogen bond is discussed.

5.1 Absolute Shieldings of the Hydrogen Halides

Absolute proton shieldings may be deduced using the absolute shielding of methane in the gas phase, 30.55 ± 0.17 ppm (see Section 2.3) and the shielding of TMS in the gas phase relative to methane (97), +0.13 ppm.

The shieldings of the hydrogen halides, as monomers in the gas phase, have been measured relative to methane (78-80). Table XII presents these values together with the absolute shieldings. The hydrogen halide shieldings observed in solution, with the exception of hydrogen fluoride in the polar solvents, were 1 to 2 ppm less than those in the gas. The difference arises from the reaction

Table XII. Proton Shieldings in parts per million of the hydrogen halides in the gas phase.

Hydrogen halide	σ_{HX} vs. CH_4	σ_{HX}, absolute
HF	-2.10 ± 0.20[a]	28.45 ± 0.26
HCl	+0.49 ± 0.01[b]	31.04 ± 0.17
HBr	+4.34 ± 0.01[c]	34.89 ± 0.17
HI	+13.25 ± 0.03[d]	43.80 ± 0.17

a. Reference 44.

b. Reference 78.

c. Reference 79.

d. Reference 80.

field of the polar molecule and van der Waals interaction with the halogenated solvents (98,99).

Table XIII presents the absolute shieldings of the bihalide ions in solution. These shieldings were determined from the absolute shieldings of TMS in the gas phase, and the relative shielding of the bihalide ions referenced to TMS as an internal standard. This procedure will tend to eliminate any small solvent effects, which are typically about -0.3 ppm for TMS (56), if the solvent effects on TMS and bihalide shieldings are about the same. These absolute shieldings of the bihalide ions in Table XIII are probably comparable to the gas phase, isolated-molecule shieldings, since the proton in the bihalide ion is near a center of symmetry, where it is subject to a zero reaction field (56), and is inaccessible to the solvent. If this is the case, the absolute shieldings are probably reliable to about 0.5 ppm, which is estimated from the uncertainty in the absolute shielding scale and from the variation observed in the shieldings of the bihalide ions in different solvents. The relative shieldings listed in Table XIII are the average values measured in sym-tetrachloroethane except those which contain fluorine, which were measured in acetonitrile.

To distinguish the complex shift, Δ_c, referenced to the shielding of the hydrogen halides in solution, from the corresponding shift referenced to the shielding of

Table XIII. Proton shielding of the bihalide ions.

Bihalide	σ_{XHY^-}, ppm vs. TMS	σ_{XHY^-}, ppm absolute	Δ_c', ppm*
FHF^-	-16.30	14.3	-14.1
$FHCl^-$	-10.34	20.3	-8.1
$FHBr^-$	-8.76	21.8	-6.5
FHI^-	-7.2	23.4	-5.0
$ClHCl^-$	-13.92	16.7	-14.3
$ClHBr^-$	-10.15	20.5	-10.5
$ClHI^-$	-7.14	22.5	-7.5
$BrHBr^-$	-10.15	20.5	-14.4
$BrHI^-$	-5.06	25.6	-9.3
IHI^-	-0.90	29.7	-14.0

*$\Delta_c' = \sigma_{XHY^-} - \sigma_{HX}$ (gas); for the heterobihalides σ_{HX} refers to the hydrogen halide containing the halogen with the smaller atomic number.

the hydrogen halide in the gas phase, the latter will be designated Δ_c'.

The same heterobihalide, XHY^-, can be formed from HX and Y^- or HY and X^-. However, if X^- is a stronger base than Y^-, the reaction of HY and X^- will involve a proton transfer reaction to form HX and Y^-. Consequently, the complex shifts for the heterobihalides are defined as

$$\Delta_c' = \sigma_{XHY^-} - \sigma_{HX}$$

where HX is the hydrogen halide containing the halogen with the smaller atomic number.

The complex shifts Δ_c' are remarkable for their size, especially in the four homobihalide ions. In all four cases, the shieldings in the homobihalide ions are about 14 ppm less than in the parent hydrogen halides. These shifts are exceptionally large since the hydrogen bond shifts are usually of the order of -5 ppm (33). The large changes in the shielding observed on the formation of the bihalide ion, together with their simple structure provides an opportunity to investigate the changes in the electronic structure of these systems.

5.2 Proton Shielding in the Homobihalide Ions

The relatively small, symmetric electronic structure of the homobihalide ions presents a challenge to

theoretical models. At present, there are accurate calculations available only for the bifluoride ion (100,101). Whether these ab initio calculations are able to predict the shieldings in the bifluoride ion has not been determined. Calculations based on a less accurate semi-empirical SCF wavefunction gave results for the proton shielding in HF and in FHF^- (102) which were in very poor agreement with the experimental values.

In this discussion, a description of the shieldings in these systems will be presented in which the changes in electronic structure and the shielding between the hydrogen halide HX, and the corresponding bihalide XHX^-, will be emphasized.

If a linear, centrosymmetric structure is assumed, the significant differences between the corresponding ion and the molecule are the H-X internuclear distance (which is roughly 20% greater in the ion) and the presence of an extra halogen center, with its electrons. In the simplest MO treatment (103), the molecule will have two bonding electrons and the ion four. Since both species are axially symmetric, the same hydrogen and halogen orbitals may be used as a basis in both.

It is proposed that the hydrogen 1s orbital population ρ_H, determines the shielding in both the bihalide ion and the related molecule. Consider, as reference

states, the completely ionic forms $X^-H^+X^-$ and H^+X^-. In each case, all the electrons are in spherical halide ion configurations. Now, the average over all orientations, of the shielding of an external nucleus by a spherical charge distribution, is zero (104). McGarvey (105) has calculated the shielding in purely ionic hydrogen halides. The only nonzero term, which arises from halogen electrons at a distance greater than the H-X distance, R, takes the form

$$\sigma_{ionic} = \frac{e^2}{3mc^2} \int_R^\infty \Psi^* (\Sigma_k r_k^{-1}) \Psi \, d\tau$$

where r_k is the vector from the nucleus to electron k. Using Slater-type orbitals with McGarvey's exponents the shieldings were evaluated in "pure ionic" hydrogen halides and bihalides, using published bond lengths (10,11, 106). In all cases, the integral at the bihalide distance had less than half its value at the molecular distance, so the bihalide shieldings, which include contributions from both halogens, were only about 1 ppm less than those in the molecules. Therefore this contribution to the shielding of ionic H^+X^- molecules is about 5 ppm, while those in the purely covalent forms are about ten times greater. Thus, one expects a correspondence between the proton shielding and the hydrogen electron population

ρ_H, which is a measure of the covalent character.

5.2.1 Theory of Proton Shielding

In this section a brief summary of the theory of hydrogen shielding in small molecules will be presented.

Ramsey (107) derived an expression for the magnetic shielding of a nucleus in a molecule which arises from the perturbation of surrounding electrons produced by an external magnetic field. This expression consists of the sum of two terms called the diamagnetic term σ_d, and the paramagnetic term σ_p. The relative magnitude of these two terms depends on the gauge, that is, the choice of the origin for the magnetic vector potential. In this discussion, only the partitioning of the shielding into σ_d and σ_p which results from the choice of the proton as the origin will be considered. The partitioning of the shielding which arises from other choices of gauge will be expressed in terms of this definition of σ_d and σ_p.

The calculation of the shielding of a nucleus in a molecule by Ramsey's expression requires an accurate set of wavefunctions for the molecule. The diamagnetic term, averaged over all orientations, can be calculated from the ground-state wavefunction by the expression (107),

[5.1] $$\sigma_d = \frac{e^2}{3mc^2} \langle 0 | \sum_k r_k^{-1} | 0 \rangle,$$

where r_k is the radial distance of the electron k from the origin. To evaluate σ_p precisely, a detailed knowledge of the energies and wavefunctions of all excited states is needed. Various approximations which eliminate the need for accurate excited-state wavefunctions have been used in theoretical calculations (108,109). These calculations of σ_p are very sensitive to the approximate wavefunctions used. This greatly limits the accuracy of theoretical calculations of nuclear shieldings, since σ_d and σ_p are usually both large in magnitude and of the opposite sign.

The partitioning of the absolute shielding into σ_d and σ_p can also be determined from the spin-rotation constant measured by molecular beam magnetic or electric resonance spectroscopy (110). For the proton shieldings in the hydrogen halides, σ_d and σ_p have been found to be of opposite sign and are of the order of 100 to 200 ppm (110).

Empirically, the shielding in the hydrogen halides can be considered as the sum of two positive terms

[5.2] $$\sigma = \sigma_H + \sigma_x$$

where σ_H arises from the hydrogen 1s electrons, and σ_x

arises from the halogen valence electrons and is proportional to the observed spin-rotation constant (110). This again implies that σ_d and σ_p contain mutually cancelling terms.

Approximate expressions for σ_d and σ_p can be used to derive simple expressions for the mutually cancelling terms. Chan and Das (111) showed that σ_p could be separated into two terms

$$\sigma_p = \sigma_p^{G} + \sigma_p^{ex}, \qquad [5.3]$$

which are defined in terms of a secondary gauge. The term σ_p^{G} depends only on ground-state wavefunctions and σ_p^{ex} involves excited-state wavefunctions. The simplest choice of secondary gauge is at the halogen nucleus. In this choice of gauge, σ_p^{G} for the hydrogen halides can be approximated by (111)

$$\sigma_p^{G} = \frac{-e^2}{3mc^2} \frac{(n - 1)}{R}, \qquad [5.4]$$

where n is the total number of electrons in the molecule and R is the bond length.

σ_d can be approximately separated into contributions from electrons centered on different nuclei by

$$\sigma_d = \sigma_d^{H} + \sigma_d^{X}. \qquad [5.5]$$

The contribution from the halogen electrons, considered as a spherical distribution centered at a distance R from the hydrogen, can be expressed as

$$[5.6] \qquad \sigma_d^X = \frac{e^2}{3mc^2} \frac{(n-1)}{R}$$

which, to the precision of the approximations, cancels the term σ_p^G

From Equations [5.3] and [5.5] , the shielding can be expressed as

$$[5.7] \qquad \sigma = \sigma_d^H + \sigma_p^{ex}$$

The shielding due to the hydrogen 1s electrons can be calculated from (34),

$$[5.8] \qquad \sigma_d^H = \frac{e^2}{3mc^2} \langle 1s | \frac{1}{r} | 1s \rangle \rho_H,$$

where ρ_H is the 1s electron density. Experience with hydrogen shieldings suggests a 1s orbital exponent of 1.2, which on evaluating equation [5.8] yields (34),

$$[5.9] \qquad \sigma_d^H = 21.4 \ \rho_H \text{ ppm.}$$

Pople (112) has formulated an expression for the halogen term σ_p^{ex}. This effect is expressed as a point magnetic dipole located at the halogen nucleus, and depends on the imbalance of the halogen valence p-orbitals. If the p_π orbitals are considered to be filled, Pople's expression

becomes

$$[5.10] \qquad \sigma_p^{ex} = \frac{e^2\hbar^2}{3m^2c^2\Delta E} \frac{(2 - \rho_p)}{R^3} ,$$

where ρ_p is the sigma-bonding p orbital population, and ΔE is the average excitation energy. To fit the observed HX shieldings, ΔE takes reasonable values of about 3 to 8 eV, decreasing from F to I.

An alternate partitioning of σ_p has been suggested by Chan and Das (111). They found σ_p^G could be evaluated from known ground state properties and accounts for a major portion of σ_p, if the electronic centroid was chosen as the origin. In this choice of gauge, $\sigma_p^{G'}$ for the hydrogen halides can be expressed as

$$[5.11] \qquad \sigma_p^{G'} = \frac{-e^2}{3mc^2} \frac{(n - 1)}{R^3} \left[\frac{\mu}{ne} R + \frac{(n - 1)}{n} R^2\right] ,$$

where μ is the dipole moment, n the total number of electrons and R the HX bond length. The dipole moment can be approximated in terms of local charge densities by

$$[5.12] \qquad \mu = eR(\rho_x - 1),$$

where ρ_x is the σ-bond electron charge density at the halogen. This yields,

$$[5.13] \qquad \sigma_p^{G'} = \frac{-e^2}{3mc^2} \frac{(n - 1)}{R} + \frac{e^2}{3mc^2} \frac{(n - 1)}{nR} (2 - \rho_x) .$$

Evaluating Equation [5.2] with the same approximations used in the previous case, one obtains

[5.14] $$\sigma = \sigma_d^H + \sigma_\Delta' + \sigma_p^{ex'}$$

where, as before,

$$\sigma_d^H = 21.4\ \rho_H$$

and

[5.15] $$\sigma_\Delta' = \frac{e^2}{3mc^2}\left[\frac{(n-1)}{nR}\right](2 - \rho_x).$$

The three shielding terms in Equation [5.14] may be interpreted as follows. The first term arises from the local diamagnetic shielding of the hydrogen 1s electrons. The second and third are associated with the halogen, and arise from the anisotropy of the diamagnetic and paramagnetic polarizability of the halogen valence shell (113).

The R^{-1} dependence of the second term suggests that the R^{-3} dependence of the entire halogen term, assumed in Equation [5.10], may not be justified. The point dipole approximation which gives rise to the R^{-3} dependence is certainly suspect for the short-range shielding effects involved in the hydrogen halides (114). As one would expect for the field on the axis near a toroidal current distribution, the R dependence of the halogen term

is somewhat more gradual than a R^{-3} dependence.

The third term ($\sigma_p^{ex'}$) cannot be evaluated in this choice of gauge without knowledge of the excited state wavefunctions. It can be deduced, and the relative importance of the three terms in Equation [5.14] assessed as follows. The electron populations can be estimated from the dipole moment by Equation [5.12] and $\rho_H = 2 - \rho_x$ is assumed. $\sigma_p^{ex'}$ is taken from Chan and Das (111), who deduced it from the observed spin rotation constant. The resulting values which are shown in Table XIV indicate that the shielding in the hydrogen halide molecules arise from hydrogen and halogen electrons in roughly equal proportions, and that σ_d^H and $\sigma_p^{ex'}$ are the dominant terms.

5.2.2 Dependence of the Shielding on the Charge Distribution

In both representations of the shielding, Equations [5.7] and [5.14], the term σ_d^H is explicitly proportional to the hydrogen charge density ρ_H. Since Equation [5.7] and [5.14] have the same expression for σ_d^H, the halogen terms must also be equal, to the extent of the approximations, and therefore,

$$\sigma_p^{ex} = \sigma_\Delta' + \sigma_p^{ex'}. \qquad [5.16]$$

Table XIV. Calculated absolute hydrogen shieldings in the hydrogen halides in ppm.

Molecule	σ_d^H	σ_Δ	$\sigma_p^{ex'}$	Total	Observed
HF	13	6	7	26	28.4
HCl	18	6	8	32	31.0
HBr	19	6	13	38	34.8
HI	20	6	22	48	43.7

Since both σ_p^{ex} and σ_Δ' are zero in the completely ionic molecule, $\sigma_p^{ex'}$ must also vanish in this case. Furthermore, if only σ-bonding is assumed, σ_p^{ex} and σ_Δ' are both proportional to the asphericity of the halogen valence shell, so $\sigma_p^{ex'}$ must also show this behavior. Consequently, if the σ-bond in the hydrogen halide is considered to be formed only from the hydrogen 1s orbital and one of the halogen 2p orbitals, then $\rho_x = \rho_p = 2 - \rho_H$ and the shielding takes the form

$$[5.17] \qquad \sigma = 21.4\ \rho_H + K_x(R)\cdot(2 - \rho_x),$$

where $K_x(R)$ is a function characteristic of the halogen x. This expression can be written in terms of the hydrogen charge density alone as

$$[5.18] \qquad \sigma(HX) = [21.4 + K_x(R)]\cdot\rho_H(HX).$$

It is apparent from the previous section that the R dependence of $K_x(R)$ is not simple, but it appears reasonable to assume that it lies between R^{-1} and R^{-3}.

The shielding in the homobihalide ions will also be proportional to the hydrogen charge density if these ions are considered to be centrosymmetric. The σ orbitals will have a symmetrized basis (103) and if the same halogen and hydrogen orbitals, used to describe the

bonding in the hydrogen halides, are used, the four electrons in σ orbitals can be partitioned as

[5.19] $$\rho_H + 2\rho_X = 4.$$

Since there are two equivalent halogen centres in a homobihalide ion, the shielding equation corresponding to Equation [5.17], will have the form

[5.20] $$\sigma(XHX^-) = 21.4\ \rho_H + 2K_X(R)\cdot(2 - \rho_X)$$

Substituting Equation [5.19] into Equation [5.20] yields

[5.21] $$\sigma(XHX^-) = [21.4 + K_X(X)]\cdot\rho_H(XHX^-).$$

Since $K_X(R)$ is the same function of R in the hydrogen halide and the corresponding bihalide ion, the shielding in the ion has the same functional form as that in the molecule.

In this discussion, the participation of the halogen 2s orbital in the σ-bonding has been neglected. However, the form of Equation [5.21] will not be affected if the hybridization in HX and XHX^- is the same since ρ_p and ρ_x will be related by a constant factor.

5.2.3 Evaluation of the Charge Densities

The hydrogen 1s electron density in the homo-

bihalide ions can be estimated as follows. $\rho_H(HX)$ is determined from the dipole moment (115) of the molecule. Using Equation [5.18], $K_x(R)$ at the HX bond distance is determined from the shielding of HX. Taking R in the bihalide ion as one-half of the halogen-halogen distance, $\rho_H(XHX^-)$ can be evaluated using Equation [5.21] if the R dependence of $K_x(R)$ is assumed. This was done assuming both R^{-1} and R^{-3} dependence, and the results are presented in Table XV.

These values of the charge densities are rather crude estimates. However, they clearly show that a significant decrease of the hydrogen charge density occurs on formation of a hydrogen bond. This conclusion does not depend on the method of evaluating the molecular charge separation; that based on the dipole moment was used as a convenient and representative example. Due to the simple R dependence of the halogen terms, the shielding midway between the halogens will have $d\sigma_x/dr = 0$, where r is the displacement along the internuclear axis. Consequently, the shielding model is not critically dependent on the symmetry of the ion; the proton could be displaced from the center of symmetry without large change in the shielding.

The neglect of the variation in excitation

Table XV. Calculation of bihalide hydrogen charge densities.

Halogen	Dipole Moment (D)[a]	Bond Lengths (Å)		Charge Densities		
		HX[b]	XHX^{-}[c]	HX	XHX^{-} (R^{-1})	XHX^{-} (R^{-3})
F	1.74	0.917	1.13	0.605	0.34	0.41
Cl	1.07	1.275	1.57	0.825	0.48	0.56
Br	0.79	1.414	1.675	0.884	0.56	0.63
I	0.38	1.604	1.9	0.951	0.70	0.82

a. Reference 115.

b. Reference 106.

c. References 10 and 11.

energy, ΔE, which explicitly appears in the term σ_p^{ex} in Equation [5.10], does not affect the arguments used to predict a lower hydrogen charge density in the bihalide ions. The halogen term arises from the mixing of the ground and excited states by the magnetic field and is proportional to the reciprocal of the energy separations between these states (112). The average excitation energy, ΔE, is an approximation which represents these energy differences. Theoretical calculations (116) have predicted that the orbital energies, of the occupied orbitals in a proton donor molecule, increase in energy on the formation of a hydrogen bond. This suggests that ΔE would be smaller in the bihalide ion than in the corresponding hydrogen halide. This change in ΔE would increase σ_x and an even lower hydrogen charge density would be required to account for the decrease in the shielding.

A recent theoretical study (100) has shown that the hydrogen charge density in FHF^- is lower than that in HF. Furthermore, other theoretical studies (116) have indicated that the decrease in the hydrogen charge density in the proton donor molecule is probably a general feature of hydrogen bonding.

BODLEIAN
LIBRARY

5.3 Proton Shielding in the Heterobihalide Ions

The contributions to the proton shielding in the heterobihalide ions are analogous to those in the homobihalide ions except that the contributions from the two halogens will no longer be equivalent. In the heterobihalide ion $X\text{-}H\cdots Y^-$, the proton shielding can be divided into three positive contributions, σ_X, σ_H, and σ_Y, each arising from the electrons associated with the corresponding nucleus. The changes in these terms on the formation of a heterobihalide can be qualitatively predicted on the basis of the shielding model for the hydrogen halides discussed in the previous section.

A simple electrostatic model does account for the trends observed in the complex shifts, Δ_c', summarized in Table XIII. As the anion Y^- approaches the positive end of the hydrogen halide molecule HX, the electrons in the bond will be polarized towards the halogen X. This polarization will produce a decrease in the proton shielding since σ_H will decrease as a result of the smaller hydrogen charge density and σ_X will decrease as a result of the larger halogen charge density. Consequently, the magnitude of Δ_c' of a given hydrogen halide would increase with the stronger electric field of the smaller anion, and the more polarizable hydrogen halides would show larger changes

when complexed to a given halide ion. All the complex shifts in Table XIII are consistent with these trends. However, this simple electrostatic model, which assumes that the electron distribution on the anion Y^- is not changed, is certainly invalid for the homobihalide ions and is presumably also invalid for the heterobihalide ions. On the formation of a centrosymmetric homobihalide ion from HX and X^-, the electron redistribution is expected to result in a lower charge density of the hydrogen and an equal sharing of the negative charge on the halogens. These changes should also occur, to a lesser extent, in the heterobihalide ions. Consequently, in the heterobihalide ion $X\text{-}H\cdots Y^-$, σ_x will be reduced due to the larger charge density on X and the larger X-H distance. The loss of the spherical electron distribution of Y^- will result in a positive shielding contribution σ_y. This contribution would be expected to increase as the hydrogen bond in $X\text{-}H\cdots Y^-$ became stronger and reach its maximum value in the homobihalide ion YHY^-.

5.4 Electrostatic Model

The importance of the shielding term σ_y, for the bihalide ion $X\text{-}H\cdots Y^-$, can be considered by estimating

the shifts Δ_C' which would arise from an electrostatic model of the hydrogen bond. In this model, the hydrogen bond is considered to result from an electrostatic interaction between the electric field of the anion, considered as a point charge, with the dipole and induced dipole of the hydrogen halide. Consequently the change in the proton shielding must be considered only in terms of the electron redistribution in the molecule. The shift Δ_E of the shielding of a proton in an electric field has been described by (98,99,117,118)

$$\Delta_E = -AE_z - BE^2 \qquad [5.22]$$

where E_z is the component of the electric field along the bond. The parameter A is a characteristic of the X-H bond, and B is usually assumed to have the hydrogen-atom value of 0.738×10^{-18} esu (119). This model has been used to explain the downfield shifts of the proton observed in weak hydrogen bonds (40,49,118,120,121). The values of A and B for HCl have been found to be 40×10^{12} esu and 0.38×10^{-18} esu respectively from studies of intermolecular shielding effects in gases (78); corresponding values for HBr have been found to be 65×10^{-2} esu and 1.60×10^{-18} esu for A and B respectively (121). Equation [5.22] cannot be accurately applied to the heterobihalide ions

since the internuclear distances are not known. However, Δ_E calculated from Equation [5.22] greatly exceeds Δ_C' for any reasonable interaction distance (assuming a linear structure). For example, to produce an electric field, evaluated at the midpoint of the HCl bond, necessary to account for the observed shift in Cl-H···I^-, the iodide ion would have to be placed at a distance of 5 Å. Since the ionic radius of the iodide ion is 2.16 Å, this is an unreasonably long distance. Moving the ion to a more reasonable position closer to the proton would result in a deshielding which is much larger than that observed. This clearly indicates the need for the additional positive contribution σ_y. The covalent bonding in the hydrogen bond would create an anisotropy in the electron distribution of the anion which would result in a positive shielding contribution.

The electrostatic model gives a surprisingly good account of the energies of formation of the bihalide ions, provided that the polarization terms are included (120). Table XVI presents the calculated ion-molecule electrostatic energies. U_{dip} is the energy of the molecular dipole, and U_{pol} the energy of the induced dipole, αE, in the ionic field (120). Both dipoles are taken at the center of the HX bond. The unknown heterobihalide halogen-halogen distances were taken as 0.5 Å less than

Table XVI. Computed Ion-Molecule Electrostatic Potential Energies (Kcal $mole^{-1}$)[a]

Ion	μ, D[b]	$\alpha_{11} \times 10^{24}$ cm^3[c]	U_{dip}	U_{pol}	Total
FHF^-	1.74	0.96	-37	-15	-52
$FHCl^-$			-25	-7	-32
$FHBr^-$			-22	-5	-27
FHI^-			-18	-4	-22
$ClHCl^-$	1.07	3.13	-12	-13	-25
$ClHBr^-$			-11	-11	-22
$ClHI^-$			-9	-8	-17
$BrHBr^-$	0.79	4.22	-8	-14	-22
$BrHI^-$			-6	-10	-16
IHI^-	0.38	6.58	-3	-13	-16

a. The available experimental values are summarized in Table I.

b. Reference 115.

c. Landolt-Bornstein, "Zahlenwerten und Funktionen" (Springer, Berlin, 1951), Vol. 1, Part 3.

the sum of the ionic radii of the halogens, which corresponds to the behavior observed in the homobihalide ions.

This simple computation reproduces the observed trends in the energies of formation for the homobihalide ions and for the series involving a common proton donor (see Table I). However, the prdicted trends in the energies of formation of the hydrogen bihalides in the series involving a common halide ion are incorrect. The energies of formation of various proton donors complexed to Cl^- in the gas phase has been found to increase in magnitude with the gas-phase acidity of the proton donor (32). Therefore the ΔH for complexes such as $X\text{-}H\cdots I^-$ should decrease in magnitude in the order

$$IHI^- > BrHI^- > ClHI^- > FHI^-$$

The calculated values in Table XV do not reproduce this trend. This may be the result of the rather drastic assumptions made regarding the interaction distances, since the relative sizes of the calculated ΔH's in this series are very sensitive to the distance used.

5.5 Dependence of Proton Shielding on Hydrogen Bond Strength

The dependence of the complex shift on the strength of the hydrogen bond, defined as $-\Delta H$ for the formation of the bond in the gas phase, cannot be directly determined

BELL FAST BOND
50% COTTON

since reliable ΔH's are not available for all of the bihalide ions. However, some indirect measures of ΔH can be used.

Kebarle and coworkers (123) found a linear correlation between the enthalpies for the formation of 1:1 hydrogen-bonded complexes between H_2O and a number of anions in the gas phase, and the proton affinities of the anions. The proton affinity of an anion B^- is defined as the enthalpy change for the gas-phase reaction

$$B\text{-}H \longrightarrow B^- + H^+,$$

and can be calculated from

$$PA(B^-) = D(B - H) + I_p(H) - EA(B),$$

where PA, D, I_p, and EA are the proton affinity, bond dissociation energy, ionization potential, and electron affinity, respectively.

The dependence of the complex shift Δ_c', for a given proton donor, on $PA(B^-)$ of the halide ions is shown in Figure 15. The data for the chloroform (120) and methanol (124) halide ion complexes have been included as examples of much weaker acids.

For a given proton donor, the decrease in the ^1H shielding on hydrogen bonding is related to the proton affinity as a measure of the proton acceptor basicity. This

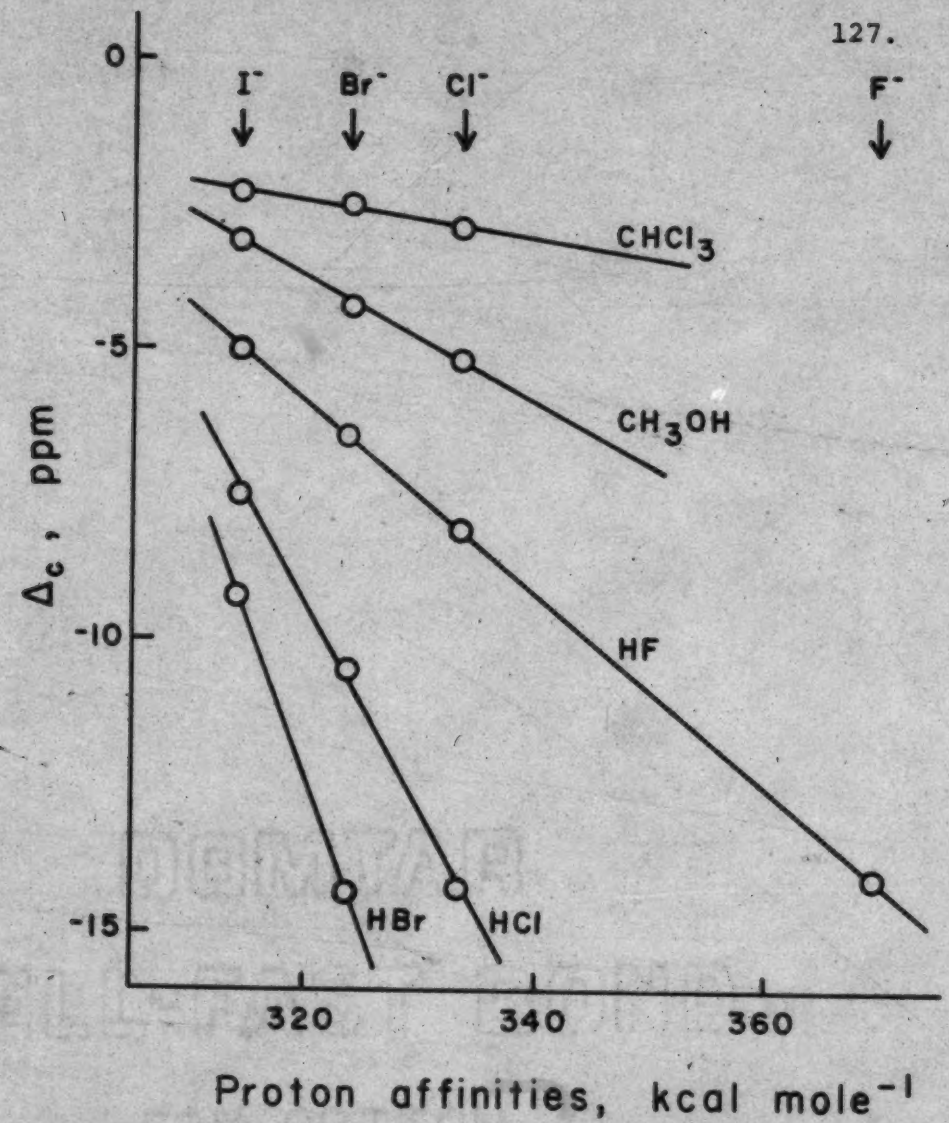

Figure 15. Dependence of the complex shifts on the proton affinities of the halide ions. Data for chloroform and methanol were taken from references 120 and 124, respectively. Complex shifts are referenced to the shielding of the proton donor in the gas phase except for chloroform.

is especially evident for the HF complexes where a wide range of base strengths is available. Since the proton affinities of the anions have been demonstrated to be proportional to the strength of the hydrogen bond formed with a given proton donor (123), the nmr shifts for a given proton donor must also be proportional to the strength of the hydrogen bond. This trend is also predicted by the energies calculated in Table XVI from an electrostatic model. Several linear enthalpy-complex shift correlations have also been found for the interactions of a proton donor with various molecular Lewis bases in inert solvents (35, 125-127).

Unfortunately the relationships shown in Figure 15 are expected to hold only for the halide ions. Consider for example, the hydrogen bonded complexes of HF of the form F-H···Y, where Y is any proton acceptor. The contribution σ_Y, produced by the electron distribution of Y, to the local magnetic field at the proton need not be related to the strength of the hydrogen bond. σ_Y is produced by the anisotropic susceptibility of the electron distribution at the bonding site of Y in the complex (34). For the halide ions, this anisotropy is created by the formation of the hydrogen bond and could be expected to be proportional to the strength of the interaction. The aniso-

tropy, created or already present, in proton acceptors with different structures would not be expected to have a simple dependence on the strength of the hydrogen bond.

This can be shown by a comparision of the complex shift between the HF complexes with the halide ions and those with the molecular bases. These shifts can be compared by using the change in the infrared stretch frequency, $\Delta\tilde{\nu}$, of the HF bond (92,128) as an approximate measure of the hydrogen bond strength (35). Figure 16 shows that Δ_c' for the bihalide ions are generally much smaller in magnitude than the Δ_c' observed in the HF complexes with the molecular bases with comparable $\Delta\tilde{\nu}$'s. This suggests that the deshielding observed in a bihalide ion, $FH\text{-}Y^-$, is smaller than that in a FH-molecular base complex with the same interaction energy. Therefore the shielding arising from the anisotropy of the halogen Y in $X\text{-}H\cdots Y^-$ is positive and important in the bihalide ions.

In summary, the behavior of the proton shielding of hydrogen fluoride complexed to various proton acceptors clearly indicates that the change in the proton shielding of a reference proton acceptor is not a reliable measure of base strengths, except for bases which are very similar in structure. For example, FHI^- is formed in acetonitrile, indicating that I^- is a stronger base than acetonitrile, although the proton shielding in FHI^- is about the same as in the FH-acetonitrile complex.

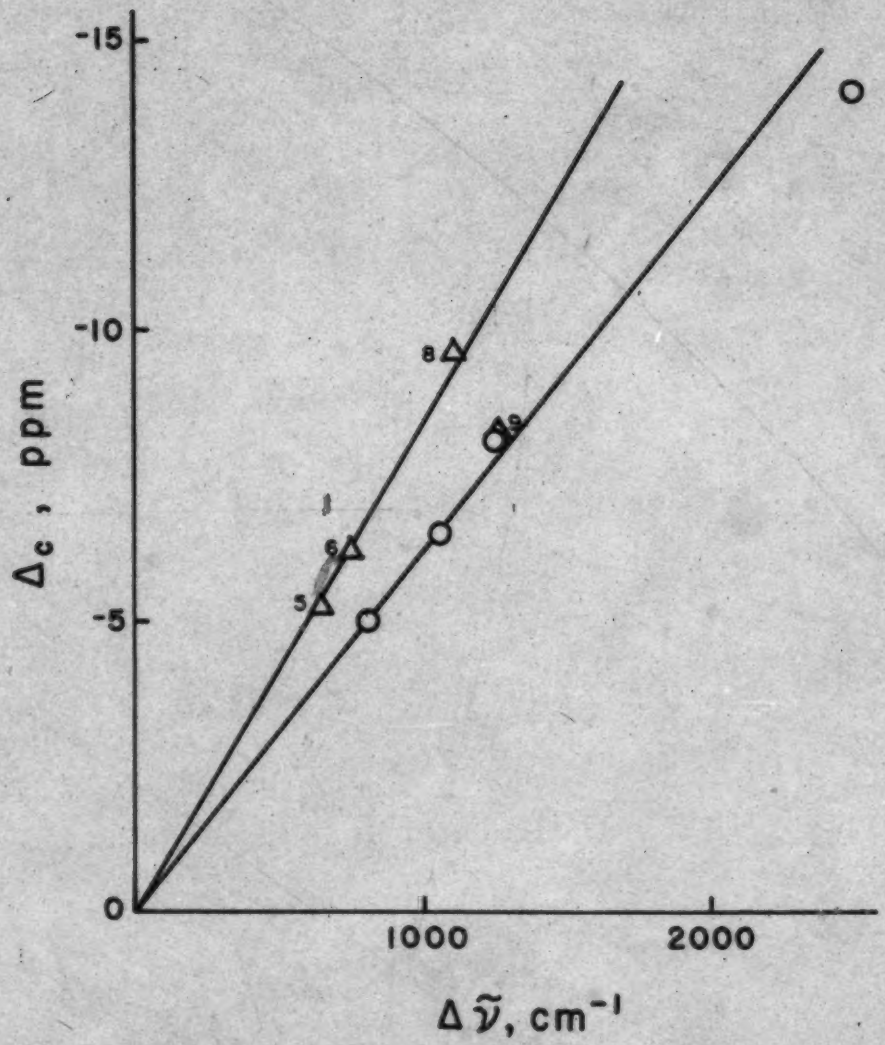

Figure 16. Correlation between the changes in the ^1H shielding and the ir stretch frequency of hydrogen fluoride: o, bihalide ions; Δ, HF in solution (numbers refer to Table XI).

There have been very few studies of the dependence of Δ_c on ΔH, for proton donors complexed to a reference base. Recently, a linear correlation between Δ_c and ΔH was found for a small number of proton donors complexed to 1-azabicyclo[2.2.2]octane (121). The enthalpy changes for the formation of the hydrogen-bonded complexes were measured in hexane and corrected for the solvation energies of the proton donors. The particular nitrogen base was chosen to minimize the neighbour anisotropy effect, and five -CH, -NH, and -OH proton donors were used.

There are a few gas-phase enthalpy measurements available for ion-molecule reactions (32). Measurements of the enthalpy of formations between various proton donors and a reference anion found the following order for $-\Delta H$ (32):

$$HBr > HCl >> CHCl_3 > HF \approx CH_3OH.$$

This trend for ΔH can be compared with the trends observed in the proton shieldings of several proton donors complexed to a reference base. In addition to Δ_c, the slopes of the lines in Figure 15 can also provide a measure of the effect of hydrogen bonding on the proton shielding of various proton donors. The slopes, defined as $d\sigma/d(PA)$, represents the rate of change in shielding with base

strength. Both Δ_c' and $d\sigma/d(PA)$ predict the same trend for for the proton donors but $d\sigma/d(PA)$ has the advantage that the gas-phase shieldings of the proton donors are not needed. The complex shifts Δ_c (referenced to the proton shielding of the proton donor in solution) measured in different solvents are difficult to compare since the shielding of the proton donor can be strongly affected by the solvent, especially in polar solvents. On the other hand, the shielding of the hydrogen-bonded complex is rather insensitive to the solvent since the hydrogen is not exposed to to the solvent. Consequently, the variation in the shieldings of various complexes, involving a common proton donor, with the base strength (such as $d\sigma/d(PA)$) should not be strongly affected by the solvent.

Figure 15 shows that the magnitudes of the changes in the proton shieldings are in the following order:

$$HBr > HCl > HF > CH_3OH > CHCl_3.$$

The changes in shielding for the hydrogen halides follows the same order as the changes in enthalpy, but the relative order of HF, CH_3OH, and $CHCl_3$ is different in these two series. This discrepancy in the order of these three proton donors is not too surprising since the range of ΔH's for these proton donors complexed to Cl^- only vary

from -14.1 to -15.2 kcal mole^{-1} (32). Consequently, other factors could control the relative order of Δ_c. The order observed for Δ_c in these five proton donors is consistent with the order of the X-H bond polarizabilities (122). A correlation has also been observed (122) between the bond polarizabilities, and the A constant in Equation [5.22] which is a measure of the electric field effects on the proton shielding. This indicates that the bond polarizability may dominate the relative order of Δ_c for complexes in which the ΔH's for the formation of the hydrogen bond are similar. If this is the case, Δ_c would be unreliable in predicting the order of ΔH for acids complexed to a reference base.

CHAPTER 6

DISCUSSION OF THE FLUORINE SHIELDINGS

In this chapter the decrease in the ^{19}F shielding of hydrogen fluoride on the formation of a hydrogen bond is discussed. A reasonable qualitative explanation for this behavior could not be found within the scope of presently accepted models which account for the shieldings in simple fluorides.

6.1 Effect of Hydrogen Bonding

The ^{19}F shieldings, observed for HF dissolved in various aprotic solvents, all show a marked decrease with respect to the shielding of HF in the gas phase. The large differences between the ^{19}F shielding of HF in the gas phase and in non-basic solvents indicate that solvent effects in addition to hydrogen bonding are appreciable. The gas-to-solution shifts of *ca.* -25 ppm should be considered as maximum values for these solvent effects since part of this shift may result from the effects of the self-association of HF in solution. The ^{19}F shieldings of HF dissolved in the basic solvents are 10 to 27 ppm less than those observed in non-polar solvents. If the non-hydrogen bonding effects are assumed to be about the same

in all these solvents, the additional deshielding in the basic solvents can be attributed to the effects of hydrogen bonding to the solvent. The ^{19}F shieldings tend to decrease with increasing base strength of the solvent defined by the Donor Number scale (94). These limited data indicate that the ^{19}F shielding generally tend to decrease with increasing strength of the hydrogen bond formed between HF and the solvent.

Even larger changes in the ^{19}F shielding are observed on the formation of the bihalide ions. A surprising feature is the virtually identical ^{19}F shielding in all four fluorine-containing bihalide ions. This behavior is in contrast to the large differences in the ^{1}H shieldings and the H-F coupling constants observed in these ions.

The decrease in both ^{1}H and ^{19}F shieldings in HF on the formation of a hydrogen bond is difficult to understand. In the previous chapter, the decrease in the ^{1}H shielding was interpreted in terms of a charge redistribution which results in a decrease in the charge density at the hydrogen and an increase in that of the fluorine. From the behavior of ^{19}F shieldings in binary fluorides, the shielding in HF would be expected to increase with a larger fluorine charge density (96). However, the available data do indicate that the decrease in the shield-

ing of the atom bonded to the electrophilic hydrogen in the proton donor molecule is a general feature of hydrogen bonding. There is a very limited number of examples in which the effect of hydrogen bonding on these shieldings has been definitely established. The ^{13}C shielding in chloroform (38) and the ^{15}N shieldings in pyrroles and indole (39) have been shown to decrease on the formation of a hydrogen bond. A decrease in the ^{17}O shielding of methanol dissolved in dichloromethane was observed on the addition of tetrabutylammonium halide. In most of the other examples mentioned in Chapter 1, the effect of forming a hydrogen bond to the electrophilic hydrogen is difficult to separate from other solvent effects.

The changes in the shielding of the heavy atom at the hydrogen bonding site are very poorly understood because of the limited amount of experimental data and the lack of theoretical studies of the shieldings in hydrogen-bonded complexes. In the following section, a theory of fluorine shieldings is presented which will be used to qualitatively discuss some of the possible explanations for the behavior of ^{19}F shieldings in hydrogen-bonded complexes of HF.

6.2 Theory of Fluorine Shielding

In the previous chapter, the proton shieldings were discussed in terms of atomic contributions. A similar model has been found to be useful in the interpretation of the large variation of the shieldings observed for ^{19}F and other heavy nuclei (129-132). The shielding of a nucleus with electrons in p orbitals can be approximately separated into two contributions,

$$\sigma = \sigma^{(1)} + \sigma^{(2)}. \qquad [6.1]$$

The local diamagnetic contribution $\sigma^{(1)}$ and the local paramagnetic contribution $\sigma^{(2)}$ arise from the electrons associated with the fluorine nucleus. The shielding contributions arising from electrons in other parts of the molecule are small compared to the local contributions (112).

Ramsey's expressions (107) for diamagnetic and paramagnetic shielding contributions contain terms which can be identified with $\sigma^{(1)}$ and $\sigma^{(2)}$ in Equation [6.1]. If the nucleus N is chosen to be the origin of the magnetic vector potential, then the total paramagnetic term σ_p for nucleus N can be related to the experimentally observed spin-rotation tensor by

$$[6.2] \qquad \sigma_p = \frac{-e^2}{3mc^2} \sum_{N \neq N'} \frac{Z_{N'}}{R_{NN'}} + \sigma_{sr}$$

where

$$[6.3] \qquad \sigma_{sr} = \frac{-e^2 h}{12Mmc^2 g_N \beta_N} \sum_{\alpha} C_{N\alpha\alpha} I_{\alpha\alpha}.$$

$Z_{N'}$ is the atomic number of nucleus N' at a distance $R_{NN'}$ from nucleus N, M is the mass of the proton, g_N is the g value of nucleus N, and β_N is the nuclear magneton. The $C_{N\alpha\alpha}$ are the three principal components of the spin-rotation tensor and $I_{\alpha\alpha}$ are the three moments of inertia.

Flygare and Goodisman (133) proposed a simple but accurate method of estimating σ_d which does not require a knowledge of the molecular wavefunction:

$$[6.4] \qquad \sigma_d = \sigma_d \text{ (free atom)} + \frac{e^2}{3mc^2} \sum_{N \neq N'} \frac{Z_{N'}}{R_{NN'}}.$$

σ_d (free atom) is the diamagnetic shielding of the isolated atom N.

The following expression for heavy atom shieldings can be obtained by substituting Equations [6.2] and [6.4] into Equation [6.1]:

$$[6.5] \qquad \sigma = \sigma_d \text{ (free atom)} + \sigma_{sr}.$$

This equation gives a good account of the fluorine shieldings in small molecules. A tabulation of the known values

of σ_{sr} for fluorine compounds has recently been published (134). In practically every case, $(\sigma - \sigma_{sr})$ was within a few ppm of the value of 471 ppm, calculated for σ_d (free atom) (135-137). For example, σ_{sr} for gaseous HF has been measured to be -57 ppm (62). Therefore Equation [6.5] predicts the ^{19}F shielding of HF to be 471 - 57 = 414 ppm, which agrees well with the established value of 410 ppm (72). This is typical of the agreement found for simple fluorine compounds in the gas phase.

The local diamagnetic contribution $\sigma^{(1)}$, in Equation [6.1], represents the expectation value of r^{-1} for the electrons associated with the nucleus. The calculated values of $\sigma^{(1)}$ for F atom and F^- ion, which represents the extreme case, differ by only 10 ppm (133, 137, 138). Therefore it is reasonable to identify $\sigma^{(1)}$ with σ_d (free atom) for fluorine shieldings in all compounds. It follows then, as suggested by Chan and Dubin (139), that $\sigma^{(2)}$ can be equated to σ_{sr}. Thus the variation in fluorine shieldings must be attributed to changes in $\sigma^{(2)}$. Empirically, $\sigma^{(2)}$ is usually negative. It is closely related to the ionic character of the bond to fluorine (96). It is zero in the isolated fluoride ion (112) and -690 ppm in F_2 (134).

Karplus and Das (130) derived an expression for

$\sigma^{(2)}$ for fluorine which can be written as,

$$[6.6] \qquad \sigma^{(2)} = \sigma_o[(P_{xx} + P_{yy} + P_{zz}) - \tfrac{1}{2}(P_{xx}P_{yy} + P_{yy}P_{zz} + P_{xx}P_{zz})]$$

where

$$[6.7] \qquad \sigma_o = \frac{-2e^2\hbar^2}{3m^2c^2\Delta E} \langle r^{-3} \rangle_{2p}.$$

P_{xx}, P_{yy}, and P_{zz} are the populations of the 2p orbitals, $\langle r^{-3} \rangle_{2p}$ is the expectation value of r^{-3} for the 2p electrons, and ΔE is the average excitation energy. This equation can be simplified to (130)

$$[6.8] \qquad \sigma^{(2)} = \sigma_o[1 - s - I + \tfrac{1}{2}(\rho_x + \rho_y)]$$

where I is the ionic character of the bond, s the degree of sp hybridization, and ρ_x and ρ_y are related to the double bond character (e.g. $\rho_x = 2 - P_{xx}$);

The most useful applications of Equation [6.8] are in calculating differences in fluorine shieldings for closely related molecules where σ_o can be assumed to be constant (130).

6.3 Application to Hydrogen Bonding of HF

The description of ^{19}F shielding in terms of

local contributions can be used to qualitatively discuss the effect of hydrogen bonding on the ^{19}F shielding of HF. The decrease in the ^{19}F shielding of HF can be assigned to changes in the local paramagnetic term since the local diamagnetic term can reasonably be expected to be nearly constant.

The expression for $\sigma^{(2)}$, in Equation [6.8], can be further simplified to

$$\sigma^{(2)} = \sigma_o(1 - I - s) \qquad [6.9]$$

if π bonding is neglected. Chan and Dubin have estimated a value of σ_o = -400 ppm for unperturbed HF by assuming s = 0 and an ionic character I of 0.86 obtained from an electronegativity versus ionic character relationship (140). Thus Equation [6.9] predicts that $\sigma^{(2)}$, for HF perturbed by a hydrogen bond, will be sensitive to changes in I or s, since the term (1 - I - s) is small. However, as summarized in the following paragraphs, changes expected in (1 - I - s) or in σ_o were either in the wrong direction or too small to account for the variation in $\sigma^{(2)}$ need to interpret the observed ^{19}F shieldings.

An electrostatic model, based on the polarization of the H-X bond by the proton acceptor, would predict an increase in the ionic character, I, of the bond, in the

sense $H^+ - X^-$. Recent theoretical calculations (116) of the electronic structure of small hydrogen-bonded complexes have also consistently predicted an increase in the electron density of X. An increase in the ionic character would reduce the magnitude of $\sigma^{(2)}$ which would tend to increase the fluorine shielding.

To explain the decrease in the ^{14}N shieldings of pyrroles, amides, and indole on the formation of hydrogen bonds to the N-H protons, a mechanism involving an electron redistribution from the nitrogen atom towards other parts of the molecule was suggested (39,40). This type of electron redistribution would not be possible in hydrogen fluoride. Consequently, other effects, which will dominate the additional shielding contribution resulting from the increase in the fluorine charge density, are required to explain the observed decrease in the ^{19}F shielding.

The change in the sp hybridization term, s, on the formation of a hydrogen bond is very difficult to estimate. However, since the degree of sp hybridization of the fluorine valence orbitals is probably small (130,137), a decrease in s cannot be expected to account for the observed increase in the magnitude of $\sigma^{(2)}$.

An increase in $\langle r^{-3} \rangle_{2p}$ in Equation [6.7] has been suggested to account for the decrease of the ^{13}C shielding

of chloroform on the formation of a hydrogen bond (38). The repulsion of the C-H electrons towards the carbon nucleus was expected to shorten the average distance of 2p orbitals and thus increase $\langle r^{-3} \rangle_{2p}$. However, in unperturbed molecules, $\langle r^{-3} \rangle_{2p}$ is expected to decrease with an increase in the electron density of the 2p orbital (131). As electrons are added to an atom, the effective nuclear charge is decreased, the orbital expands, and r^{-3} becomes smaller causing a increase in the shielding. The dependence of $\langle r^{-3} \rangle_{2p}$ on the bond length has also been considered (132). $\langle r^{-3} \rangle_{2p}$ was shown to decrease as the bond length increased. If this is the case, hydrogen bonding to HF would result in a decrease in $\langle r^{-3} \rangle_{2p}$, due to the larger charge density on the fluorine and the larger bond length, which would tend to increase the shielding.

The average excitation energy, ΔE in Equation [6.7], was introduced to approximate the individual energy differences between the ground and excited states, in order to reduce the summation over excited states to a single term depending only on the ground-state wavefunction (130). In this process the exact physical interpretation of ΔE is lost and ΔE must be considered as a semi-empirical parameter. The value of ΔE is usually assumed to be not less than the lowest electronic transition from the ground to

the excited state (96). Theoretical studies on hydrogen bonding have shown that the molecular orbital energies of the proton donors increase in energy, and that there is a good correlation between the average change in the molecular orbital energies and the total energy change (141) involved in the formation of a hydrogen bond. Increases of up to 10% were calculated for the orbital energies in the proton donor molecule for a complex such as $FH\cdots NH_3$ (141). Therefore the effective ΔE in the expression for $\sigma^{(2)}$ should be smaller in the hydrogen-bonded complex than in the unassociated proton donor molecule. The decrease in ΔE is in the right direction needed to produce a decrease in the shielding but does not appear to be large enough to account for the observed trend.

The interpretation of the effect of hydrogen bonding on the ^{19}F shielding contributions is thus unsatisfactory. This model, which has been successfully applied to unperturbed molecules, would predict an increase in the ^{19}F shielding on the basis of the increased ionic character of H-F bond expected on the formation of a hydrogen bond. Although the decrease in the energy separations between the occupied and unoccupied molecular orbitals are important, there is no indication that this effect will dominate, and control the observed trends in the shield-

ings.

A more elaborate model appears to be needed to explain the behavior observed in the ^{19}F shieldings. The expression for $\sigma^{(2)}$ given by Equation [6.7] does not appear to adequately describe the local paramagnetic shielding in hydrogen-bonded complexes. The ionic character or even accurate gross atomic orbital populations may not accurately reflect the electron distribution which gives rise to the paramagnetic term. Calculations based on accurate molecular wavefunctions for the hydrogen-bonded complexes are probably needed to interpret the shielding of the nuclei in heavy atoms.

CHAPTER 7

DISCUSSION OF THE COUPLING CONSTANT

In this chapter the effect of hydrogen bonding on the H-F coupling constant of hydrogen fluoride is discussed. The increased ionic character of the H-F bond in the hydrogen-bonded complex is suggested as a possible explanation for the trend observed in the H-F coupling constants.

7.1 Effect of Hydrogen Bonding

The H-F coupling constant in gaseous hydrogen fluoride, deduced from molecular beam electric resonance measurements, is +530 ± 23 Hz (62). In liquid hydrogen fluoride at low temperatures, a coupling constant of 521 Hz was observed in the nmr spectra (61). The H-F coupling constant decreases when hydrogen fluoride is dissolved in a basic aprotic solvent or complexed to a halide ion. The effect of hydrogen bonding on the coupling constant in hydrogen fluoride is exceptionally large compared to the fractional changes previously reported for other one -bond coupling constants. The fractional change in J(HF) is about a factor of five larger than that observed for ^{13}C-H (56,59,60) or ^{15}N-H (43) proton donor dissolved in

the same basic solvents. A more interesting difference is the direction of the change in the coupling constants. An increase in the magnitude of $^{1}J(^{13}CH)$ of C-H proton donors has been consistently observed on the formation of a hydrogen bond (56-58). The increase observed in the magnitude of $^{1}J(^{15}NH)$ in aniline has also been attributed to the formation of a hydrogen bond to N-H (43).

In order to compare the direction of the change in the coupling constant in the absolute sense, it is useful to use the reduced coupling constant defined as (143)

$$[7.1] \qquad K(AB) = \frac{2\pi}{\hbar\gamma_A\gamma_B} J(AB),$$

where $\gamma_A\gamma_B$ is the product of the magnetogyric ratios of the coupled nuclei. The reduced coupling constant depends only on the electronic environment which couples the nuclei and does not depend on nuclear magnetic properties.

The reduced coupling constants between ^{1}H directly bonded to ^{13}C, ^{15}N, and ^{19}F are all positive (62, 142). Therefore the decrease of K(HF) in hydrogen fluoride on hydrogen bonding is also in the opposite direction to the changes in $^{1}K(^{13}CH)$ and $^{1}K(^{15}NH)$, in the absolute sense.

7.2 Theory of Nuclear Spin-Spin Coupling

The theory of the electron coupled interactions between nuclear spins in a molecule was originally proposed by Ramsey (144). The interaction energy between two nuclei, which gives rise to the observed coupling in the high resolution nmr spectra of fluorine, takes the form

$$E_{AB} = K(AB)\ \mu_A \cdot \mu_B .$$

Thus, the reduced coupling constant K(AB) is defined as the proportionality constant between the interaction energy, E_{AB}, of the two nuclear spins, and the product of their magnetic moments.

In Ramsey's theory, the interactions arises from three distinct mechanisms:

(1) a nuclear magnetic moment induces orbital electronic currents which in turn produce magnetic fields at the site of the second nucleus

(2) the dipole interaction between the magnetic moment of a nucleus and the electron spins produces a magnetic field which acts on the other nucleus

(3) a Fermi contact interaction between nuclear moments and electron spins in s orbitals, which leads to electron spin polarization.

Ramsey developed general formula for these three contributions to the coupling constant using quantum-mechanical perturbation theory. Of these three interactions, the Fermi contact term is usually considered to be predominant (especially if protons are involved) and most attempts at calculating coupling constants are based on this term alone (145,146).

Pople and Santry (143) have expressed the coupling constant due to the Fermi contact term in molecular orbital form. If only the valence s orbitals are considered, the reduced coupling constant can be written in the form,

$$[7.2] \qquad K(AB) = \frac{64\pi^2\beta^2}{9} S_A^2(o)\, S_B^2(o)\, \pi_{AB},$$

where

$$[7.3] \qquad \pi_{AB} = 4 \sum_{i}^{occ} \sum_{j}^{unocc} (\varepsilon_i - \varepsilon_j)^{-1} C_{iA}C_{iB}C_{jA}C_{jB}.$$

$S_N^2(o)$ represents the electron density of the valence s orbital at nucleus N and β is the Bohr magneton. $(\varepsilon_i - \varepsilon_j)$ is the energy difference between the ith occupied and jth unoccupied molecular orbitals, and C_{iN} and C_{jN} are the coefficients of the valence s atomic orbital of atom N in these molecular orbitals.

Calculations of the coupling constant in HF us-

ing Equation [7.2] (or a form involving fewer approximations) have not been successful. Problems arise due to the sensitivity to cancellation of large terms of opposite sign in the summation involved in the term π_{AB}. Several calculations of J(HF) have been carried out using wavefunctions which involve only one unoccupied molecular orbital (143,147). In all cases, a negative value of J(HF) was calculated and the magnitude of J(HF) was found to be very sensitive to the wavefunction used.

Kato and Saika (147) also applied this perturbation approach with a basis set involving several unoccupied molecular orbitals. Although they calculated a positive value of J(HF) in good agreement with the experimental value, there was no indication of convergence in the summation over excited states. A more rigorous calculation using the same basis set (148) and other larger basis sets (149) have found the same behavior. This defect has been attributed to the poor description of the unoccupied molecular orbitals rather than to deficiencies in the calculation of the coupling constant from the wavefunctions (149).

At present, a detailed understanding of the contributions to the coupling constant in hydrogen fluoride based on Equation [7.2] is not available. However, the

theoretical calculations have shown that the Fermi contact interaction dominates the coupling constant in HF (147) and that this interaction arises predominantly from the molecular orbitals involving the fluorine 2s orbital (143,147-149).

Calculations of the coupling constant in HF have also been carried out using other approaches than that of Equation [7.2]. Pople et al (150,151) have introduced a finite perturbation method for calculating the term π_{AB} in Equation [7.2]. The application of this method to HF was unsuccessful. A coupling constant of +19.7 Hz was obtained by a CNDO calculation, and a value of -150 Hz by the more rigorous INDO method (151). Positive coupling constants in good agreement with the experimental value have been calculated by the variational procedure (152) and the perturbed Hartree-Fock method (153). However, these methods have not been extensively tested.

In the next section, the variation in J(HF) will be discussed using Equation [7.2] since it provides the simplest conceptual basis for interpreting coupling constant mechanisms.

7.3 Interpretation of Hydrogen Bonding Effects on the Coupling Constant

The conceptual basis for interpreting the mechanisms which lead to the change in the coupling constant on hydrogen bonding is not very well developed. There have been very few theoretical calculations on this effect (58). Consequently even qualitative interpretations are difficult to justify since the dependence of the coupling constant on the various features of the electronic environment is not very well understood.

The observed increase in the ^{13}C-H coupling constant on hydrogen bonding has been attributed to the effect of the electric field produced by the electrons at the bonding site in the proton acceptor (59,60). Significant changes in the C-H bond length were ruled out in the case of $CHCl_3$, on the basis of the small changes in the infrared C-H stretch frequency on hydrogen bonding (59). This electric field dependence of $^1J(^{13}C\text{-}H)$ has also been observed in situations where the electric field arises from longer range electrostatic interactions. $^1J(^{13}C\text{-}H)$ has been found to increase in the presence of an electric field arising from a cation complexed to another part of the molecule (154,155), or from the reaction field of a polar solvent (156,157), when the field is oriented in such a way as to polarize the electrons in the C-H bond

towards the carbon. Theoretical calculations have predicted a linear dependence of $^{1}J(^{13}C\text{-}H)$ in the presence of a uniform electric field in the range expected from a reaction field mechanism (158).

The mechanism by which these interactions effect a change in $^{1}J(^{13}C\text{-}H)$ is not very well understood. It has been argued that the polarization of electrons towards the carbon by the electric field would increase the carbon 2s orbital contribution to the C-H bond, and result in an increase in the coupling constant (59,60,156,157). However, there is no theoretical justification to indicate that such a mechanism can account for the electric field effects on coupling constants (58).

The difference in the effect of hydrogen bonding on the coupling constant of HF compared with other proton donors is surprising. There have been indications that the direction of the change in the magnitude of the coupling constants for the same type of interaction may be a method for determining the relative signs of the coupling constant (159). The difference between the effect of hydrogen bonding on the coupling constant in the H-F and C-H bonds can be considered using Equation [7.2].

Pople and Santry (143) have proposed a simple model of the bonding in HF which was used to show where the contributions to the coupling constant arise. The

bonding in HF was considered to mainly involve a fluorine 2p and the hydrogen 1s atomic orbitals, since the fluorine 2s atomic orbital is of much lower energy than that of the 2p orbital. The molecular orbitals formed from these atomic orbitals can be described by,

$$\psi_3 = (|p\rangle - |h\rangle)/\sqrt{2}$$

$$\psi_2 = (|p\rangle + |h\rangle)/\sqrt{2}$$

$$\psi_1 = |s\rangle$$

where s, p, and h represent the fluorine 2s, 2p and hydrogen 1s atomic orbitals respectively, if the bond is considered to be non-polar and the overlap integral is neglected. The orbital energies increase from ψ_1 to ψ_3 and the lower two molecular orbitals are doubly occupied. However, to have a non-zero coupling constant by a Fermi contact interaction, there must be some bonding between the fluorine and hydrogen s orbitals. By considering the bonding between s and h as a small perturbation, the molecular orbitals of HF were described as,

$$\psi_3 = (|p\rangle - |h\rangle + x|s\rangle)/\sqrt{2}$$

$$\psi_2 = (|p\rangle + |h\rangle - x|s\rangle)/\sqrt{2}$$

$$\psi_1 = (|s\rangle + x\,|h\rangle),$$

where $0 \leq x << 1$.

The small amount of bonding between s and h in ψ_1 produces a corresponding anti-bonding character in ψ_2 and ψ_3.

In this model, the term π_{HF} in Equation [7.3] has contributions from two excitations, $\psi_1 \rightarrow \psi_3$ and $\psi_2 \rightarrow \psi_3$. These contributions involve the products of the coefficients of the s orbitals and the coupling constant will be proportional to

$$\pi_{HF} = - \frac{2x^2}{\varepsilon_1 - \varepsilon_3} + \frac{x^2}{\varepsilon_2 - \varepsilon_3}$$

On the basis of this model, a negative coupling constant was predicted since the negative contribution from $\psi_2 \rightarrow \psi_3$ was expected to dominate because of the smaller energy difference. Calculations using the coefficients which have been more accurately determined by molecular orbital calculations also gave negative coupling constants (143, 147).

Although this bonding description does not predict the correct sign of the coupling constant, it does provide a basis for rationalization of the changes in the coupling constant on hydrogen bonding. In this description, the coupling constant is controlled by the small amount of bonding between the fluorine 2s and the hydro-

gen 1s orbitals. This bonding could be expected to decrease in a hydrogen-bonded complex since the H-F bond becomes more ionic. The decrease in the covalent bonding would be reflected in a decrease in the coefficient x which would produce a decrease in the magnitudes of both the negative and positive contributions. This would result in a smaller coupling constant.

The contributions to the coupling constant are also a function of the excitation energies, which are approximated in Equation [7.3] by the differences in orbital energies. Theoretical calculations have found that the occupied orbital energies of the proton donor molecule increase in energy, and that the absolute change in energy is approximately the same for all orbitals (140). An increase of 5 to 10% in the orbital energies were calculated for HF complexed to H_2O and NH_3 as the proton acceptors. This would result in a decrease in the terms $(\varepsilon_i - \varepsilon_j)$ which would increase the magnitude of the individual contributions to the coupling constant. Since the changes in these contributions will not be the same magnitude, the net effect is difficult to estimate from the rather uncertain description of the coupling constant in HF. However, it is not clear that the changes in the excitation energies can produce the trends observed.

A simple bonding model can be used to show the differences in the dependence of the coupling constant in F-H and C-H proton donors on hydrogen bonding. If the bonding is described in terms of the hydrogen 1s orbital and the 2s and a 2p orbital on the heavy atom, the bonding molecular orbital can be represented as

$$\psi_1 = a_1 |h\rangle + b_1 |s\rangle + c_1 |p\rangle$$

and the unoccupied antibonding orbital as

$$\psi_2 = a_2 |h\rangle + b_2 |s\rangle + c_1 |p\rangle.$$

The proportion of $|s\rangle$ and $|p\rangle$ in the molecular orbitals can be fixed by requiring $b_i^2 = c_i^2/n$. For example, sp^3 hybridization would require $n = 3$. In terms of these molecular orbitals the coupling constant is proportional to

$$\pi = \frac{a_1\, b_1\, a_2\, b_2}{\Delta E}$$

This expression can be transposed to

[7.4] $$\pi = \frac{a_1^2\, b_1^2}{\Delta E} = \frac{a_1^2\,(1 - a_1^2)}{\Delta E(n + 1)},$$

by using the relationships which result from requiring Ψ_1 and Ψ_2 to be orthonormal, and neglecting overlap intergrals. Equation [7.4] has been found to adequately describe

the coupling constant in a non-polar ^{13}C-H bond (143). This expression is not intended to adequately describe the coupling constant in HF, but does provide a basis for considering the differences in the qualitative behavior of $^{1}J(HF)$ and $^{1}J(^{13}CH)$ on hydrogen bonding.

The observed trend in $^{1}J(HF)$ on hydrogen bonding is consistent with an increase in the charge separation or ionic character of the H-F bond in the direction H^{+}-F^{-}. The increased ionic character will be reflected in a decrease in a_1^2 in Equation [7.4] which would result in a smaller coupling constant if this effect dominated the change in the H-F coupling constant. In contrast the observed increase in $^{1}J(^{13}CH)$ on hydrogen bonding clearly indicates that this mechanism does not dominate the coupling constant in C-H bonds.

A possible explanation for this difference is the variation of π in Equation [7.4] with changes in a_1 which is shown in Figure 17, assuming ΔE and n are constant. π increases from zero for the completely ionic bond, $X^{-} - H^{+}$, and reaches a maximum for a non-polar bond where $a_1 = 1/\sqrt{2}$. Figure 17 also shows that the partial derivative $\partial\pi/\partial a_1$, which reflects the sensitivity of π to changes in a_1, goes to zero for completely ionic and completely non-polar bonds. Since C-H proton donors can be consi-

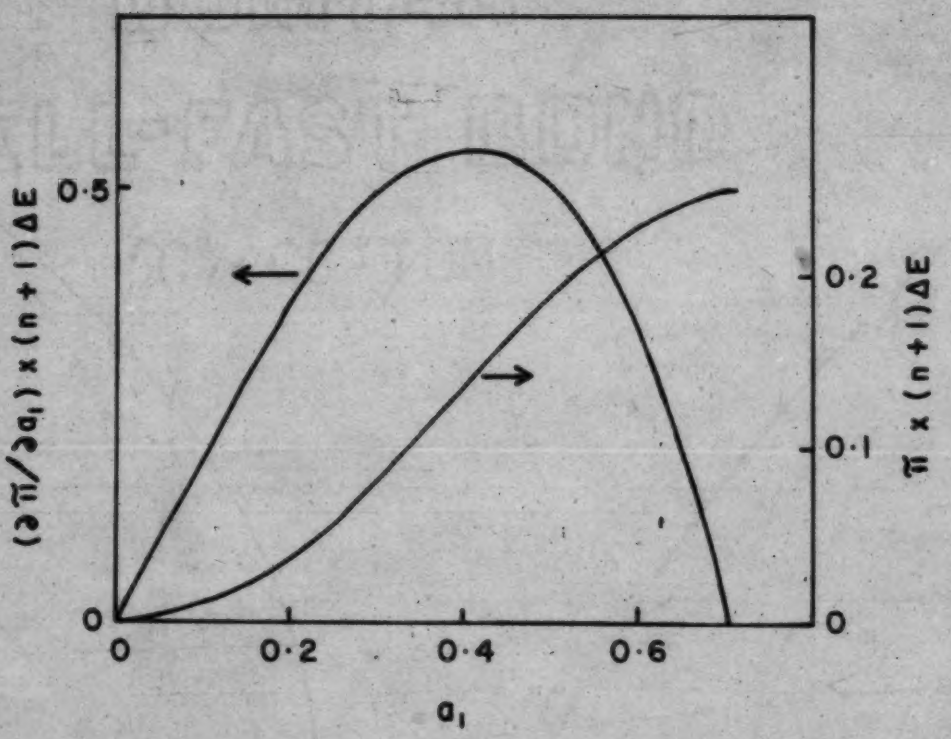

Figure 17. Variation of π_{AB} with a_1.

dered to be near the non-polar region, π will not be very sensitive to changes in the ratios of the coefficients and could be dominated by other effects, such as changes in hybridization (59,60,156,157). The relative insensitivity of $^{1}J(^{13}CH)$ to changes in bond polarity has also been used to explain substituent effects (160). In this bonding description, a value of 0.4 for a_1 would be a reasonable estimate for HF (161), which is near the region where $\partial\pi/\partial a_1$ is at a maximum. Therefore a dependence of $^{1}J(FH)$ on the changes in the H-F bond polarity appears to be reasonable.

In larger basis sets, the important excitations which contribute to the coupling constant will arise from the occupied molecular orbitals involving the fluorine 2s and hydrogen 1s atom orbitals (147-149). These contributions should show corresponding sensitivity to changes in bond polarity since they involve the product of the unequal coefficients of the hydrogen and fluorine s orbitals in the occupied molecular orbitals.

There is certainly a need for further theoretical studies before the effects of hydrogen bonding on coupling constants can be understood. There has been one calculation of the coupling constant in HF and FHF^- reported. Coupling constants of -331 and -82.9 Hz were calculated for HF and FHF^- respectively, by an INDO calcu-

lation based on Equation [7.2] (162). While the sign of the coupling constant in HF was incorrect, the calculations did predict with remarkable accuracy that these two coupling constants would be in the ratio 4:1.

7.4 Variation of J(HF) with Base Strengths

The variation of the coupling constant in HF may be a useful measure of the strength of the hydrogen bond and thereby provide a measure of the base strength of the proton acceptors. The changes in the ^{1}H shieldings are not a very reliable measure of the strength of the hydrogen bond since they are influenced by magnetic fields produced by nearby electrons which are not necessarily related to the strength of the hydrogen bond. The differences in the behavior of the ^{19}F shieldings between the bihalide ions and the HF complexes with the molecular bases, clearly demonstrate that this parameter is not generally correlated with enthalpy change associated with the hydrogen bond. There are very few measurements of the enthalpy change associated with the formation of a hydrogen bond to HF. An ir study of the temperature dependence of the equilibrium constant for the formation of the HF-diethyl-ether complex in the gas found $\Delta H = -7.2$ kcal mole^{-1} (163). The ΔH for the formation of $FHCl^{-}$ has been estimated as

-14 kcal mole^{-1} on the basis of the trend observed for the gas phase reaction between several proton donors and Cl^- (32). The observed ΔH's for the formation of FHF^- in alkali metal crystals were corrected for crystal lattice effects to give ΔH = -60 kcal mole^{-1} (31). There is a linear relationship between these values of ΔH and the corresponding H-F coupling constants which suggests that the coupling constant may be a reliable measure of ΔH.

The decrease in the H-F stretching frequency, $\Delta\tilde{\nu}$, has been used as an estimate of the strength of the hydrogen bond (35). Figure 18 presents a plot of $\Delta\tilde{\nu}$, referenced to the gas-phase monomer frequency of HF, versus J(HF). It is encouraging that the trends in $\Delta\tilde{\nu}$ and in J(HF) reflect the same relative order of the proton acceptors. This indicates that J(HF) may provide a useful scale for comparing the hydrogen bond acceptor strengths of both molecular and anionic proton acceptors. However, much more data, in particular better ΔH's, are necessary to judge the quantitative accuracy of an enthalpy-coupling constant correlation.

The point for the bifluoride ion was omitted from Figure 18 because the changes in the infrared stretch frequency and the coupling constant were very much larger than those for the other complexes. Since the change in

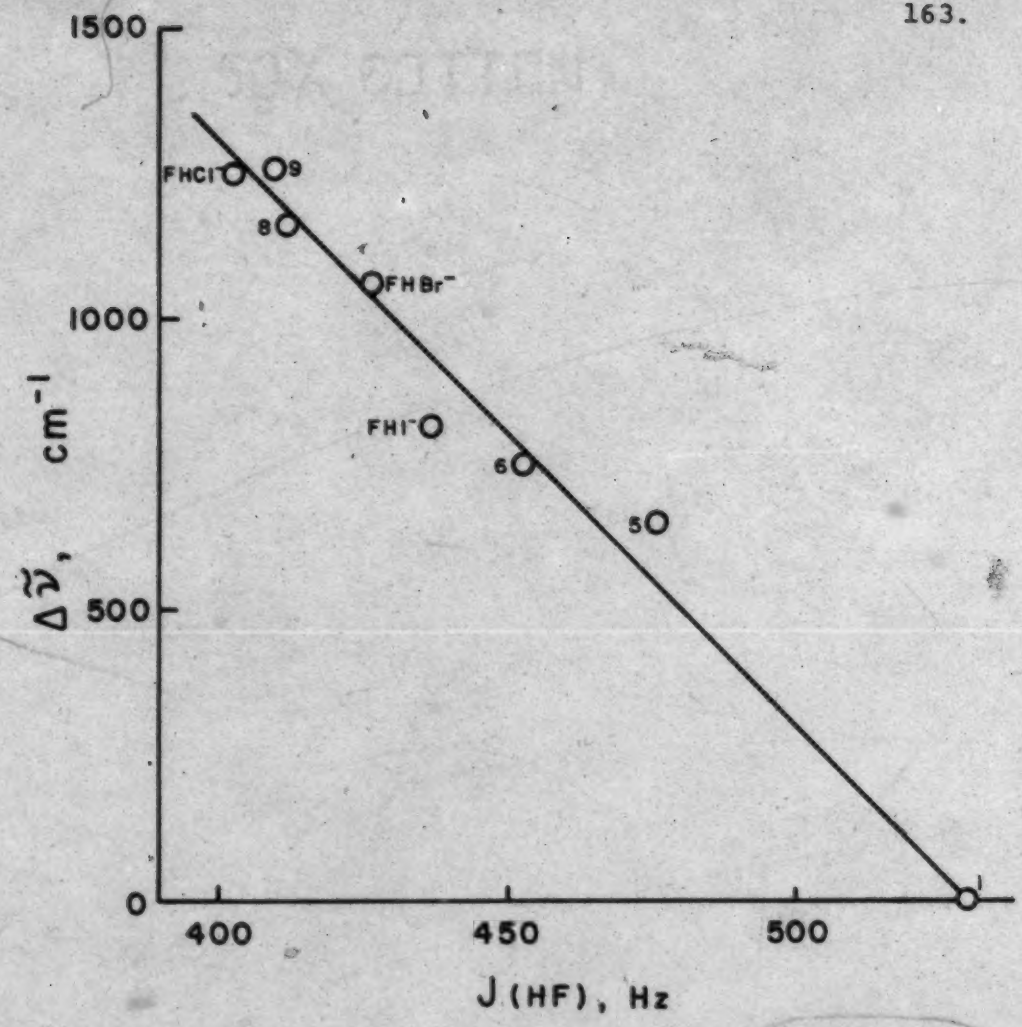

Figure 18. Correlation between the changes in the coupling constant and the ir stretch frequency of hydrogen fluoride (numbers refer to Table XI).

the coupling constant on the formation of FHF^- is so large, it is not certain that the coupling constant is still positive. However, the agreement with the trend predicted in Figure 18 is much better if the coupling constant in the bifluoride ion is assumed to be positive.

The consistent trend between the decrease in J(HF) and the base strength of the proton acceptor also supports the suggestion that the increased polarity of the H-F bond in the complex causes the decrease in the coupling constant.

CHAPTER 8

CONCLUSION

Hydrogen halides associate with the halide ions of tetraalkylammonium salts in suitable aprotic solvents to form bihalide ions. Solutions containing a hydrogen halide in the presence of an excess of halide ion can be described by a single equilibrium involving the formation of a bihalide ion, if the conjugate base of the hydrogen halide is not a weaker base than the halide ion added. When the halide ion added to a solution is a stronger base than the conjugate base of the hydrogen halide present, the proton is transfered from the hydrogen halide to the halide ion. The nmr and ir spectra of these solutions could be adequately described by assuming a quantitative proton transfer reaction. The proton shieldings decrease on the formation of the bihalide ion and two consistent trends are apparent in the proton complex shifts (defined only for the formation of a bihalide ion which does not involve a proton transfer process):

(1) the magnitude of the complex shift of a given hydrogen halide increases with the base strength of the halide ion and reaches a maximum value for the homobihalide ion.

(2) the magnitude of the complex shifts of the hydrogen halides complexed to a given halide ion increases with acid strength of the hydrogen halide and reaches a maximum value for the homobihalide ion.

This study has definitely shown that the ^{19}F shielding of hydrogen fluoride decreases on the formation of a hydrogen bond to the electrophilic hydrogen. This behavior of the ^{19}F shielding has been previously observed only in a very limited number of cases (44,45,50,51). There is now at least one clear example of the effect of hydrogen bonding on the heavy atom shielding in each of the C-H, N-H, O-H, and F-H proton donors. In all cases, the formation of a hydrogen bond results in a decrease of the shielding in the atom bonded to the electrophilic hydrogen (see section 1.2.3).

There is an approximate correspondence between the decrease in the ^{19}F shielding of hydrogen fluoride on the formation of a hydrogen bond, and the decrease of the corresponding ^{1}H shielding and H-F coupling constant, and the increase in the base strength of the proton acceptor, except for the bihalide ions. The ^{19}F shielding in all four bihalide ions are the same, to within the experimental uncertainty, and are over 70 ppm less than the

shielding in gaseous hydrogen fluoride.

The first examples of the effect of hydrogen bonding on the H-F coupling constant of hydrogen fluoride have been observed. The H-F coupling constant decreases on the formation of a hydrogen bond which is in contrast to the behavior of the corresponding coupling constants in ^{13}C-H and ^{15}N-H proton donors (43,59). The H-F coupling constant in hydrogen fluoride is very sensitive to the strength of the hydrogen bond formed, and the variation in this coupling constant appears to be a useful measure of the base strength of both molecular and anionic Lewis bases.

The interpretation of the mechanisms which result in the decrease in the proton shieldings and the H-F coupling constants complements the theoretical studies of hydrogen bonding. These theoretical studies have predicted the following changes on the formation of a hydrogen bond (116):

(a) a "charge shift" or polarization of the bond in the proton donor

(b) a charge transfer from the proton acceptor to the proton donor

(c) a decrease in the charge density of the bridging hydrogen

(d) an increase in the bond length in the proton donor.

A description of the proton shielding in terms of local contributions was used to show that the hydrogen charge density must be smaller in the homobihalide ion than in the corresponding hydrogen halide. The trends in the proton shieldings appear to be dominated by the polarization of the hydrogen halides by the electric field of the Lewis base. This results in a decrease in the local diamagnetic shielding due to the decrease in the hydrogen electron density, and a decrease in the shielding arising from the neighbour anisotropy effect of the halogen. However, in the bihalide ions an additional significant shielding contribution is present which arises from the anisotropy created in the halide ion on the formation of the hydrogen bond. This effect is consistent with the predicted charge transfer from the proton acceptor to the proton donor.

The decrease in the H-F coupling constant was interpreted in terms of an increase in the ionic character of the H-F bond in the hydrogen-bonded complex.

An interpretation of the decrease in the ^{19}F shielding could not be found which was compatible with an increase in the fluorine charge density. This is probably due to the inadequacy of the shielding model since the

fluorine charge density in a complex such as FHF^- is undoubtedly larger than that in HF.

Quantitative calculations of the nuclear shieldings and coupling constant in hydrogen-bonded complexes are certainly needed. Theoretical calculations have been successful in describing many of the properties of hydrogen-bonded complexes but very few attempts have been made to calculate the nuclear magnetic properties of these complexes. The observations reported here should provide a useful contribution to the data necessary to test these calculations.

REFERENCES

1. S. A. Harrel and D. H. McDaniel, J. Amer. Chem. Soc., 86, 4497 (1964).
2. W. C. Hamilton and J. A. Ibers, "Hydrogen Bonding in Solids" (W. A. Benjamin, New York, 1968), pp. 108-113.
3. D. G. Tuck in "Progress in Inorganic Chemistry," ed. F. A. Cotton (Interscience, New York, 1968), Vol. 9, p. 161.
4. T. C. Waddington in "Main Group Elements," ed. V. Gutmann (Butterworths, London, 1972), p. 85.
5. F. Kaufler and E. Kunz, Chem. Ber., 42, 385 (1909).
6. H. F. Herbrandson, R. T. Dickerson, Jr., and J. Weinstein, J. Amer. Chem. Soc., 76, 4046 (1954).
7. M. M. Davis, "Acid-Base Behavior in Aprotic Organic Solvents," National Bureau of Standards Monograph 105 (United States Department of Commerce, Washington, D.C., 1968).
8. J. M. Kolthoff and M. K. Chantooni, Jr., J. Amer. Chem. Soc., 85, 2195 (1963).
9. G. Pimentel and A. L. McClellen in "Annual Review of Physical Chemistry," ed. H. Eyring (Annual Review Inc., Palo Alto, California, 1971), p. 360.
10. L. W. Schroeder and J. Ibers, Inorg. Chem., 7, 594 (1968).

11. J. M. Ready, K. Knox, and M. B. Rubin, J. Chem. Phys., 40, 1082 (1964).

12. J. W. Swanson and J. M. Williams, Inorg. Chem., 6, 3697 (1967).

13. J. C. Evans and G. Y-S. Lo, J. Phys. Chem., 70, 11 (1966).

14. L. W. Schroeder, J. Chem. Phys., 52, 1972 (1970).

15. J. W. Nibler and Pimentel, J. Chem. Phys., 47, 710 (1967).

16. G. C. Sterling, C. J. Ludman and T. C. Waddington, J. Chem. Phys., 52, 2730 (1970).

17. G. Herzberg, "Infrared and Raman Spectra of Polyatomic Molecules" (Van Nostrand, New York, 1945), p. 252.

18. G. C. Pimentel and A. L. McClellan, "The Hydrogen Bond" (W. H. Freeman, San Francisco, 1960).

19. T. E. Haas and S. M. Welsh, J. Phys. Chem., 71, 3363 (1967).

20. C. J. Ludman, T. C. Waddington, J. A. Salthouse, R. T. Lynch, and J. A. S. Smith, J. Chem. Soc. D, 1970, 405.

21. J. C. Evans and G. Y-S. Lo, J. Phys. Chem., 71, 3697 (1967).

22. J. C. Evans and G. Y-S. Lo, J. Phys. Chem., 71, 3942 (1967).

23. D. E. Milligan and M. E. Jacox, J. Chem. Phys., 53, 2034 (1970).

24. D. E. Milligan and M. E. Jacox, J. Chem. Phys., 55, 2550 (1971).

25. P. N. Noble and G. C. Pimentel, J. Chem. Phys., 49, 3165 (1968).

26. V. Bondybey, G. C. Pimentel, and P. N. Noble, J. Chem. Phys., 55, 540 (1971).

27. D. H. McDaniel and R. E. Vallee, Inorg. Chem., 2, 996 (1963).

28. R. L. Benoit, M. Rinfret, and R. Domain, Inorg. Chem., 11, 2603 (1972).

29. T. C. Waddington, Trans. Faraday Soc., 54, 25 (1958).

30. H. D. B. Jenkins and T. C. Waddington, Nature, 232, 5 (1971).

31. H. P. Dixon, H. D. B. Jenkins, and T. C. Waddington, J. Chem. Phys., 57, 4388 (1972).

32. R. Yamdagni and P. Kebarle, J. Amer. Chem. Soc., 93, 7139 (1971).

33. J. W. Emsley, J. Feeny, and L. H. Sutcliffe, "High Resolution Nuclear Magnetic Resonance Spectroscopy," (Pergamon Press, Oxford, 1965), pp. 534-551.

34. J. A. Pople, W. G. Schneider, and H. J. Bernstein, "High Resolution Nuclear Magnetic Resonance" (McGraw-Hill, New York, 1959).

35. A. S. N. Murthy and C. N. R. Rao, Appl. Spectrosc. Rev., 2, 69 (1968).

36. Reference 34, Chap. 10.

37. J. C. Davis, Jr., and K. K. Deb in "Advances in Magnetic Resonance," ed. J. S. Waugh (Academic Press, New York, 1970), Vol. 4, p. 201.

38. R. L. Lichter and J. D. Roberts, J. Phys. Chem., 74, 912 (1970).

39. H. Saito and K. Nukada, J. Amer. Chem. Soc., 93, 1072 (1971).

40. H. Saito, Y. Tanaka, and K. Nukada, J. Amer. Chem. Soc., 93, 1077 (1971).

41. A. E. Florin and M. Alei, Jr., J. Chem. Phys., 47, 4268 (1967).

42. W. H. Litchman, M. Alei, Jr., and A. E. Florin, J. Chem. Phys., 50, 1031 (1969).

43. L. Paolillo and E. D. Becker, J. Mag. Resonance, 2, 168 (1970).

44. D. K. Hindermann and C. D. Cornwell, J. Chem. Phys., 48, 2017 (1968).

45. E. L. Mackor, C. MacLean and C. W. Hilbers, Recueil, 87, 655 (1968).

46. W. H. Litchman, M. Alei, Jr., and A. E. Florin, J. Amer. Chem. Soc., 91, 6574 (1969).

47. J. Reuben, J. Amer. Chem. Soc., 91, 5725 (1969).

48. Z. Luz and G. Yagil, J. Phys. Chem., 70, 554 (1966).

49. R. D. Green, J. S. Martin, W. B. M. Cassie, and J. B. Hyne, Can. J. Chem., 47, 1639 (1969).

50. K. Schaumburg and C. Deverell, J. Amer. Chem. Soc., 90, 2495 (1968).

51. J. Soriano, J. Shamir, A. Netzer, and Y. Marcus, Inorg. Nucl. Chem. Letters, 5, 209 (1969).

52. P. M. Borodin and E. N. Sventitskii, Dokl. Acad. Nauk. SSSR, 175, 473 (1967), English translation.

53. A. Loewenstein and Y. Margalit, J. Phys. Chem., 69, 4152 (1965).

54. H. Saito, K. Nukada, H. Kato, T. Yonezawa, and K. Fukui, Tetrahedron Letters, 1965, 111.

55. H. A. Christ and P. Diehl, Helv. Phys. Acta, 36, 170 (1963).

56. P. Laszlo in "Progress in Nuclear Magnetic Resonance Spectroscopy," eds. J. W. Emsley, J. Feeney, and L. H. Sutcliffe (Pergamon Press, Oxford, 1967), Vol. 3, Chap. 6.

57. S. L. Smith, Top. Current Chem., 27, 119 (1972).

58. M. Barfield and M. D. Johnston, Jr., Chem. Rev., 73, 53 (1973).

59. D. F. Evans, J. Chem. Soc., 1963, 5575.

60. V. S. Watts and J. H. Goldstein, J. Phys. Chem., 70, 3887 (1966).

61. C. MacLean and E. L. Mackor in "Proceedings of the Colloque Ampère," Eindhoven, 1962, ed. J. Smidt (North-Holland Publishing Co., Amsterdam, 1963), p. 571.

62. J. S. Muenter and W. Klemperer, J. Chem. Phys., 52, 6033 (1970).

63. N. V. Sidgwick, "The Chemical Elements and their Compounds" (Oxford University Press, London, 1950), Vol. II, p. 1168.

64. N. H. Furan, "Standard Methods of Chemical Analysis" (Van Nostrand, New York, 1962), 6th ed., p. 441.

65. H. H. Willard, N. H. Furan and C. E. Bricker, "Elements of Quantitative Analysis" (Van Nostrand, New York, 1956), p. 262.

66. W. T. Miller, Jr., J. H. Fried, and H. Goldwhite, J. Amer. Chem. Soc., 82, 3091 (1960).

67. R. T. Morrison and R. N. Boyd, "Organic Chemistry" (Allyn and Bacon, Boston, 1959), p. 553.

68. T. Myint, D. Kleppner, N. F. Ramsey, and H. G. Robinson, Phys. Rev., 17, 405 (1966).

69. E. D. B. Lambe, Ph.D. thesis, Princeton University, 1959; Dissertation Abstr., 21, 2330 (1961).

70. P. F. Winkler, F. G. Walther, M. T. Myint, and D. Kleppner in "Physics of One and Two Electron Atoms," ed. F. Bopp and H. Kleinpoppen (North-Holland Publishing Co., Amsterdam, 1969), p. 146.

71. H. Grotch and R. A. Hegstrom, Phys. Rev. A, 4, 59 (1971).

72. D. K. Hindermann and C. D. Cornwell, J. Chem. Phys., 48, 4148 (1968).

73. H. A. Benesi and J. H. Hildebrand, J. Amer. Chem. Soc., 71, 2703 (1949).

74. R. L. Scott, Rec. Trav. Chim., 75, 787 (1956).

75. W. B. Pearson, J. Amer. Chem. Soc., 87, 167 (1965).

76. D. A. Deranleau, J. Amer. Chem. Soc., 91, 4044 (1969).

77. J. F. Coetzee in "Progress in Physical Organic Chemistry," eds. A. Streitwieser, Jr., and R. W. Taft (Interscience, New York, 1967), Vol. 4, p. 45.

78. W. T. Raynes, A. D. Buckingham, and H. J. Bernstein, J. Chem. Phys., 36, 3481 (1962).

79. L. Petrakis and C. H. Soderholm, J. Chem. Phys., 35, 1174 (1961).

80. W. G. Schneider, H. J. Bernstein, and J. A. Pople, J. Chem. Phys., 28, 601 (1958).

81. R. D. Green, Ph.D. thesis, University of Alberta, 1968.

82. G. J. Janz and S. S. Danyluk, J. Amer. Chem. Soc., 81, 3846 (1959).

83. E. Allenstein and A. Schmidt, Spectrochim. Acta, 20, 1451 (1964).

84. S. W. Peterson and J. W. Williams, J. Amer. Chem. Soc., 88, 2866 (1966).

85. Reference 33, pp. 841-851.

86. R. St. C. Smart and N. Sheppard, Proc. Roy. Soc., A320, 417 (1971).

87. R. L. Reddington and T. E. Reddington, J. Phys. Chem., 72, 2456 (1968).

88. J. C. Evans and G. Y-S Lo, J. Phys. Chem., 70, 20 (1966).

89. J. A. Salthouse and T. C. Waddington, J. Chem. Soc., 1964, 4664.

90. J. I. Brauman and L. K. Blair, J. Amer. Chem. Soc., 92, 5986 (1970).

91. R. L. Benoit, A. L. Beauchamp, and R. Domain, Inorg. Nucl. Chem. Letters, 7, 557 (1971).

92. P. Van Huong and M. Couzi, J. Chim. Phys., 67, 1994 (1970).

93. R. M. Adams and J. J. Katz, J. Mol. Spectrosc., 1, 306 (1957).

94. V. Gutmann, "Coordination Chemistry in Non-Aqueous Solutions" (Springer-Verlag, New York, 1968), p. 19.

95. W. T. Raynes and M. A. Raza, Mol. Phys., 20, 555 (1971).

96. J. W. Emsley and L. Phillips in "Progress in Nuclear Magnetic Resonance Spectroscopy," eds. J. W. Emsley, J. Feeney, and L. H. Sutcliffe (Pergamon Press, Oxford, 1971), Vol. 7.

97. H. Spiesecke and W. G. Schneider, J. Chem. Phys., 35, 722 (1961).

98. A. D. Buckingham, Can. J. Chem., 38, 300 (1960).

99. T. Yonemoto, Can. J. Chem., 44, 223 (1966).

100. P. A. Kollman and L. C. Allen, J. Amer. Chem. Soc., 92, 6101 (1970).

101. P. N. Noble and R. N. Kortzeborn, J. Chem. Phys., 52, 5375 (1970).

102. M. Zaucer, J. Koller, and A. Azman, Z. Naturforsh A25, 1769 (1970).

103. G. C. Pimentel, J. Chem. Phys., 19, 446 (1951).

104. A. Salès, F. Cabaret, and J. Guy, J. Phys. Radium, 23, 258 (1962).

105. B. R. McGarvey, J. Chem. Phys., 27, 68 (1957).

106. G. Herzberg, "Spectra of Diatomic Molecules" (Van Nostrand, New York, 1950).

107. N. F. Ramsey, Phys. Rev., 78, 699 (1950).

108. W. N. Lipscomb, in "Advances in Magnetic Resonance,"

ed. J. S. Waugh (Academic Press, New York, 1966) Vol. 2, pp. 138-176.

109. D. E. O'Reilly in "Progress in Nuclear Magnetic Resonance Spectroscopy," eds. J. W. Emsley, J. Feeney, and L. H. Sutcliffe (Pergamon Press, London, 1966), Vol. 2, pp. 1-62.

110. N. F. Ramsey, Amer. Scientist, 49, 509 (1961).

111. S. I. Chan and T. P. Das, J. Chem. Phys., 37, 1527 (1962).

112. J. A. Pople, Proc. Roy. Soc. (London), A239, 550 (1957).

113. C. P. Slichter, "Principles of Magnetic Resonance" (Harper and Row, New York, 1963), Chap. 4.

114. A. A. Bothner-By and J. A. Pople in "Annual Review of Physical Chemistry," ed. H. Eyring (Annual Reviews, Inc., Palo Alto, California, 1965), Vol. 16, p. 43.

115. A. L. McClellan, "Table of Experimental Dipole Moments" (W. H. Freeman, San Francisco, 1963).

116. P. A. Kollman and L. C. Allen, Chem. Rev., 72, 283 (1972).

117. A. D. Buckingham, T. Schaefer, and W. G. Schneider, J. Chem. Phys., 32, 1227 (1960).

118. P. J. Berkeley and M. W. Hanna, J. Amer. Chem. Soc., 86, 2990 (1964).

119. T. W. Marshall and J. A. Pople, Mol. Phys., 1, 199 (1958).

120. R. D. Green and J. S. Martin, J. Amer. Chem. Soc., 90, 3659 (1968).

121. F. L. Slejko and R. S. Drago, Inorg. Chem., 12, 176 (1973).

122. G. Widenlocker and E. Dayan, Compt. Rend., 260, 6856 (1965).

123. J. D. Payzant, R. Yamdagni, and P. Kebarle, Can. J. Chem., 49, 3038 (1971).

124. S. Ormondroyd, E. A. Phillpot, and M. C. R. Symons, Trans. Faraday Soc., 67, 1253 (1971).

125. T. D. Epley and R. S. Drago, J. Amer. Chem. Soc., 89, 5770 (1967).

126. A. D. Sherry and K. F. Purcell, J. Phys. Chem., 74, 3535 (1970).

127. L. Joris, J. Mitsky, and R. W. Taft, J. Amer. Chem. Soc., 94, 3438 (1972).

128. J. C. Evans and G. Y-S. Lo, J. Phys. Chem., 70, 543 (1966).

129. A. Saika and C. P. Slichter, J. Chem. Phys., 22, 26 (1959).

130. M. Karplus and T. P. Das, J. Chem. Phys., 34, 1683 (1961).

131. M. Karplus and J. A. Pople, J. Chem. Phys., 38, 2803 (1963).

132. A. B. Strong, D. Ikenberry, and D. M. Grant, J. Mag. Resonance, 9, 145 (1973).

133. W. H. Fylgare and J. Goodisman, J. Chem. Phys., 49, 3122 (1968).

134. S. C. Wofsy, J. S. Muenter and W. Klemperer, J. Chem. Phys., 55, 2014 (1971).

135. W. C. Dickinson, Phys. Rev., 80, 563 (1950).

136. R. A. Bonham and T. Strand, J. Chem. Phys., 40, 3447 (1964).

137. S. Frage and G. Malli, "Many-Electron Systems: Properties and Interactions" (W. B. Saunders, Philadelphia, 1968).

138. T. W. Sidwell and R. P. Hurst, J. Chem. Phys., 37, 203 (1962).

139. S. I. Chan and A. S. Dubin, J. Chem. Phys., 46, 1745 (1967).

140. D. P. Dailey and C. H. Townes, J. Chem. Phys., 23, 118 (1955).

141. P. A. Kollman and L. C. Allen, J. Amer. Chem. Soc., 93, 4991 (1971).

142. W. McFarlane, Quart. Rev., 23, 187 (1969).

143. J. A. Pople and D. P. Santry, Mol. Phys., 8, 1 (1964).

144. N. F. Ramsey, Phys. Rev., 91, 303 (1953).

145. M. Barfield and D. M. Grant in "Advances in Magnetic Resonance," ed. J. S. Waugh (Academic Press, New York, 1965), Vol. 1, p. 149.

146. J. N. Murrell in "Progress in Nuclear Magnetic Resonance Spectroscopy," eds. J. W. Emsley, J. Feeney, and L. H. Sutcliffe (Pergamon Press, Oxford, 1971), Vol. 6, p. 1.

147. Y. Kato and A. Saika, J. Chem. Phys., 46, 1975 (1967).

148. J. N. Murrel, M. A. Turpin, and R. Ditchfield, Mol. Phys., 18, 271 (1970).

149. W. Adam, A. Grimison, and P. A. Sprangle, Theor. Chim. Acta, 18, 385 (1970).

150. J. A. Pople, J. W. McIver, Jr., and N. S. Ostlund, J. Chem. Phys., 49, 2960 (1968).

151. J. A. Pople, J. W. McIver, Jr., and N. S. Ostlund, J. Chem. Phys., 49, 2965 (1968).

152. D. E. O'Reilly, J. Chem. Phys., 36, 274 (1962).

153. P. M. Getzin, Ph.D. Thesis, Columbia University, 1967.

154. W. T. Raynes and T. A. Sutherley, Mol. Phys., 17, 574 (1969).

155. J. C. Hammel, J. A. S. Smith, and E. J. Williams,

J. Chem. Soc. A, 1969, 1461.

156. R. H. Cox and S. L. Smith, J. Mag. Resonance, 1, 376 (1970).

157. C. L. Bell and S. S. Danyluk, J. Mol. Spectrosc., 35, 376 (1970).

158. M. D. Johnston and M. Barfield, J. Chem. Phys., 54, 3083 (1971).

159. C. L. Bell and S. S. Danyluk, J. Amer. Chem. Soc., 88, 2344 (1966).

160. N. Muller and D. E. Pritchard, J. Chem. Phys., 31, 768 (1959).

161. C. A. Coulson, "Valence," (Oxford University Press, London, 1961), p. 107.

162. A. Azman, B. Borstnik, and J. Koller, Theor. Chim. Acta, 13, 262 (1969).

163. R. K. Thomas, Proc. Roy. Soc. (London), A322, 137 (1971).

APPENDIX

The equilibrium concentrations of the species present in solutions containing a hydrogen halide, HA, and the tetrabutylammonium salt of the halide ion B^-, where B^- is a stronger base than A^-, were calculated assuming a quantitative proton transfer from HA to B^-.

The following equations were used to describe solutions where the number of moles of B^- added were less than or equal to the initial amount of HA:

[A.1] $$HA + B^- \longrightarrow HB + A^-$$

[A.2] $$HA + A^- \rightleftharpoons AHA^- \qquad K_1 = \frac{[AHA^-]}{[HA][A^-]}$$

[A.3] $$HB + A^- \rightleftharpoons BHA^- \qquad K_2 = \frac{[BHA^-]}{[HB][A^-]}$$

If the initial concentrations are defined as

$$[HA]_\circ = a$$

$$[B^-]_\circ = b$$

where $a \geq b$, the equilibrium concentrations are

$$[AHA^-] = x \qquad [HA] = a - b - x$$

$$[BHA^-] = y \qquad [HB] = b - y$$

$$[B^-] = 0 \qquad [A^-] = b - x - y$$

The following equations can be derived from the expressions for the associations constants:

$$[A.4] \qquad y = \frac{bx}{\frac{K_1}{K_2}(a - b) - x\left(\frac{K_1}{K_2} - 1\right)}$$

$$[A.5] \qquad K_1\left(\frac{K_1}{K_2} - 1\right)x^3 - \left\{\frac{2aK_1^2}{K_2} - \frac{bK_1^2}{K_2} - K_1(a - b) + \frac{K_1}{K_2} - 1\right\}x^2 + \left\{\frac{K_1^2}{K_2}(a^2 - b^2) + \frac{K_1}{K_2}(a - b)\right\}x - \frac{K_1^2}{K_2}b(a - b)^2 = 0$$

In the region where $a \leq b$ the following equilibria will be present:

$$[A.6] \qquad HB + A^- \rightleftharpoons BHA^-$$

$$[A.7] \qquad HB + B^- \rightleftharpoons BHB^- \qquad K_3 = \frac{[BHB^-]}{[HB][B^-]}$$

The equilibrium concentrations are given as

$$[BHA^-] = y \qquad [HB] = a - y - z$$

$$[BHB^-] = z \qquad [B^-] = b - a - z$$

$$[HA] = 0 \qquad [A^-] = a - y.$$

The following equations can be derived from the expressions for the association constants:

$$y = \frac{az}{\frac{K_3}{K_2}(b - a) - z\left(\frac{K_3}{K_2} - 1\right)}$$

$$K_3\left(\frac{K_3}{K_2} - 1\right)z^3 - \left\{\frac{2bK_3^2}{K_2} - \frac{aK_3^2}{K_2} - K_3(b - a) + \frac{K_3}{K_2} - 1\right\}z^2$$

$$+ \left\{\frac{K_3^2}{K_2}(b^2 - a^2) + \frac{K_3}{K_2}(b - a)\right\}z - \frac{K_3^2}{K_2}a(b - a)^2 = 0 \quad ..$$

In every case an unique solution was found.

Since these species in solution are undergoing rapid proton exchange, the average shielding can be calculated from

$$\sigma = \sum_i f_i \sigma_i$$

where f_i is the fraction of species i with shielding σ_i.

Tables XVII, XVIII, and XIX present the calculated and observed shieldings for solutions in sym-tetrachloroethane at 34°. The average values of the association constants and proton shieldings presented in Chapter 3 were used. The largest deviations between the calculated and observed shieldings occurs in solutions which contain an excess of hydrogen halide. These deviations are in the direction expected if complexes of the type $X^-(HY)_n$ are present.

Table XVII. Proton shieldings in solutions containing 0.1M HBr and Bu_4NCl in sym-tetrachloroethane

$[Cl^-]$ added	σ Calculated (ppm)	σ Observed (ppm)	Difference
0.0101	1.14	0.90	+0.24
0.0198	-0.33	-1.10	+0.97
0.0267	-1.32	-1.87	+0.55
0.0558	-4.84	-5.50	+0.66
0.0943	-7.49	-8.33	+0.84
0.1083	-8.40	-8.87	+0.47
0.1290	-9.84	-9.80	-0.04
0.1817	-12.04	-12.24	+0.20
0.2796	-13.24	-13.15	-0.09
0.4614	-13.64	-13.40	-0.24
0.6762	-13.75	-13.70	-0.05

Table XVIII. Proton shieldings in solutions containing 0.2M HI and Bu_4NCl in sym-tetrachloroethane

$[Cl^-]$ Added	σ Calculated (ppm)	σ Observed (ppm)	Difference
0.0585	5.94	4.90	+1.04
0.1261	0.52	-0.05	+0.57
0.2126	-5.39	-5.68	+0.29
0.2961	-9.38	-9.78	+0.40
0.3503	-11.29	-11.58	+0.29
0.4363	-13.01	-12.84	-0.17
0.6192	-13.64	-13.52	-0.12
0.8768	-13.78	-13.88	+0.10
1.118	-13.82	-14.05	+0.13

Table XIX. Proton shieldings in solutions containing 0.2M HI and Bu_4NBr in sym-tetrachloroethane

$[Br^-]$ Added	σ Calculated (ppm)	σ Observed (ppm)	Difference
0.0999	3.94	3.55	0.39
0.2002	-2.37	-2.84	0.47
0.4461	-8.82	-8.87	0.05
0.6105	-9.55	-9.65	0.10
0.9283	-9.88	-10.02	0.14